Characterisation and Description of Compressible Rubbery Materials for Component Modelling

Nathan Townsend

A dissertation submitted in partial fulfilment of the requirements for the degree of MPhil

Department of Engineering, Design and Mathematics, University of the West of England, Bristol

October 2015

ABSTRACT

Rubbery foams and similar highly compressible rubbery solids form an important class of materials for technology. In order for components made from such materials to be modelled, in Finite Element Analysis (FEA) for example, appropriate constitutive laws are required.

The review of the literature revealed that rubbery foams lacked the array of comprehensive data sets that have been published for near-incompressible rubbery materials for example. Moreover there were important contradictions between accounts of how rubbery foams behaved at finite strains. The review of the literature also raised some doubts on what the value of Poisson's ratio (v) should be for such materials in simple extension – let alone in compression.

Most finite strain FEA of rubbery foams seems to use in the constitutive law a finite strain version of v based on logarithmic strains: here called the Poisson index, υ. Some of the implications of such approaches have been explored via theory and experiments. Some doubt has thereby been cast on such approaches.

In this project experiments performed in simple compression on a normal natural rubber latex foam have confirmed that the apparent Poisson ratio can fall to very low values even at rather small strains; the apparent Young modulus can drop to low values even at very small strains. The experiments have also indicated that: v, and therefore υ at small strain simple extension, can be well below the value of 1/3 usually assumed; the value of υ can rise as extension progresses and can exceed ½.

Table of contents

5 EXPERIMENTAL WORK

5.1 Materials for experiments

5.1.1 Introduction
5.1.2 Measurement of the density of the natural rubber latex foam
5.1.3 Finding the volume fraction of rubber in the foam
5.1.4 Finding the volume fraction of closed cells in the foam
5.1.5 Removal of “skin” from the Pentonville Foam natural rubber latex foam
5.1.6 Conditioning of the test piece

5.2 Simple shear test

5.2.1 Apparatus and experimental procedure
5.2.2 Results and discussion for simple shear test

5.3 Simple extension tests

5.3.1 Apparatus
5.3.2 Deformation measurement
5.3.3 Experimental procedure.

5.4 Simple compression tests

5.4.1 Apparatus and procedures
5.4.2 Results and discussion for simple extension and compression tests

5.5 Pressure-volume tests

5.5.1 Apparatus and procedures
5.5.2 Experimental method
5.5.3 Results and discussion for bulk modulus test

LIST OF FIGURES

Acknowledgements

I would like to thank everyone who has helped, encouraged and supported me throughout the years I have spent studying for my MPhil.

In particular I would like to express my sincere gratitude to my director of studies Dr VA Coveney for all his tireless effort, support and encouragement.

Special thanks also to Dr G Chagnon whose work with Dr VA Coveney was referred to throughout this study.

I would also like to thank Professor M Smith for help and support as director of studies during the final years of this study.

Thanks also to my additional supervisor Dr A Farooq for offering help and advice when needed.

Finally thanks to Dr D Cole for help and advice with experimental work, and for checking and proof reading my dissertation.

1. INTRODUCTION

This project focuses on highly compressible materials, mainly rubbery foams, and the constitutive models used to describe these. Rubbery foams are important materials and widely used in health, transport and many other technical areas. Their functions include shock and impact reduction, noise absorption and isolation from vibration.

Rubbery materials without voids can undergo large strains of hundreds of percent in tension as well as in compression more or less elastically. For materials without voids the shear modulus (μ) is ~1 MPa, whereas the bulk modulus (K) is ~2 GPa.
Because K/μ is so high these materials have Poisson ratios close to ½ and are sometimes called near incompressible.

Voided or cellular rubbery solids otherwise known simply as rubbery foams have shear moduli that are generally lower and bulk moduli much lower than those for solid rubbers. Foam materials can have open or closed cells with geometry that can be either regular or irregular. They can be composites, with hollow or otherwise highly compressible inclusions e.g. cork. The single most important feature of a rubbery foam material is the fraction of the volume occupied by solid rather than air or another gas. This is the volume fraction (Φ) of the foam; provided the density of the gas can be ignored it is equal to the density of the cellular material divided by the density of the solid from which it is formed, ρ/ρ_S . Ultra low density foams can have a volume fraction as low as 0.001. General purpose polymeric foams have a volume fraction of between 0.05 and 0.2. A foam material is normally described as having a volume fraction of below about 0.3. Above this value the dense foam is sometimes described as a solid containing isolated pores (Gibson & Ashby, 1997).

Foam materials are especially good at absorbing energy in impacts while keeping the peak force below a level that would cause damage. They will always give a lower peak force than a non-foam solid of the matrix material (Gibson & Ashby, 1997). The buckling and collapse of cells can allow a large amount of energy to be absorbed at a near constant load (Gibson & Ashby, 1997). A number of mechanisms can be at work when a foam is absorbing energy. Some relate to the elastic deformation of the cells while others depend on the compression or flow of the fluid within the cell walls (Gibson & Ashby, 1997). So the behaviour of a particular foam depends on the cell wall material; it also depends on whether there are open cells so that they are interlinked or closed cells so that the cells are isolated (Schwaber, 1973).

In order for rubbery foams have component modelling done in Finite Element Analysis for example, appropriate constitutive laws are required. Such material models usually need to describe elastic behaviour up to large deformations; this is the principal subject of the present work. Such constitutive laws should give physically plausible and accurate stress and dimensional changes for a wide variety and range of deformations in compression and tension up to around 100% strain. A material needs to be characterised throughout a wide range of modes of deformation and combinations of these modes in order to properly simulate conditions a component will encounter. For example a seat cushion will be subject to compression but will also experience deformation in tension at the edges of the loaded area. Published data up to these large strains for rubbery foam is limited and often of indifferent quality. One set of data found in the open literature covering a range of modes of deformation for foam is that of Blatz & Ko (1962). Further work has been done by Storåckers (1986) on two vulcanised foam rubbers for the same mode of extension and compression over a wide range of deformation. Gent & Thomas (1959, 1963) also performed simple, uniaxial,

extension and compression experiments on natural rubber foams. More recently tests were carried out on two types of polyurethane foam by El-Ratal & Mallick (1996), Mills & Gilchrist (1997) also tested polyurethane foam. The same authors also attempted macroscopic modelling of foams. Gibson & Ashby (1997) carried out extensive work on rubbery foams and many other related cellular solids including cork, wood and bone.

There is generally thought to be a marked and abrupt change in behaviour in compression, probably associated with a marked reduction in Poisson's ratio in turn associated with cell buckling (Dienes & Solem, 1999; Mills, 2007; Gibson & Ashby, 1997). When the foam is made from suitably rubbery material such presumed buckling does appear recoverable (Gent & Thomas, 1959, 1963). Other authors have performed particular experiments on auxetic materials – materials exhibiting negative Poisson ratios (Lakes, 1993; Alderson & Evans, 1997).

2 LITERATURE REVIEW

The main subject of the current dissertation is the behaviour of isotropic compressible elastic materials at finite strains, however any valid model of the behaviour of such materials must correspond to an infinitesimal strain model at such strains.

2.1 Elasticity at infinitesimal strains and the Poisson ratio (ν)

At infinitesimal strains in linear elastic materials, stresses are proportional to strains. Please see Figure 1.

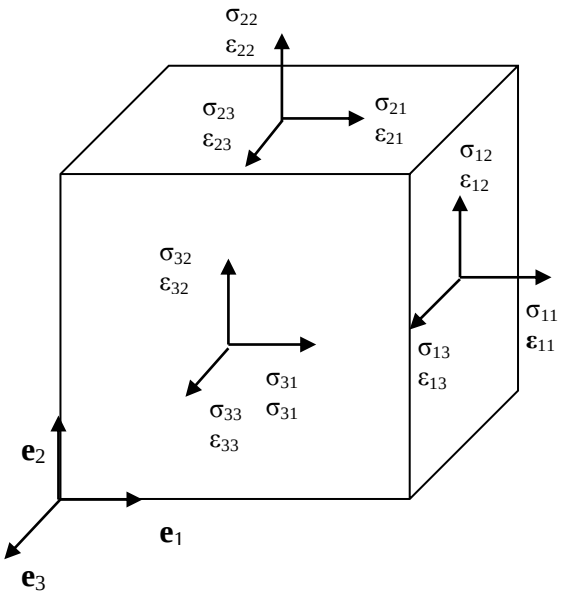

Figure 1. Unit vectors in the 1, 2 and 3 directions and conventional strain ε_{ij} and stress σ_{ij} components for a cuboid of material.

Linear elastic, isotropic solids, Hookean or Lamé solids, are characterised, at infinitesimal strains, by any two of the elastic constants: Λ, μ, K, E and ν (the 1st Lamé constant, the 2nd Lamé constant or shear modulus, the bulk modulus, the Young modulus and the Poisson ratio). The constants relate stresses to strains; the Poisson ratio can also be used to relate principal strains (ε_i) to each other. The Poisson ratio is best known for relating lateral strain to simple extension; more generally ν gives the strain in the 3rd direction if the other two strains are specified in general biaxial strain under plane stress conditions. Consider a cuboid of material aligned with the direction of principal strain (so that $\varepsilon_{ij} = 0$, $i \neq j$) if ε_{11} and ε_{22} are applied and faces in the 3 direction are stress free, ε_{33} (i.e. ε_3) is given by

$$\varepsilon_3 = \frac{-\nu}{1-\nu}(\varepsilon_1 + \varepsilon_2) \qquad (2.1)$$

(See Mars, 2006 and Appendix I.)

Schematic examples of modes of test are shown in Figure 2 and Appendix II .

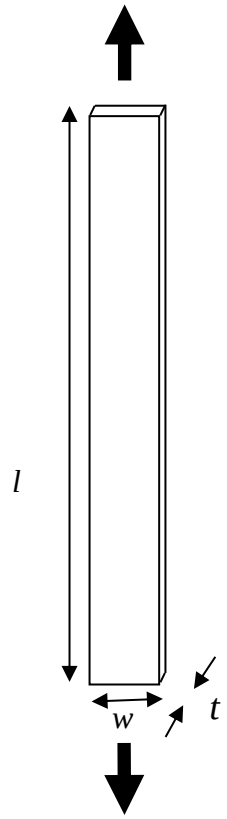

a. Simple extension
($l >> w$; $l >> t$)

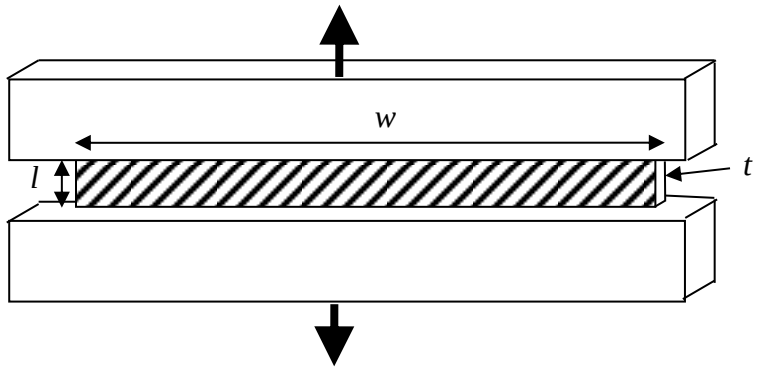

b. Fixed width or planar extension
($w >> l > t$ to minimise end effect)

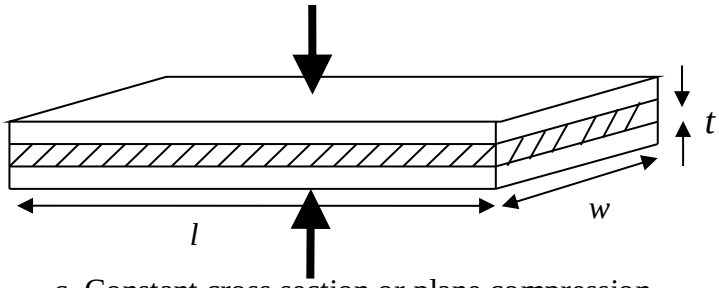

c. Constant cross section or plane compression
(l &$w >> t$ and bonded to rigid plates)

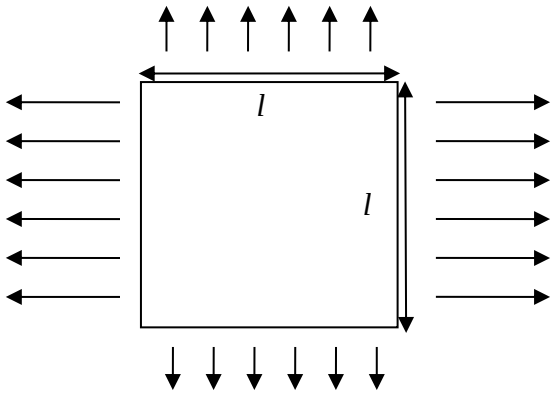

d. General biaxial extension

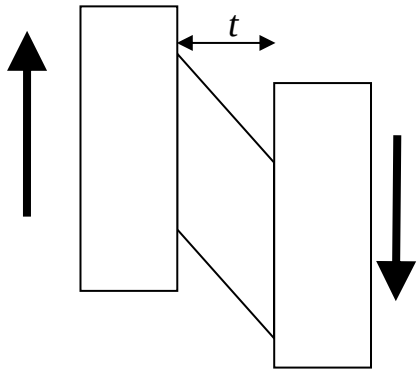

e. Simple shear
(l & $w >> t$ and bonded to plates - see (c))

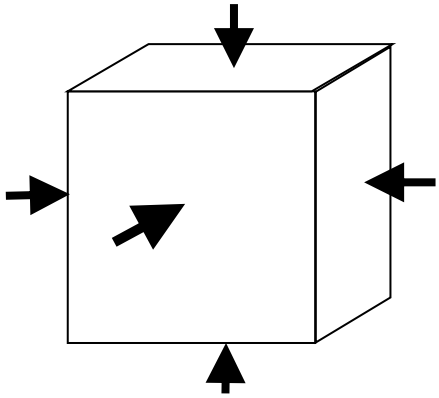

f. Pure volume decrease

Figure 2. Modes of test for material properties (schematic)

Although most solids have Poisson ratios of around 0.3, $-1 < \nu < ½$ is generally accepted as being the permissible range in principle for isotropic solids (Mott & Roland, 2009 and 2013; Greaves et al, 2011); *K* falls to zero at the lower limit and rises towards infinity at the upper. Clearly, neither the lower nor the upper limit can be reached for any real material, nevertheless the upper limit gives an idealisation widely-used in rubber modelling (Treloar, 1975; Rivlin, 1992). The range $0 \leq \nu < ½$ corresponds to "non-auxetic" and $-1 < \nu < 0$ to "auxetic" behaviour - see Gibson & Ashby (1997) and Alderson & Evans (1997) for example). By considering several modes deformation Mott & Roland (2009 and 2013) argue that the non-auxetic range should be further divided and that all normal isotropic elastic solids, to which the Lamé framework of elasticity is applicable, have $1/5 \leq \nu < ½$.

2.2 Finite deformations

2.2.1 Measures of finite deformation

In what follows **F** is the deformation gradient $\partial\mathbf{x}/\partial\mathbf{X}$ or $F_{ij} = \dfrac{\partial x_i}{\partial X_j}$ in component form (Holtzapfel, 2000; Bower, 2009); **X** and **x** are material and spatial coordinates respectively – corresponding to the reference configuration and the current configuration .

For isotropic materials that are elastic up to finite strains, deformation is usually measured using one of the following (Rivlin, 1992; Holzapfel 2000; Treloar 1976).

(a) The principal scalar invariants (I_1, I_2, I_3) of the Cauchy-Green deformation tensor, right (**C)** or, here, left (**B**, sometimes written **b)**; Holtzapfel (2000), Oden (1972, 2000), Rivlin (1992), Bower, 2009.

(b) The eigenvalues ($\lambda_1^2, \lambda_2^2, \lambda_3^2$) of **B (**or **C)** or their square roots, the principal extension ratios or stretches (Eihlers & Eipper, 1998; Storåckers, 1986; Bruhns et al, 2001; Bower, 2009).

(c) Simple rearrangements of (a) such as the volume ratio $J = \sqrt{I_3}$ and invariants of "volume neutralised" **B** and **C**, $\overline{\mathbf{B}} = J^{-2/3}\mathbf{B}$ and $\mathbf{C} = J^{-2/3}\overline{\mathbf{C}}$ i.e. invariants modified to remain unchanged for pure volume change ($\bar{I}_1$ and $\bar{I}_2$) – see Penn (1970), Treloar (1975), Ehlers & Eipper (1998), Gough et al (1999) or Bower (2009) for example. *(d)* Simple rearrangements of (b) such as the natural logarithmic or Hencky strains (principal values $e_i = \ln \lambda_i$) or the volume neutralised principal extension ratios (Simo & Taylor, 1991; Gough et al, 1999; Bruhns et al, 2001).

In the above the principal extension ratios and first two principal invariants volume neutralised can of course be obtained from the volume neutralised $\overline{\mathbf{F}} = \mathbf{F}/J^{1/3}$. Please see Appendix III for more details.

2.2.2 Modelling of elastic behaviour at finite strain and the definition of the Poisson index (υ)

What is called herein the Poisson index (υ) is a finite strain version of the Poisson ratio relating logarithmic strains ($e_i = \ln \lambda_i$) – please see Blatz & Ko, 1962; Ogden, 1972a). As Ogden (1972b) points out, υ will, in general, be a function of the deformation – see also: Alderson et al (1997); Pierron, 2010). There is disagreement between various authors on the extent to which υ varies with deformation of rubbery foams; some workers indicate that υ varies little if at all with extension (Blatz & Ko, 1962; Storåckers, 1986) – others indicate that υ varies by a surprisingly large amount: El-Ratal & Mallick (1996) and see later in this dissertation.

Using Kirchoff stress (Bruhns et al, 2001) some authors use the direct Hencky, (1928) approach to extend the equations of isotropic elasticity at infinitesimal strain to calculate the stresses at finite strains via logarithmic strain (e_i). $e_i = \ln(\lambda_i)$. Some other models, such as the Blatz & Ko form of constitutive law (please see below and Blatz & Ko, 1962) or Ogden's model that has come to be known as the hyperfoam model as usually implemented also use the Poisson index (υ) and assume that it can be regarded as a constant (Storåckers, 1986.).

Chagnon & Coveney (2008, 2011) argue that irrespective of whether υ is constant or not, it can be defined for a particular state of strain, if faces in the 3 direction are stress free, by

$$e_3 = \frac{-\upsilon}{1-\upsilon}(e_1 + e_2) \qquad (2.2a)$$

or

$$\lambda_3 = (\lambda_1 \lambda_2)^{\frac{-\upsilon}{1-\upsilon}} \qquad (2.2b)$$

Please see Figure 1.

It should be noted, though, that such a definition hypothesises that aspects of the Hencky (1928) approach are appropriate for the material being modelled.

As the logarithmic principal strains (e_i) become smaller they tends towards the infinitesimal principal strains ε_i, so at infinitesimal strain the Poisson index υ equals the Poisson ratio (ν).

2.3 Forms of constitutive law for rubbery materials – treated as isotropic and elastic up to large strains

2.3.1 Rubbery materials without voids

Solid rubbery materials are described as near incompressible because the bulk modulus (K) is very large compared with the shear modulus (μ). It is usual to assume that a Helmoltz free energy function (W) of the deformation gradient (**F**) can be used to describe them:

$$W = W(\mathbf{F}) \qquad (2.3)$$

W, also known as the strain energy density, is defined per unit volume in the reference configuration (Rivlin, 1992; Gough et al, 1999; Holtzapfel, 2006). Treating rubber as incompressible, Rivlin (1948, 1992) used symmetry to argue that because W is a function of the deformation gradient it must also be a function of the first two principal invariants of the left or the right Cauchy-Green deformation tensor **B** or **C**:

$$W = W(I_1, I_2) \qquad (2.4)$$

So the current view is that the strain energy density of any isotropic elastic incompressible material can be described by equation 2.4 and the stresses found from its derivatives – as explained by Rivlin (1948, 1992), Rivlin & Sawyers (1976), Holzapfel (2006), Bower (2009) and elsewhere.

Maclaurin expansion gives what has come to be known as the Rivlin series form of constitutive law (Rivlin & Saunders, 1951):

$$W = \sum C_{ij} (I_1 - 3)^i (I_2 - 3)^j \qquad (2.5)$$

If $\partial W/\partial I_1$ and $\partial W/\partial I_2$ are taken to be constants $C_{10} = C_1$ and $C_{01} = C_2$ respectively, equation 2.5 simplifies to the Mooney, or Mooney-Rivlin, form:

$$W = C_1(I_1 - 3) + C_2(I_2 - 3) \qquad (2.6)$$

Here $2C_1 + 2C_2 = \mu$, the shear modulus. If $\partial W/\partial I_2$ is taken to be zero, equation 2.6 simplifies to the neo-Hookean form (Treloar, 1975):

$$W = \frac{\mu}{2}(I_1 - 3) \qquad (2.7)$$

Equation 2.7 is also given by the Gaussian statistical theory of rubber elasticity with μ proportional to absolute temperature (Treloar, 1975). In the neo-Hookean form, the stresses associated with shape changes are calculated with knowledge of just one material constant: the shear modulus μ – as is the case at infinitesimal strains.

Rivlin & Sawyers (1976) "advance the view that if one adopts the position that W is a function of I_1 and I_2, then, from the viewpoint of the numerical solution of boundary value

problems, the fitting of these experimental results by an algebraic expression for W is, in large measure, an empty exercise… Indeed, if the solution of the problem involves the use of a computer, one could just as well take the experimentally determined dependence of $\partial W/\partial I_1$ and $\partial W/\partial I_2$ on I_1 and I_2 as a constitutive input to the problem."

The experimental investigation of how $\partial W/\partial I_1$ and $\partial W/\partial I_2$ depend on I_1 and I_2 has centred on general biaxial extension of sheets of rubber in the plane stress condition (see Figure 2). Treloar (1975) shows, for an incompressible material, the loci of simple extension /compression, equibiaxial extension/compression and fixed width extension/compression on the I_1, I_2 plane. The loci are replotted in Figure 3. The curves of simple extension /compression and equibiaxial extension/compression give the boundaries of what are possible values of I_1, and I_2 for general biaxial extension. Note that, as expected the loci for simple extension/compression, equibiaxial extension/compression merge in to that for fixed width extension/compression as the values of I_1 and I_2 approach 3.

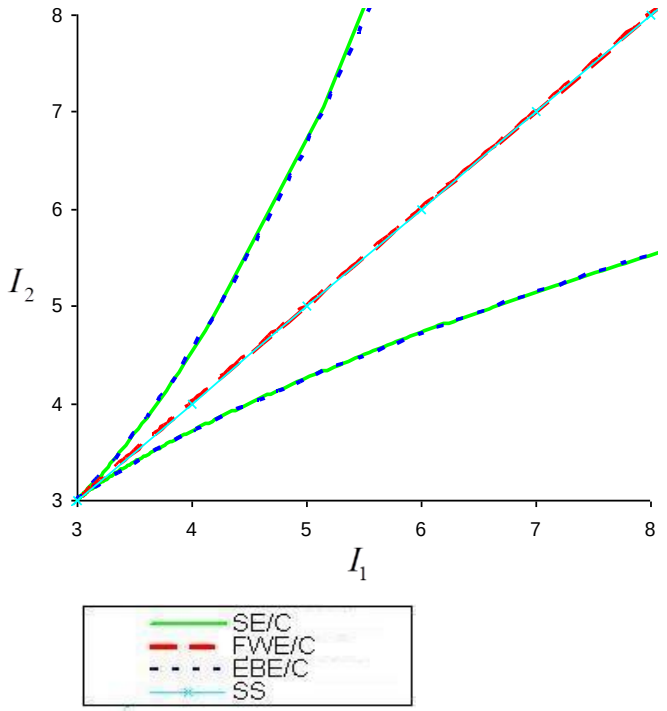

Figure 3. Loci of simple extension/compression (SE/C), equibiaxial extension/compression(EBE/C), fixed width extension/compression(FWE/C) and simple shear (SS) for an incompressible material on the I_1, I_2 plane.

Gent & Rivlin (1951), Rivlin (1992) and Gough et al (1999) have discussed the experimental evidence on how W or rather $\partial W/\partial I_1$ and $\partial W/\partial I_2$ for rubbery materials without voids depend on I_1 and I_2. All three publications make it clear that wherever it is possible to distinguish well between $\partial W/\partial I_1$ and $\partial W/\partial I_2$, because strains are sufficiently large, $\partial W/\partial I_1$ is at least five times larger than $\partial W/\partial I_2$. Gent & Rivlin (1951) suggest, on the basis of their data and the data of others, that $\partial W/\partial I_2$ is associated with energy dissipation and speculate that structurally it may be associated with some form of secondary, relatively fragile reformable, crosslinks. Kawabata (1973) performed plane stress general biaxial measurements on natural rubber and SBR (styrene-butadiene rubber) materials over a temperature range of 20 to 100 °C. He found that $\partial W/\partial I_1$ was approximately proportional to absolute temperature (see equation 2.7) but

that $\partial W/\partial I_2$ was substantially temperature independent. He found that the relaxation behaviour of $\partial W/\partial I_2$ closely resembled that of $\partial W/\partial I_1$ and that the relaxation time was almost the same.

Gough et al (1999) warned that the common practice of applying conditioning cycles of deformation to a test piece may produce anisotropy. They say that their data and the data of others for a number of practical rubbery materials is consistent with $\partial W/\partial I_2$ being zero but not for one material. They point out that when strains are insufficiently large it is no longer possible to distinguish between I_1 and I_2.

Edwards & Vilgis (1986) have proposed modifying the Gaussian statistical theory of rubber elasticity to allow for chain slippage at small strains and to account for stiffening at large strains via the tube concept.

Because the role of $\partial W/\partial I_2$ is, at most, less important than that of $\partial W/\partial I_1$ in rubber elasticity and because dropping $\partial W/\partial I_2$ in a model gives benefits, a number of authors have decided to do this, including: Yeoh (1990), Arruda & Boyce (1993), Davies et al (1994), Gent (1996) and Marlow (2003) who proposes direct use of experimental results for $W(I_1)$ in finite element analysis. Some of these approaches seem to work well – see Boyce & Arruda (2000) for example.

A number of authors, including Mooney (1940), Carmichael & Holdaway (1961) and Valanis & Landel (1967) have hypothesised that W can be expressed as a sum of functions of the principal extension ratios, or their squares:

$$W = w(\lambda_1) + w(\lambda_2) + w(\lambda_3) \qquad (2.8)$$

Rivlin & Sawyers (1976) showed that forms of W conforming to equation 2.8, the "Valanis-Landel" hypothesis, imply that the dependence of W on I_1 and I_2 conforms to the following:

$$\frac{\partial}{\partial I_1}\left(\frac{\partial^2 W}{\partial I_1^2} + I_1\frac{\partial^2 W}{\partial I_1 \partial I_2}\right) = -\frac{\partial}{\partial I_2}\left(\frac{\partial^2 W}{\partial I_2^2} + I_2\frac{\partial^2 W}{\partial I_1 \partial I_2}\right) \qquad (2.9)$$

As pointed out by Gough et al (1999) strain energy density functions conforming to the Valanis-Landel hypothesis have "been found to work well in practice, at least for unfilled rubber up to moderately large strains [by] Obata et al, 1970; Valanis & Landel, 1967; Jones & Treloar, 1975; Ogden, 1972". However, they go on to point out that Gent's (1996) strain energy density function (designed for use up to high strains) does not conform to equation (2.9). The same will be true of any strain energy density function which has $\partial W/\partial I_2 \equiv 0$ but which includes high powers of I_1 .

w in equation 2.8 may, in turn, be expanded as a series of integer powers of λ_i (Mooney, 1940) or as a general power series (Ogden, 1972a):

$$W = \sum \frac{\mu_i}{\alpha_i}\left(\lambda_1^{\alpha_i} + \lambda_2^{\alpha_i} + \lambda_3^{\alpha_i} - 3\right) \qquad (2.10)$$

Here the powers, α_i can be have any real value. Note that some authors use eigenvalues of **B** in the Ogden series; these are the squares of the principal extension ratios but also often written λ_i.

If there is still debate about the possible role of I_2 and its origin and about the suitability of the Valanis-Landel hypothesis there is further debate about how best to represent the compressibility of rubbery materials without voids.

If the ideal, isotropic elastic material is compressible, equation 2.3 gives (Rivlin, 1992; Bower, 2009)

$$W = W(I_1, I_2, I_3) \qquad (2.11a)$$

[note that the use of W on the right hand of each of equations 2.3, 2.4, 2.11a, 2.11b means that the strain energy density is a function of the variables written but <u>not</u> that the functional is the same in each case.]

or equivalently, but with different C_{ijk}

$$W = W(\bar{I}_1, \bar{I}_2, J) \qquad (2.11b)$$

Maclaurin series expansion gives (Oden, 1972, 2000):

$$W = \sum C_{ijk} (I_1 - 3)^i (I_2 - 3)^j (I_3 - 3)^k \qquad (2.12a)$$

or equivalently

$$W = \sum C_{ijk} (\bar{I}_1 - 3)^i (\bar{I}_2 - 3)^j (J - 3)^k \qquad (2.12b)$$

The Cauchy stress can be found by using a formula such as the following – see Appendix IV or Chagnon (2003) or Bower (2009) for example:

$$\boldsymbol{\sigma} = \frac{2}{J}\left[\overline{\mathbf{B}} - \frac{1}{3}\bar{I}_1\mathbf{I}\right]\frac{\partial W}{\partial \bar{I}_1} + \frac{2}{J}\left[\bar{I}_1\overline{\mathbf{B}} - \overline{\mathbf{B}}^2 - \frac{2}{3}\bar{I}_2\mathbf{I}\right]\frac{\partial W}{\partial \bar{I}_2} + \frac{\partial W}{\partial J}\mathbf{I} \qquad (2.13)$$

Rivlin (1992) emphasises the difficulty in experimental determination for equations 2.11 or 2.12 if there are no simplifications; this is because $\partial W / \partial \bar{I}_1, \partial W / \partial \bar{I}_2$ and $\partial W / \partial J$ can each be functions of $\bar{I}_1, \bar{I}_2$ and J. A widely used simplification suggested by Flory (1960; see also Gough et al, 1999) is to separate W into an isochoric part purely due to shape change (W_s) and a dilational part purely due to volume change (W_v):

$$W = W_s(\bar{I}_1, \bar{I}_2) + W_v(J) \qquad (2.14a)$$

or equivalently

$$W = W_s(\bar{\lambda}_1, \bar{\lambda}_2) + W_v(J) \qquad (2.14b)$$

Note that $\bar{\lambda}_1\bar{\lambda}_2\bar{\lambda}_3 \equiv 1$ so that any two of $\bar{\lambda}_1, \bar{\lambda}_2, \bar{\lambda}_3$ can be used.

Forms conforming to equation 2.14(a) can be called shape-volume uncoupled – e.g. in equation 2.14 $\partial W_v / \partial \bar{I}_1 = \partial W_v / \partial \bar{I}_2 = \partial W_s / \partial J = 0$.

Blatz & Ko (1962) put forward the following form that is a modification of the Mooney form (equation 2.6) allowing for compressibility via a constant Poisson index (υ):

$$W = C_1\left[I_1 - 3 + \frac{1-2\upsilon}{\upsilon}\left(J^{-2\upsilon/(1-2\upsilon)} - 1\right)\right] + C_2\left[\frac{I_2}{J^2} - 3 + \frac{1-2\upsilon}{\upsilon}\left(J^{2\upsilon/(1-2\upsilon)} - 1\right)\right] \qquad (2.15)$$

where $C_1 + C_2 = \mu/2$ – please see Treloar (1975) and equations 4.2.2 and 4.2.18.

The volume neutralised principal invariants are

$\bar{I}_1 = J^{-2/3} I_1$ and $\bar{I}_2 = J^{-4/3} I_2$

so we can write

$$W = C_1\left[J^{2/3}\bar{I}_1 - 3 + \frac{1-2\upsilon}{\upsilon}\left(J^{-2\upsilon/(1-2\upsilon)} - 1\right)\right] + C_2\left[J^{-2} J^{4/3}\bar{I}_2 - 3 + \frac{1-2\upsilon}{\upsilon}\left(J^{2\upsilon/(1-2\upsilon)} - 1\right)\right]$$

or

$$W = C_1\left[J^{2/3}\bar{I}_1 - 3 + \frac{1-2\upsilon}{\upsilon}\left(J^{\frac{-2\upsilon}{1-2\upsilon}} - 1\right)\right] + C_2\left[J^{-2/3}\bar{I}_2 - 3 + \frac{1-2\upsilon}{\upsilon}\left(J^{\frac{2\upsilon}{1-2\upsilon}} - 1\right)\right] \qquad (2.16)$$

Equation 2.16 shows the Blatz & Ko equation in a way that emphasises that there is a particular sort of coupling between shape changes and volume changes in the calculation of *W*.

Penn (1970) measured volume change of rubber in simple extension and found that the results were not consistent with shape-volume separation in the strain energy density (equation 2.14). Ogden (1972b) referred to Penn's work (1970) to argue in favour of the type of shape-volume coupling used in the Blatz & Ko model (equation 2.16). Gough et al (1999) however said that the experimental errors in Penn's (1970) measurements of volume change were such that shape-volume separation could not be refuted on the basis of his data. They do, though, argue for a form of W_v that is an uneven function of (J-1) and that "rises towards infinity as it must when the volume approaches zero". Ehlers & Eipper (1998) on the other hand find that shape-volume uncoupled models can lead to unrealistic behaviour with cross-section *increasing* at high degrees of simple extension and *decreasing* at high degrees of simple compression. The volume of natural rubber increases slightly at simple extensions up to about 100% but decreases at strains of hundreds of percent, because of crystallisation, where the nominal Poisson index will therefore exceed ½ (Ogden, 1972b; Treloar, 1975). According to Ogden (1972b) at $\lambda_1 = 8$, $J = 0.98$

Now $J = \lambda_1 \lambda_2 \lambda_3 = \lambda\, \lambda^{-\upsilon}\, \lambda^{-\upsilon} = \lambda^{1-2\upsilon}$ $\quad\therefore\quad \upsilon = \frac{1}{2}\left(1 - \frac{\ln J}{\ln \lambda}\right) = 0.505$ (2.17)

2.3.2 Rubbery foams and other highly compressible materials

If there is some question about whether shape-volume coupling is necessary for rubbery materials without voids, for highly compressible rubbery materials (e.g. rubbery foams) shape-volume coupling seems difficult to argue against – especially if they are likely to undergo large deformation in compression as well as in extension. Equations 2.11 and 2.12 show the general descriptions but, as stated above, consideration of the dependence of *W*, or its three derivatives, in $\bar{I}_1, \bar{I}_2$ and J space would be a major undertaking, perhaps because of this, the Blatz & Ko form (equations 2.15 and 2.16) and what is now known as the hyperfoam form (Ogden, 1972b; Hill, 1978; Storåckers, 1986; Mills & Gilchrist, 2000a)

$$W = \sum_i \frac{2\mu_i}{\alpha_i^2}\left[J^{\alpha_i/3}\left(\bar{\lambda}_1^{\alpha_i} + \bar{\lambda}_2^{\alpha_i} + \bar{\lambda}_3^{\alpha_i}\right) - 3\right] + \sum_i \frac{2\mu_i}{\alpha_i^2 \beta_i}\left[J^{-\alpha_i \beta_i} - 1\right] \qquad (2.18)$$

are widely used. Of the constants, α_i and β_i can take any real value, the initial shear modulus $\mu_0 = \sum_i \mu_i$ also $\beta_i = \frac{\upsilon_i}{1-2\upsilon_i}$ so multiple constant (sub) Poisson indices can, in principle, coexist. However, in practice, a single constant Poisson index is generally chosen (Storåckers, 1986; Mills & Gilchrist, 2000a and see below). It can be seen that the hyperfoam form is a generalisation of the Blatz & Ko form – please see equation 2.16 and Storåckers (1986) for example.

2.4 Existing sets of data for rubbery foam and micromechanical models

Blatz & Ko (1962), Blatz (1963) tested a polyurethane rubbery foam - or rubbery solid with pores - with a fraction of rubber by volume of the foam (Φ) of 0.53; unlike some polyurethane foams this one was more likely to be isotropic because of the way it was made (Blatz & Ko, 1962; Gibson & Ashby, 1997). The material was tested in simple, equibiaxial and fixed-width extensions. Their method implied that equation 2.2 was being used. Their data shows little scatter and a value of $\upsilon = 0.25$ was obtained, by means of particularisations of equation 2.2. After having decided that υ should be 0.25 Blatz & Ko went on to compare the stresses given by their equation (equation 2.15) to the measured stresses. They came to the surprising conclusion from this comparison that C_1 in equation 2.15 was small and could be ignored and so arrived at what has come to be known as the Blatz-Ko form of strain energy density function implemented in some commercial Finite Element Analysis software (Bower, 2009).

Storåckers (1986) questioned the results of Blatz & Ko (1962) and obtained $\upsilon = 0.32$ from for simple, equibiaxial and fixed-width extension of a natural rubber (NR) foam and $\upsilon = 0.49$ for (b) an EPDM (ethylene-propylene-diene) rubber foam. His method implied that equation 2.2 was being used. The value of υ for NR foam is well within the expected range but the value for the EPDM foam seems high. Storåckers said only that the NR foam was highly compressible and the EPDM foam was slightly so. Unfortunately Storåckers preconditioned his materials by applying cycles of deformation prior to his tests (please see above and Gough et al, 1999). Like Blatz & Ko (1962) strains of up to 50 or 100% were attained in Storåckers' tests.

Gent & Thomas (1959, 1963) described a simple micromechanical model, for an idealised open cell rubbery foam, of strands of rubber; a Poisson ratio (ν) of ¼ was predicted. They performed simple (uniaxial) extension experiments on 15 natural rubber latex foams of volume fractions (rubber volume divided by foam volume) Φ varying from 0.093 to 0.568, checking that the rubber matrices were all similar. The method of manufacture of the foams meant that the foams were likely to be essentially isotropic (Gent & Thomas,1959, 1963).They measured ν at about 10% simple extension as 0.33 ± 0.04; their set of data suggested that ν did not vary with Φ. Gibson & Ashby (1982) described a relatively simple micro-mechanical model for open and closed cell foams. Gibson & Ashby's model, based on bending of members, predicted a ν of 0.33. The experimental results of Gent & Thomas (1959, 1963), Gibson & Ashby (1982, 1997) and others covering a very wide range of Φ together with the model of Gibson & Ashby pointed to ν for open and closed cell foams varying little for "all values" of Φ, i.e. up to $\Phi = 0.6$ at least; the combined experimental results Gibson & Ashby (1982, 1997) presented showed considerable scatter but "there is no systematic variation with density [relative density i.e. Φ]..The average value is about 1/3." A graph summarising published experimental data for ν against Φ is shown in Figure 4. Some of Gibson & Ashby's (1982) results fell outside the range of ν for normal materials, but they did not comment on this. They did not state at what strain or strains they made the Poisson ratio measurements.

Results presented by Gent & Thomas (1959) included plots of, presumed, nominal stress against engineering strain ($\varepsilon = \lambda - 1$) in simple extension and also for, nominal, simple compression for test pieces of natural rubber latex foam of $\Phi = 0.125$. λ was from 0.6 to 1.15. The plot of stress against λ is essentially linear in extension but shows a sudden drop in tangential stiffness (slope of the graph) at small compressive strain (i.e. between $\lambda \approx 1$ and 0.97). Such behaviour is thought to be associated with the onset of buckling of the cell walls or ligaments in the foam (Gent & Thomas, 1959; Gibson & Ashby, 1997).

There have been many publications on attempts at micromechanical modelling of rubbery foam since 1963, Gong et al (2005a&b) reviewed some of this work as well as producing their own micromechanical models of increasing complexity and performing some physical experiments – unfortunately all the experiments were on anisotropic foams. It is noted that the modelling results of Gong et al (2005a) for isotropic foam predicted that ν will tend towards 0.5 as Φ tends towards zero (please see Figure 4). Gan et al (2005) have also reviewed micromechanical modelling of solid foam and also produced a model that predicted that ν will tend towards 0.5 as Φ tends towards zero. Neither sets of authors commented on the fact that this prediction differed from the predictions of other models and from what most of the published experimental data seem to show.

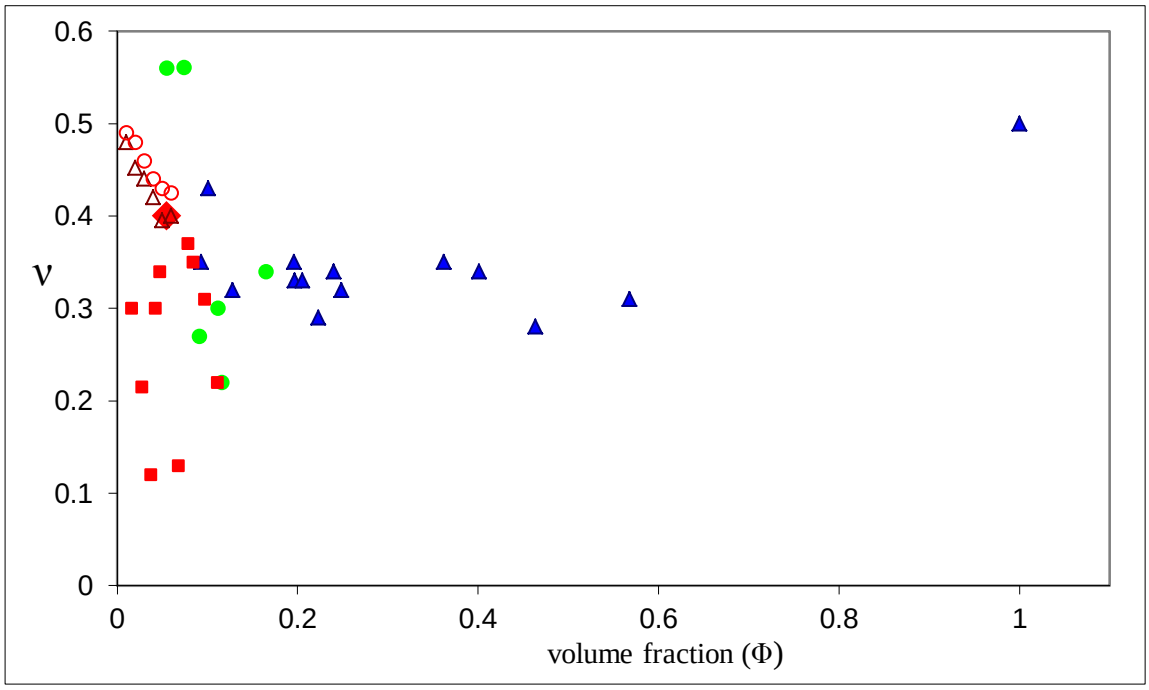

▲ Gent & Thomas (1959) natural rubber latex; ▮ Gibson & Ashby (1982) polyurethane;
♦ Lakes (1987) polyurethane; ● Gibson & Ashby (1982) polyethylene;
Gong et al (2005) mathematical models with uniform (○) and (△) non-uniform cross sections.

Figure 4. Poisson's ratio (ν) versus volume fraction (Φ) for a range of real and modelled foams.

As indicated above, Blatz & Ko (1962) and Storåckers (1986) found that υ did not vary with simple extension, equibiaxial extension and fixed width deformation. El-Ratal & Mallick (1996) performed simple extension tests on (a) a "seat foam" and (b) a "commercial foam" – both polyurethane. For foam (a) they found that υ at $\lambda = 1.1$ was about 0.25 but at $\lambda = 1.4$, υ was approximately 0.6. For foam (b) υ at $\lambda = 1.1$ was about 0.35 but at $\lambda = 1.4$, υ was approximately 0.75. These high values of υ correspond to volume ratios (J) as low as 0.8 in simple extension (equation 2.17). Such volume reductions seem surprising but may be possible for rubbery foams at such extensions.

As just described, there is some doubt about whether the Poisson index (υ) can be considered constant in extension. However, notwithstanding the findings of Gibson & Ashby (1982), there seems to be a consensus that υ does vary considerably in compression. Gibson & Ashby (1982) reported measuring the Poisson ratio (ν) in tension and compression. However they did not report that values differed depending on whether the test piece was in tension or compression. They stated that, in agreement with their theory, there was no systematic variation of ν with density and that the average value was about 1/3. However, Mills & Gilchrist (2000a) stated "For an open cell foam under uniaxial compression, it is a reasonable approximation that the Poisson's ratio $\nu = 0$ [Poisson index, $\upsilon = 0$]". They tested a polyether polyurethane foam with a density of 38kg/m^3. Their compressive stress-strain plot shows a sharp reduction in tangential stiffness at compressive strains of a few percent – presumably

associated with buckling of cells; the two-term hyperfoam form (equation 2.18) does not represent this feature well, showing that it would be difficult to model extension *and* compression. Mills & Gilchrist (2000a) went on to state "when uniaxial compression and simple shear data were entered, the [commercial Finite Element Analysis] program could not find a convergent fit to the data either for $N = 1$ or 2 [single term or two term hyperfoam form]". Pierron (2010) tested a "standard low density polyurethane foam" with a density of 30kg/m^3. Under conditions approximating to simple compression Pierron's data shows a steep plunge in a tangential, or incremental, Poisson ratio (ν_t) as extension ratio λ decreased, between $\lambda = 1$ and 0.95. Despite some increase in ν_t on further compression, it was still negative when compression ended at $\lambda \sim 0.2$.

A principal observation in Pierron's work was the prevalence of localised behaviour, including the propagation of zones associated with particular ranges of ν_t through the material. He states "Here, the compression process starts where the load is introduced (top and bottom edges) which is consistent with observations from (2) and then propagates in bands towards the centre. This results in highly heterogeneous strain maps. This was reported in (1) on a very similar foam. ..buckling elastic collapse of whole rows of cells by buckling of the cell walls." Gent & Cho (1999) and Gent (2005) discuss surface instabilities in rubber without voids; for the material without voids such instabilities are predicted to form in a rubber test-piece in simple compression or in bending when $\lambda = 0.444$ has been reached. However instabilities were observed by Gent & Cho (1999) at $\lambda = 0.65$ in bending of rubber without voids.

2.5 The work of Chagnon & Coveney (2008, 2011)

In unpublished work, Chagnon & Coveney (2008, 2011) used equations 2.2 and 2.13 together to obtain the following expression for the class of forms of model of isotropic elastic material in which compressibility is expressed by the Poisson index (υ) – as discussed by Ogden (1972b) and Hill (1978):

$$\frac{\partial W}{\partial J} = \frac{2}{J}\left[\left(\frac{\bar{I}_1}{3} - J^{-r}\right)\frac{\partial W}{\partial \bar{I}_1} - \left(\frac{\bar{I}_2}{3} - J^{r}\right)\frac{\partial W}{\partial \bar{I}_2}\right] \qquad (2.19)$$

where $r = \frac{2}{3} \cdot \frac{1+\upsilon}{1-2\upsilon}$.

For infinitesimal strains, $r = K/\mu$ because $\nu = \frac{3K - 2\mu}{2(3K + \mu)}$.

So equation 2.19 is a finite strain version of the small strain equation relating bulk modulus, Poisson ratio and shear modulus (K, ν, μ). At finite strains, though, the shear modulus can have two parts $2\partial W/\partial \bar{I}_1$ and $2\partial W/\partial \bar{I}_2$ and they, υ and $\partial W/\partial J$ are, in general, functions of $\bar{I}_1, \bar{I}_2$ and J. Using equation 2.19 Chagnon and Coveney generated the Blatz & Ko form (equation 2.15 or 2.16) that is a modified Mooney first order form. They then generated a third order polynomial form, in which $\bar{I}_2$ does not appear, that is a modified Yeoh (1990) form: the BKY form. They tried to fit the BKY form to Gent & Thomas' (1959) combined

simple extension and compression data for a $\Phi = 0.125$ natural rubber latex foam. Similarly to the difficulties Mills & Gilchrist (2000a) experienced with the hyperfoam form, with the BKY form Chagnon & Coveney (2008, 2011) were unable to obtain an acceptable fit to the combined extension-compression data and concluded that this was almost certainly due to rather abrupt changes in the Poisson index when λ is less than but close to 1.

Note that equation 2.19 can be used to modify Cauchy stress equation 2.13 for this class of forms to (Chagnon & Coveney, 2011):

$$\boldsymbol{\sigma} = \frac{2}{J}\left[\overline{\mathbf{B}} - J^{-r}\mathbf{I}\right]\frac{\partial W}{\partial \bar{I}_1} + \frac{2}{J}\left[\bar{I}_1\overline{\mathbf{B}} - \overline{\mathbf{B}}^2 - \bar{I}_2\mathbf{I} + J^{r}\mathbf{I}\right]\frac{\partial W}{\partial \bar{I}_2} \qquad (2.20)$$

2.6 General discussion

Regarding

(i) the direct Hencky (1928) approach,

(ii) the Blatz & Ko equation (equation 2.15 or 2.16),

(iii) generalisations of the Blatz and Ko approach suggested by Chagnon & Coveney (2008, 2011)

and (iv) the hyperfoam form as normally applied,

none are general descriptions for an ideal, isotropic elastic material (in contrast to $W = W(\underline{F})$ or $W = W(\lambda_1, \lambda_2, \lambda_3)$ or equation 2.11). All of (i) to (iv) explicitly or implicitly use equation 2.2. This means that one of the ways in which (i) – (iv) are not general is that if, under plane stress conditions, $\lambda_1\lambda_2 = 1$ then $\lambda_2 = 1$.

It is not a given that a Poisson index (υ) approach is always valid or useful. However for normal isotropic rubbery foams there seems a general view that the Poisson ratio and so the Poisson index at almost zero strain is close to 0.33 for volume fractions of rubber in the range $\Phi = 0.01 - 0.6$ (please see above and Gibson & Ashby, 1982).

As Ogden (1972b) said, it would be convenient if the Poisson index υ could be taken to be constant. The data of Blatz & Ko (1963) and Storåkers (1986) points to υ being almost constant with strain for simple, equibiaxial and fixed-width extensions - although the value of υ given by Blatz & Ko from their data (1963) is surprising: 0.25. In contrast to Blatz & Ko (1962) and Storåkers (1986), El-Ratal & Mallick (1996) found that υ varied quite strongly with simple extension. There is clearer direct and indirect evidence that υ varies abruptly in simple compression.

In practical applications, rubbery foam is often subjected to extension, shear and compression but here seems to be lack of experimental data combining, for example, comprehensive shear, simple extension and simple compression data for the same rubbery foam in order that conclusions can be made about the variation of W and/or its derivatives and of υ with deformation. Gent & Thomas (1959) did give simple extension and compression data for the

same rubbery foam but did not give information on how volume varied with extension and compression – apart from giving the Poisson ratio as close to 0.33.

Regarding the question of $\partial W / \partial \bar{I}_1$ and $\partial W / \partial \bar{I}_2$, it would be convenient if one or other could be ignored for rubbery foams. Blatz & Ko (1962) suggested that $\partial W / \partial \bar{I}_1$ could be ignored for their foam – the opposite of what is often the case for rubbery materials without voids. However, Blatz & Ko's method of data analysis involved use of abscissae of $\lambda_1^{-2}\lambda_2^{-2}$; this gave strong emphasis to the higher deformations where a Mooney form is least likely to be applicable (see also, Treloar, 1975). On giving equal weightings at all levels of deformation Chagnon & Coveney (2008) found that setting $C_1 = 0$ in equation 2.16 "gave a particularly poor fit to Blatz & Ko's own data"; they found "a much improved fit was obtained with $C_1 \approx C_2$ in equation 2.16 and an almost equally good a fit was obtained with $C_2 = 0$". It should also be noted that Blatz & Ko (1962) and Storåkers (1986) reported no tests in compression.

It would be helpful if guidance regarding the behaviour of $\partial W / \partial \bar{I}_1$, $\partial W / \partial \bar{I}_2$, $\partial W / \partial J$ and υ in deformation could be obtained from micromechanical modelling of isotropic foams as well as physical tests on foams. Unfortunately, the results of some recent micromechanical modelling show serious differences with other evidence.

3 RESEARCH QUESTIONS, AIMS, OBJECTIVES & PLAN OF WORK

3.1 Key points from literature review in relation to this piece of work

(i) For isotropic hyperelastic modelling of rubbery materials without voids it seems clear, from investigations by Rivlin & Saunders, 1951) and others (Rivlin, 1992) that the importance of the derivative of the strain energy function (W) with respect to the second principal invariant of the Cauchy-Green deformation tensors ($\partial W/\partial I_2$) is minor compared to $\partial W/\partial I_1$.

(ii) As indicated previously, rubbery foams lack the array of comprehensive data sets published for finite deformation of unvoided rubbery materials.

(iii) Regarding the modelling of rubbery foam at small strains, Gibson & Ashby (1982) seem to be quite definite that the Poisson ratio of normal rubber foams should be close to 0.33. But there is considerable scatter in the summary data that Gent & Thomas (1959, 1963) and they present. Moreover, Blatz & Ko (1962) found their dense foam had a Poisson ratio (ν) of 0.25; El-Ratal & Mallick's (1996) data points to ν of a slightly lower value for a polyurethane "seat foam".

(iii) Concering (i) above but for rubbery foam, there is a general lack of information in the literature. Blatz & Ko (1962) indicate that for their relatively dense rubbery material $\partial W/\partial I_1$ is negligible, although their findings have been questioned by Storåckers, (1986) and by Chagnon & Coveney (2008).

(iv) The Poisson index (υ) is a particular finite strain version of the Poisson ratio (ν). The Blatz & Ko (1962) and hyperfoam (Ogden, 1972b; Storåckers, (1986); Mills & Gilchrist, 2000a) constitutive laws for rubbery foams use a constant Poisson index (υ) approach to describe the way in which the shape-dependent and volume-dependent parts of the constitutive laws are coupled. This feature gives attractive analogies with infinitesimal strain but means that both constitutive laws are not fully general.

(v) In modelling with the Blatz & Ko or hyperfoam forms the Poisson index (υ) is assumed constant (Blatz & Ko, 1962; Storåckers, 1986; Mills & Gilchrist, 2000a). It seems unlikely that υ is the same in compression as it is in extension, but in extension the results of Blatz & Ko (1962) and Storåckers (1986) point to constant υ. However, the simple extension results of El-Ratal & Mallick's (1996) show υ increasing from values at or below 0.33 at small strains to values well above ½ at large strain.

3.2 Research questions arising

Central questions arising from the literature review are the following.

(a) How does the Poisson index (υ) vary with deformation? There seems to be a particular lack of published data showing this for extension and compression for the same rubbery foam.

(b) How can the validity of constitutive laws using the Poisson index method, other types of shape-volume coupling or no shape-volume coupling be assessed?

(c) Do the experimental methods adopted by Blatz & Ko (1962) and Storåckers (1986) seem effective for answering (b)?

(d) Do the experimental methods adopted by Blatz & Ko (1962) and Storåckers (1986) seem effective for answering the question posed by Rivlin (1992) and others about the relative sensitivity of W to changes in the principal invariants. Answering such questions has the potential to lead to simplified constitutive laws as has been the case for rubbery materials without voids.

3.3 Aims, objectives & outline plan of work

(i) Perform experiments to determine how the Poisson index (υ) for a rubbery foam varies with extension and compression.

(ii) Considering the modes of deformation they used and the measurements they made, assess how effective the methods used by Blatz & Ko (1962) and Storåckers (1986) were in: assessing the validity of constitutive laws using the Poisson index; answering questions about the relative sensitivity of W to changes in the principal invariants – q.v. (i) in 3.1.

(iii) Examine other ways in which the validity of constitutive laws using the Poisson index method, other types of shape-volume coupling or no shape-volume coupling could be assessed. Attempt such an assessment.

(iv) Consider other ways in which questions about the relative sensitivity of W to changes in the principal invariants could be assessed. Begin such an assessment.

4 THEORY

4.1 Loci in $\bar{I}_1, \bar{I}_2, J$ space, for constant Poisson index (υ), of various modes of deformation

In this section loci in $\bar{I}_1, \bar{I}_2, J$ space, of various modes of deformation are shown for various constant values of the Poisson index (υ).

As explained in the literature review, J, the volume ratio is the ratio of the volume a piece of material in the current, deformed, configuration to its volume in the reference, undeformed, configuration. $\bar{I}_1$ and $\bar{I}_2$ are the 1st and 2nd principal invariants of the volume-neutralised left Cauchy-Green deformation tensor $\overline{\mathbf{B}}$ or the right, $\overline{\mathbf{C}}$; $\bar{\lambda}_1^2$, $\bar{\lambda}_2^2$ and $\bar{\lambda}_3^2$, the eigenvalues of $\overline{\mathbf{B}}$ or $\overline{\mathbf{C}}$, are the squares of the volume-neutralised principal extension ratios: $\bar{\lambda}_i = \lambda_i / J^{1/3}$. So $\bar{\lambda}_1 \bar{\lambda}_2 \bar{\lambda}_3 \equiv 1$. Also $\bar{I}_1$ and $\bar{I}_2$ are not affected by purely volume change. Now $\bar{I}_1 = \bar{\lambda}_1^2 + \bar{\lambda}_2^2 + \bar{\lambda}_3^2$ and, because of volume-neutralisation, $\bar{I}_2 = \bar{\lambda}_1^{-2} + \bar{\lambda}_2^{-2} + \bar{\lambda}_3^{-2}$. $\bar{I}_1$ or $\bar{I}_2$ *each give the amount of shape change of an element of material* – but $\bar{I}_1$ and $\bar{I}_2$ can have different values for different types of shape change so the combined values of $\bar{I}_1$ and $\bar{I}_2$ give the *type and magnitude of shape change*; this information can be shown by projecting onto a plane of constant J loci ("trajectories") in $\bar{I}_1, \bar{I}_2, J$ space. It should be noted that $3 \le \bar{I}_1 < \infty$ and $3 \le \bar{I}_2 < \infty$ but $0 < J < \infty$, where $\bar{I}_1 = \bar{I}_2 = 3$ and $J = 1$ in the undeformed state.

Because the generally accepted permissible range of the Poisson ratio is $-1 < \nu \le ½$ this range of the Poisson index (υ) is covered in the constant υ loci ("trajectories") shown in Figure 5. See however Mott & Roland (2009, 2013) and chapter 2. Also, it is possible for values of $\upsilon >$ ½ to occur at finite strain: for example natural rubber "strain crystallises" at high extension ratio; thereby increasing its density - although only slightly (i.e. up to a maximum of around 3% at λ around 8 in simple extension - see Treloar, 1975 pp 20 – 22); this suggests that υ can be a function of one or more of $\bar{I}_1$ or $\bar{I}_2$ or J and can sometimes exceed ½.

As shown below, for small changes in shape, all shape changes share the same locus projected on the $\bar{I}_1, \bar{I}_2$ plane of constant J: $\bar{I}_1 = \bar{I}_2$. Shear gives the same locus, $J = 1, \bar{I}_1 = \bar{I}_2$, at all levels of deformation but other types of shape change give loci which deviate from $\bar{I}_1 = \bar{I}_2$ as the level of deformation increases.

As explained in chapter 3 one of the main aims of this MPhil is to begin an examination of possible classes of mathematical descriptions for highly compressible rubbery material and to propose tests towards such an examination. As described in chapter 2, Ogden's (1972b) hyperfoam form of strain energy density function (W) is often used in finite element analysis of such materials and the Blatz & Ko (1962) form is sometimes used; both, explicitly or implicitly, use constant Poisson index (υ) quantities. The correctness or otherwise of using υ in W for such materials will be discussed later in this dissertation. Certainly, though, υ can be expected to vary with deformation of a rubbery foam. Consider a rubbery foam containing a low or moderate volume fraction of rubber (Φ). The indications are that at very small strains the Poisson index (υ) would not be greater than 0.4. However if such a material is deformed such that the volume ratio (J) falls to Φ the voids are expected to close up. Here it seems

likely that the material will behave rather like a rubbery material without voids so the Poisson index is expected to rise to close to 0.5. As discussed above, υ may also be a function of one or both of the 1st two principal scalar invariants of the volume-neutralised Cauchy-Green deformation tensor, $\bar{I}_1$ and $\bar{I}_2$.

Nevertheless, plotting the loci for constant υ fulfils at least two useful functions. Firstly such plots give some indication of how effective or otherwise a set of tests will be in covering $\bar{I}_1, \bar{I}_2, J$ space. For an isotropic elastic incompressible material the combination of simple extension, equibiaxial extension and fixed-width extension tests cover the I_1, I_2 plane reasonably well. (Please see Figure 3 in chapter 2, Rivlin & Saunders, 1951, or Treloar, 1975). Blatz & Ko (1962) and Storåckers (1986) both chose this combination of tests for rubbery foams. Such loci can help answer the question of how appropriate this choice was for highly compressible materials.

Secondly the loci plots give a visual indication of what a particular value or range of values of υ would imply about the way J would change with particular modes of deformation.

Perhaps the simplest loci are for pure volume change (the locus follows the J axis, with $\bar{I}_1 = \bar{I}_2 = 3$) and for simple shear. For simple shear, by definition volume is unchanged so J = 1 and the locus is simply a straight line such that $\bar{I}_1 = \bar{I}_2$, as mentioned earlier. Both loci are independent of the value of υ. (Please see Figure 2 for diagrams of modes of test). At υ = ½ volume is constant so that "planar" (or "fixed width") extension/compression becomes "pure shear" (i.e. shear without rotation of the principal axes); in this particular case, therefore,

$$\lambda_3 = \bar{\lambda}_3 = 1 \text{ and } \bar{\lambda}_2 = \lambda_2 = 1/\lambda_1 = 1/\bar{\lambda}_1$$

Since $\bar{I}_1 \equiv \bar{\lambda}_1^2 + \bar{\lambda}_2^2 + \bar{\lambda}_3^2$ and $\bar{I}_2 \equiv 1/\bar{\lambda}_1^2 + 1/\bar{\lambda}_2^2 + 1/\bar{\lambda}_3^2$

it immediately follows that $\bar{I}_1 = \bar{I}_2$ (4.1.1)

For other modes of deformation use is made of equation 2.2b rewritten here:

$$\lambda_3 = (\lambda_1 \lambda_2)^{\frac{-\upsilon}{1-\upsilon}} \quad (4.1.2)$$

Equation 4.1.2 gives for the volume ratio in plane stress general biaxial deformation:

$$J = \lambda_1 \lambda_2 \lambda_3 = (\lambda_1 \lambda_2)^{\frac{1-2\upsilon}{1-\upsilon}} \quad (4.1.3)$$

For simple extension/compression (SE/C), fixed width extension/compression (FWE/C), equibiaxial extension/compression (EBE/C):

$$\lambda_2 = \lambda_3 = \lambda_1^{-\upsilon} \quad \text{SE/C} \quad (4.1.4)$$

$$\lambda_3 = \lambda_1^{\frac{-\upsilon}{1-\upsilon}} \text{ and } \lambda_2 = 1 \quad \text{FWE/C} \quad (4.1.5)$$

$$\lambda_3 = \lambda_1^{\frac{-2\upsilon}{1-\upsilon}} \text{ and } \lambda_2 = \lambda_1 \quad \text{EBE/C} \quad (4.1.6)$$

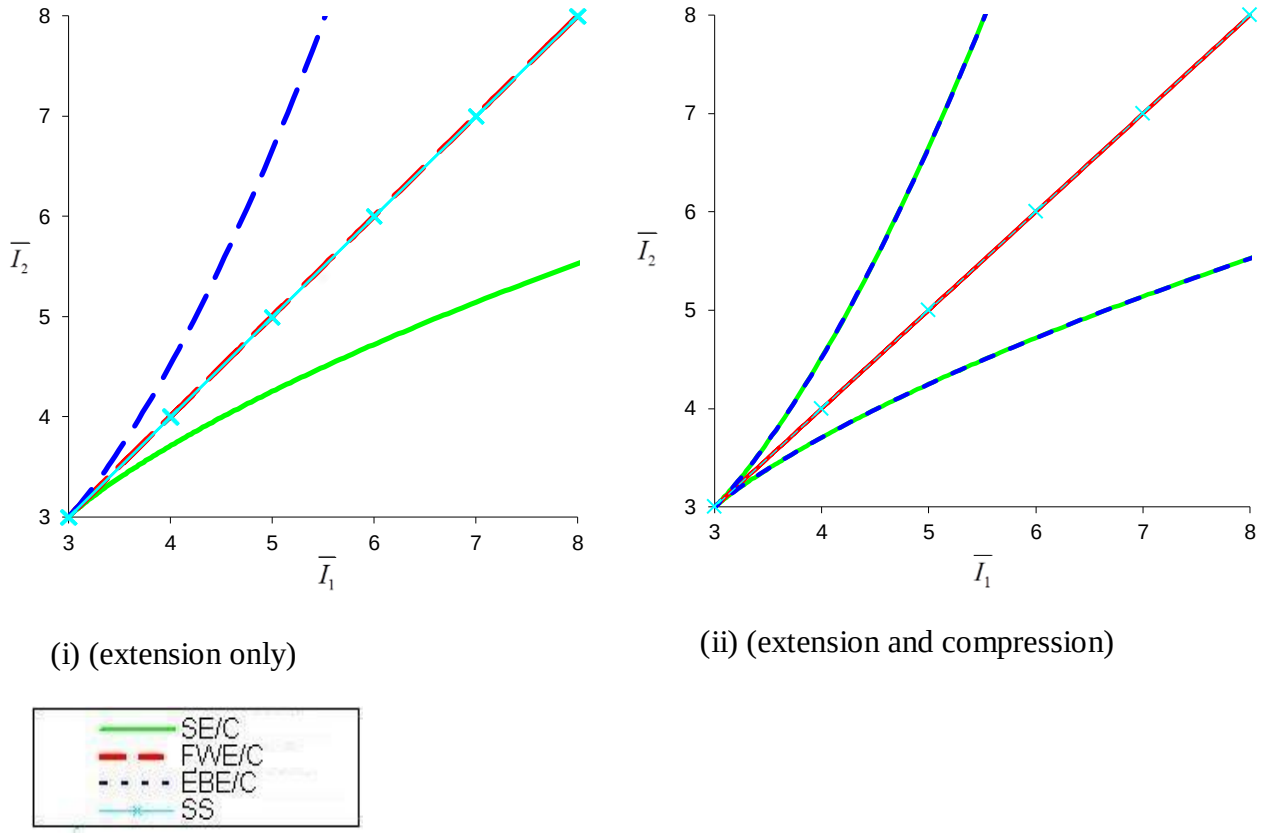

Figure 5.a. Loci for simple extension and compression (SE/C), equibiaxial extension and compression (EBE/C) fixed width extension and compression (FWE/C) and simple shear (SS) for υ = 0.5.

The simplest pattern of loci is given for the incompressible case (υ = ½, figure 5a; see also Literature Review and Treloar, 1975). In this case: J = 1 by definition; the locus for fixed-width extension compression (FWE/C) coincides with that for simple shear (SS); the locus for equibiaxial compression coincides with that for simple extension; the locus for simple compression coincides with that for equibiaxial extension.

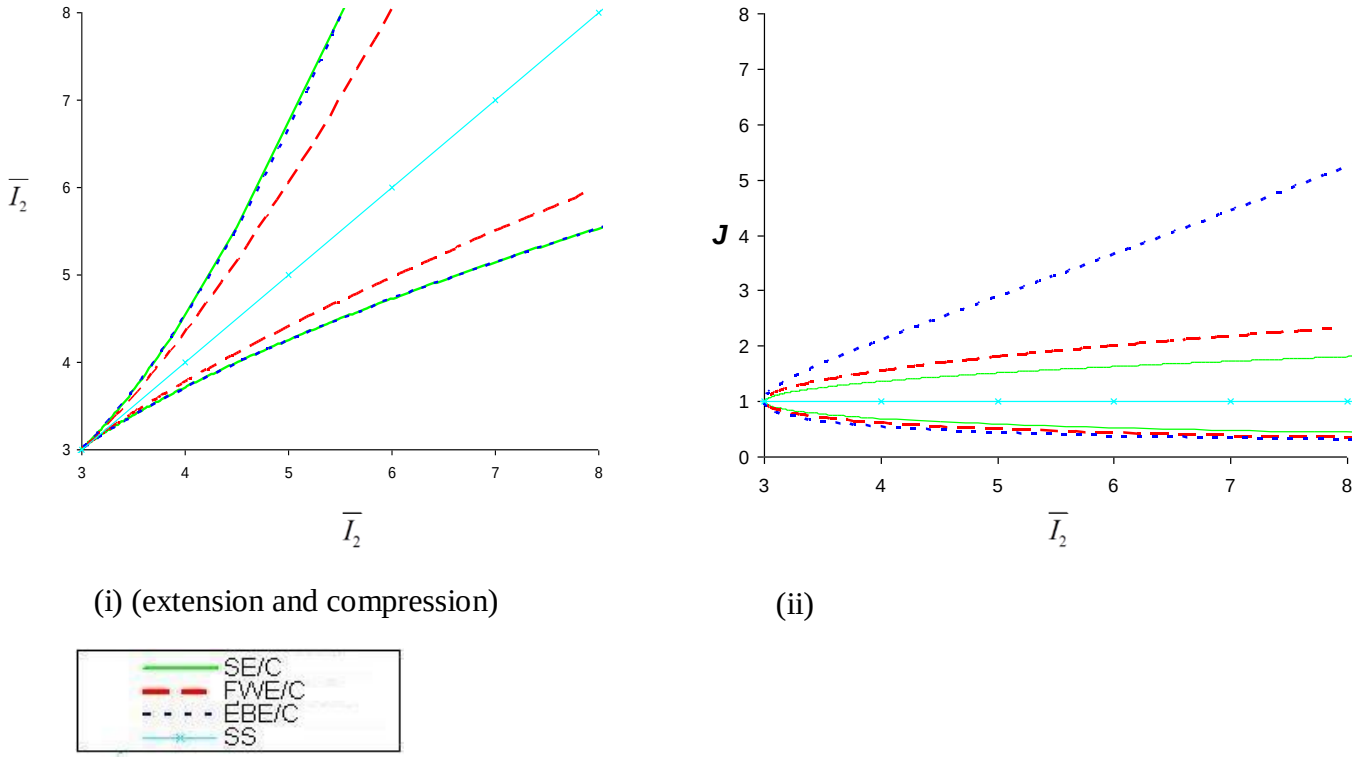

(i) (extension and compression)

(ii)

Figure 5.b. Loci for simple extension and compression (SE/C), equibiaxial extension and compression (EBE/C) fixed width extension and compression (FWE/C) and simple shear (SS) for $\upsilon = 0.25$.

Figure 5.b shows loci for $\upsilon = 0.25$. A value of 0.25 coincides with: the value predicted (in extension) by the simple structure-based model of Gent & Thomas (1959, 1963) for Poisson's ratio (ν); the value of the Poisson ratio which Blatz & Ko found for a rubbery foam in SE, EBE and FWE. Also, a value of $\upsilon = 0.25$ is quite close to: Mott & Roland's lower limit for ν for normal elastic solids (0.2); the value indicated by the data of Storåkers (1986) for a natural rubber foam ($\upsilon \approx 0.33$); the average value of Poisson's ratio (ν) found by Gent & Thomas for 13 natural rubber latex foams ($\nu \approx 0.33$) – see also the summary graph in the literature review; the value of ⅓ predicted by the Gibson & Ashby (1982) model.

The projections onto an $\bar{I}_1$, $\bar{I}_2$ plane of constant J for the loci for SE/C and EBE/C remain coincident with each other and are on the same curves as they were for the incompressible case; this holds true for all $-1 < \upsilon \leq ½$. However, it is clear that for a given value of $\bar{I}_1$ the values of J are very different in simple extension (SE) and equibiaxial extension (EBE).

As expected, Figure 5.b shows that the locus for SS at $\upsilon = 0.25$ is as it was at $\upsilon = 0.5$: it remains a straight line of $J = 1$, $\overline{I_1} = \overline{I_2}$; as stated above, this holds true for all $-1 < \upsilon \leq ½$. However the locus for FWE/C is no longer coincident with that for SS. Instead, the loci for FWE/C and for SE/C have become rather close in $\bar{I}_1$, $\bar{I}_2$, J space.

For a given $\overline{I_1}$ and for $J > 1$ the value of J for the various modes of deformation are in the order: SS (lowest, $J = 1$), SE/C, FWE/C, EBE/C (highest).

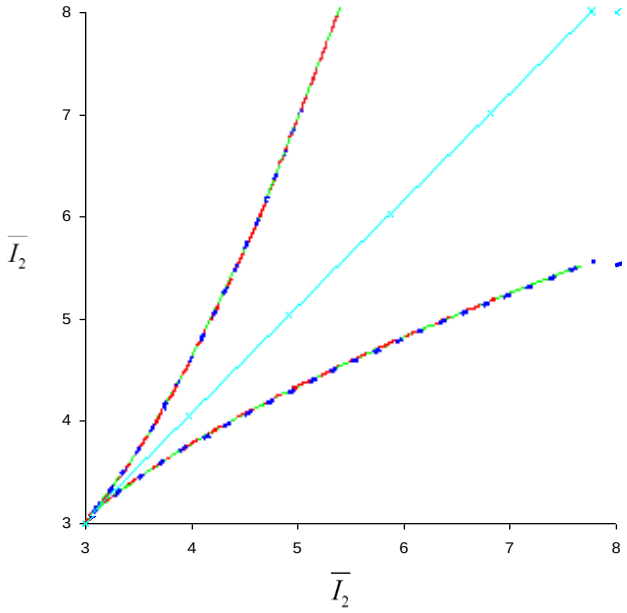

(i) (extension and compression)

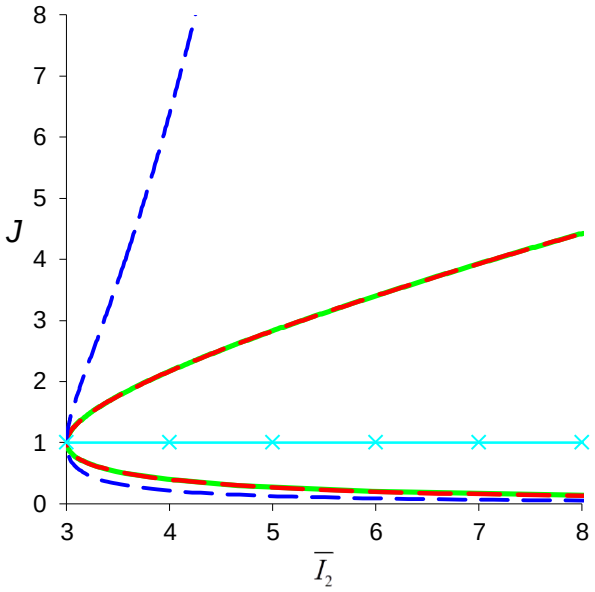

(ii)

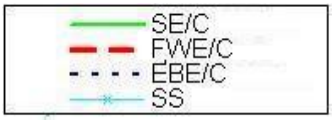

Figure 5.c (i-ii). Loci for simple extension and compression (SE/C), equibiaxial extension and compression (EBE/C) fixed width extension and compression (FWE/C) and simple shear (SS) for $\upsilon = 0$.

Figure 5.c shows loci for $\upsilon = 0$ and marks the boundary between 'normal' and auxetic behaviour. (But see Mott & Roland, 2013.) As might be expected, the loci for FWE/C and SE/C are now coincident in $\bar{I}_1$, $\bar{I}_2$, J space. However, unsurprisingly, the locus for EBE/C shows considerably greater volume increase (at any given $\bar{I}_1$) than do the loci for FWE/C and SE/C.

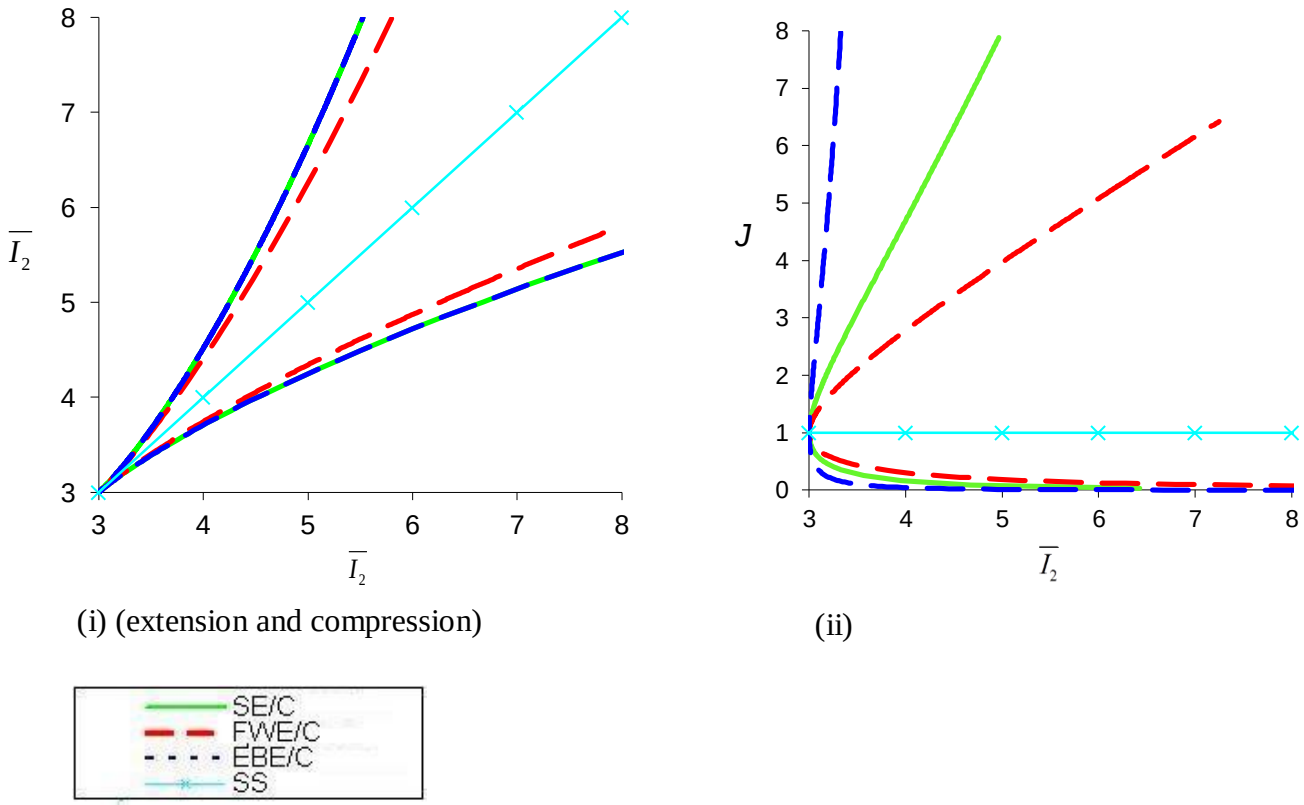

Figure 5.d (i-ii). Loci for simple extension and compression (SE/C), equibiaxial extension and compression (EBE/C) fixed width extension and compression (FWE/C) and simple shear (SS) for υ = -0.25.

Figure 5.d shows loci for υ = -0.25 and thus gives some insight into auxetic behaviour. The locus of FWE/C on the $\overline{I_1}, \overline{I_2}$ plane has moved back inwards from the locus of SE/C and EBE/C. For a given $\overline{I_1}$ and for $J > 1$ the value of J for the various modes of deformation are now in the order: SS (lowest, $J = 1$), FWE/C, SE/C, EBE/C (highest). (For $J < 1$ the order is reversed.) So compared to what was the case for υ = 0.25, FWE/C and SE/C have changed places; this holds true for all $-1 < \upsilon < 0$.

Except for SS, J changes strongly as $\overline{I_1}$ varies for each mode of deformation at υ = -0.25.

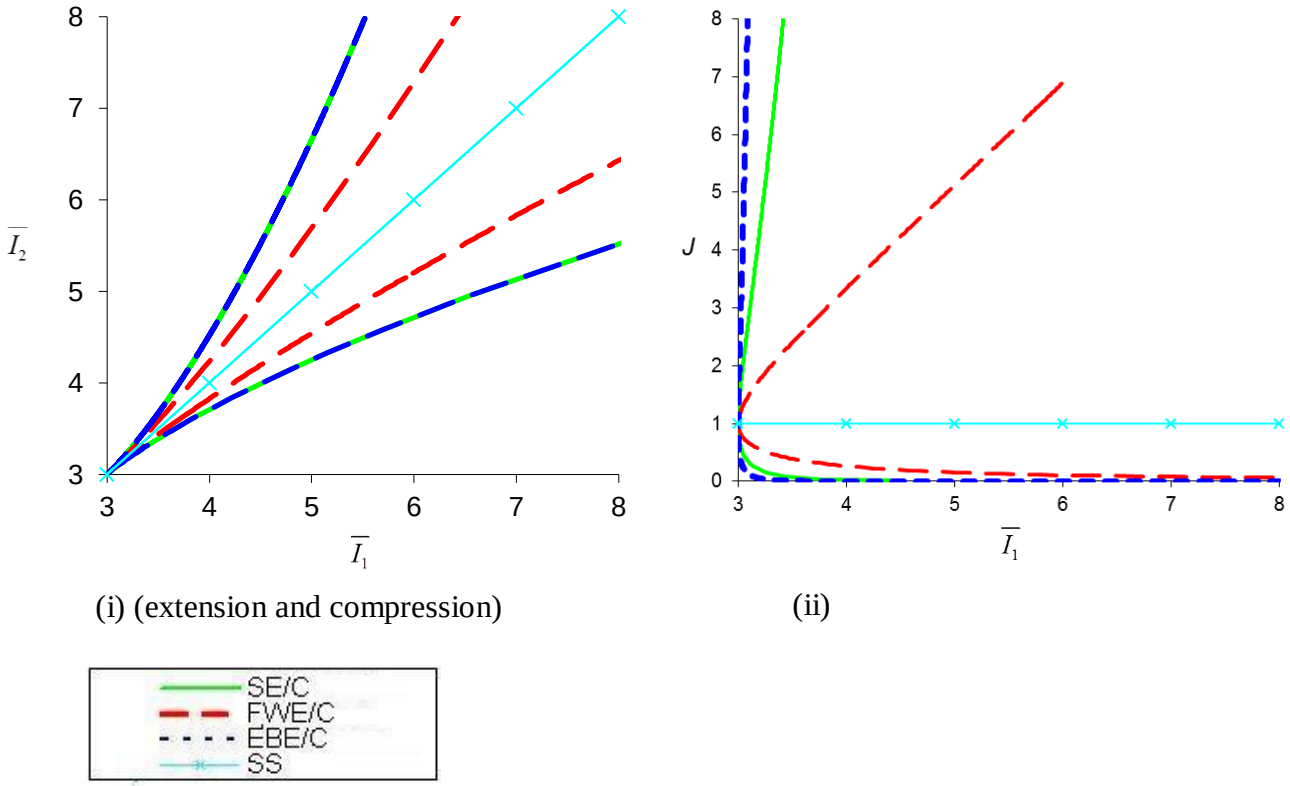

(i) (extension and compression) (ii)

Figure 5.e (i-ii). Loci for simple extension and compression (SE/C), equibiaxial extension and compression (EBE/C) fixed width extension and compression (FWE/C) and simple shear (SS) for υ = -0.5.

Figure 5.e shows loci for υ = -0.5 and thus gives some insight into more auxetic behaviour. The locus of FWE/C on the $\overline{I_1}, \overline{I_2}$ plane has moved inwards further from the locus of SE/C and EBE/C.

For EBE/C and SE/C *J* changes noticeably more strongly with $\overline{I_1}$ than was the case at υ = -0.25.

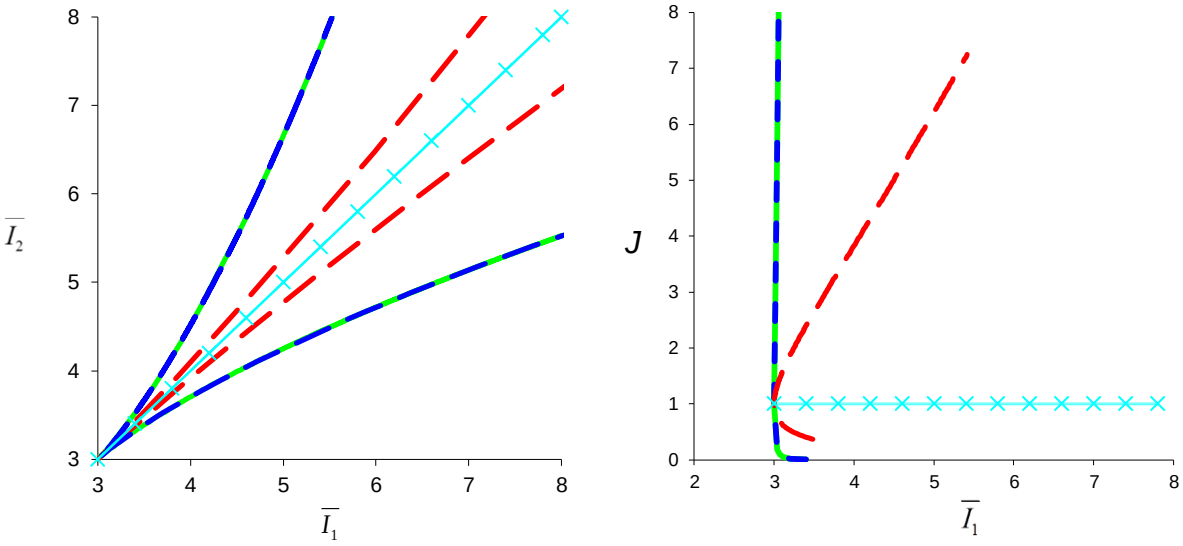

(i) (extension and compression) (ii)

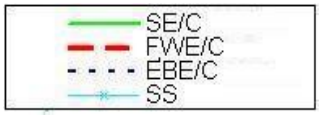

Figure 5.f (i-ii). Loci for simple extension and compression (SE/C), equibiaxial extension and compression (EBE/C) fixed width extension and compression (FWE/C) and simple shear (SS) for υ = -0.75.

Figure 5.f shows loci for υ = -0.75 and thus gives some insight into still more auxetic behaviour. The locus of FWE/C on the $\overline{I_1}, \overline{I_2}$ plane is now quite close to the locus of SS.

For EBE/C and SE/C the dependence of J on $\overline{I_1}$ is now so strong that, except at very small values of J, it is difficult to distinguish the loci from a line parallel to the J axis and passing through $\overline{I_1}$ = 3.

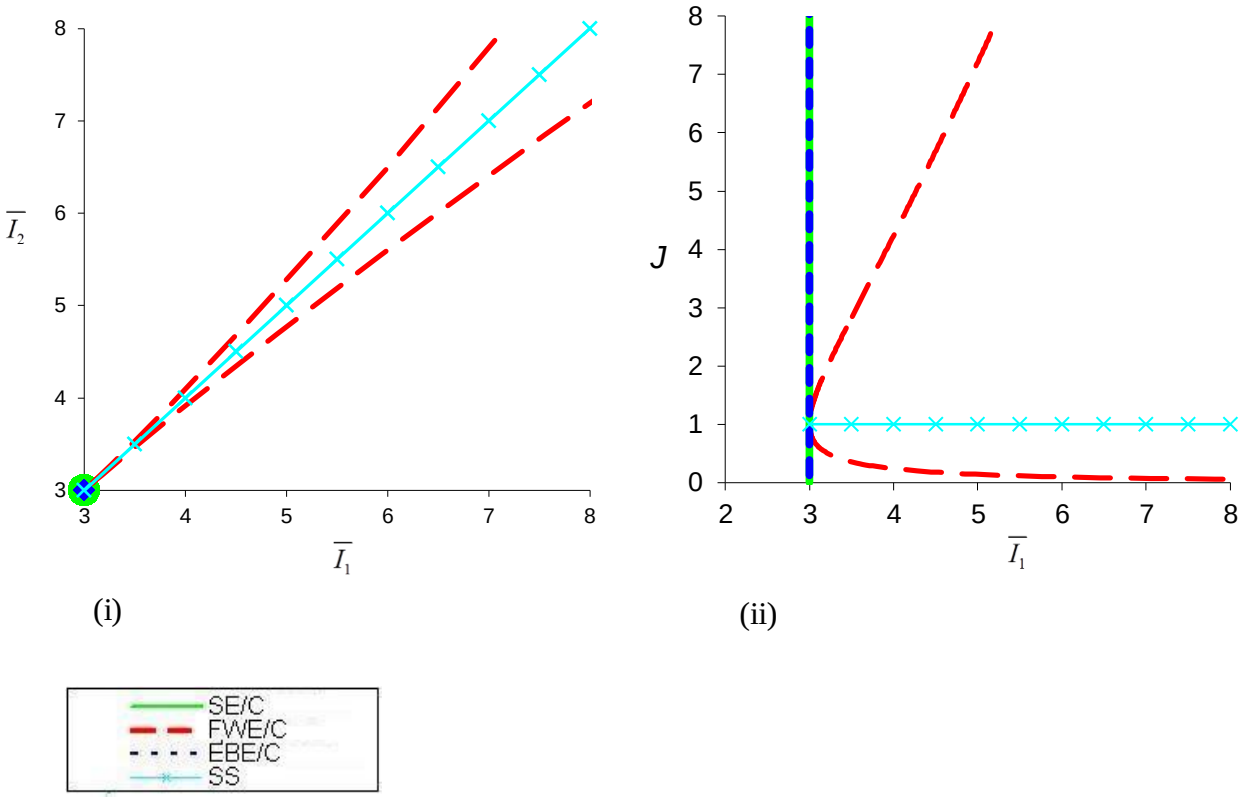

Figure 5.g (i-ii). Loci for simple extension and compression (SE/C), equibiaxial extension and compression (EBE/C) fixed width extension and compression (FWE/C) and simple shear (SS) for υ = -0.9999.

Figure 5.g shows loci for υ = -0.9999 and thus gives some insight into still more extreme auxetic behaviour. The locus of FWE/C on the $\overline{I_1}, \overline{I_2}$ plane is now essentially coincident with the locus of SS – qv figure 5.a.

For EBE/C and SE/C the dependence of J on $\overline{I_1}$ is now so strong that it is virtually impossible to distinguish the loci from a line parallel to the J axis and passing through $\overline{I_1}$ = 3. For FWE/C the dependence of J on $\overline{I_1}$ at υ = -0.9999 is somewhat similar to that at υ = -0.75.

Summary of work on loci in $\bar{I}_1, \bar{I}_2, J$ space

The plots showing loci in $\bar{I}_1, \bar{I}_2, J$ space (for constant υ) of various modes of deformation bring into clear view the size of the task for comprehensive characterisation of a highly deformable and compressible elastic material. If, as might be expected, υ is a function of deformation, the plots shown earlier in this section provide hints as to confusions that might arise in interpretation of experimental data – particularly with regard to analysis of data from fixed width extension/compression (FWE/C, "planar tension") tests, where the locus changes in position on the $\bar{I}_1, \bar{I}_2$ plane as υ changes. At υ = 0.25 - which seems not far from a typical reported value for a rubbery foam in extension, the loci on the $\bar{I}_1, \bar{I}_2$ plane for FWE/C and simple extension/compression (SE/C) are rather close. This in turn means that doing both tests, rather than just one of the two, may add little information or insight and may quite possibly lead to confusion – especially given experimental errors and the possibility that υ varies with deformation. (Please see earlier discussion of the work of Blatz & Ko (1962) and Storåkers (1986) in the Literature Review.) It appears that simple shear would be a better choice of test than fixed width extension compression (FWE/C). As might be expected, the loci for values of $\upsilon < 0.2$ seem very strange (see also Mott & Roland, 2013).

4.2 Generalisation of Blatz & Ko's approach and behaviour in specific modes of deformation

4.2.1 Generalisation of Blatz & Ko's approach

As indicated in chapter 2 Blatz & Ko (1962) described an isotropic hyperelastic compressible material by:

$$W = C_1\left[J^{2/3}\bar{I}_1 - 3 + \frac{1-2\upsilon}{\upsilon}\left(J^{\frac{-2\upsilon}{1-2\upsilon}} - 1\right)\right] + C_2\left[J^{-2/3}\bar{I}_2 - 3 + \frac{1-2\upsilon}{\upsilon}\left(J^{\frac{2\upsilon}{1-2\upsilon}} - 1\right)\right] \qquad (4.2.1)$$

where:

W is the strain energy density;

$\bar{I}_1$ and $\bar{I}_2$ are the first two principal invariants of $\bar{B}$, the volume neutralised left Cauchy – Green deformation tensor;

J is the volume ratio;

υ is the Poisson index.

This is a particularisation of the general approach (see Rivlin, 1992 for example) in which the material is described by the dependence of W on $\bar{I}_1, \bar{I}_2$ and J or $\partial W/\partial\bar{I}_1, \partial W/\partial\bar{I}_2$ and $\partial W/\partial J$ on $\bar{I}_1, \bar{I}_2$ and J. In equation 4.2.1:

(a) the dependence of $\partial W/\partial J$ on $\bar{I}_1, \bar{I}_2$ and J is described via the Poisson index (υ);

(b) the Poisson index does not vary with $\bar{I}_1, \bar{I}_2$ or J;

(c) $\partial W/\partial\bar{I}_1$ and $\partial W/\partial\bar{I}_2$ do not vary with $\bar{I}_1$ or $\bar{I}_2$ - so Blatz & Ko's equation 4.2.1 can be described as a Mooney-related form of constitutive law.

For Blatz & Ko's form

$$\frac{\partial W}{\partial\bar{I}_1} = C_1 J^{2/3} \qquad (4.2.2a)$$

$$\frac{\partial W}{\partial\bar{I}_2} = C_2 J^{-2/3} \qquad (4.2.2b)$$

$$\frac{\partial W}{\partial J} = C_1\left(J^{-1/3} + \frac{1-2\upsilon}{\upsilon} J^{\frac{-1}{1-2\upsilon}}\right) + C_2\left(J^{-5/3} + \frac{1-2\upsilon}{\upsilon} J^{\frac{4\upsilon-1}{1-2\upsilon}}\right) \qquad (4.2.2c)$$

It seems rather unlikely that propositions (b) and (c) would be correct for situations where there are compressions and large extensions so Chagnon & Coveney (2007 & 2011) proposed that (b) and (c) be dropped. Propositions (a) and (b) will be returned to in the experimental chapter. Here preparations for the examination of proposition (a) will be made by setting out expressions for stresses written in terms of $\partial W/\partial\bar{I}_1$, $\partial W/\partial\bar{I}_2$ and υ – each allowed to vary

with $\bar{I}_1, \bar{I}$ and J – for various modes of deformation; a material described in such a way will be called a Generalised Blatz & Ko (GBK) material. The steps leading to the expressions are given in Appendix V.

4.2.2 Simple uniaxial extension and compression (SE/C)

Consider a cuboid of material, with sides aligned with the principal axes of deformation, with normal stresses applied to the 1 faces. The 2 and 3 faces are stress free. λ is the extension ratio in the 1 direction. For a GBK material description, the Cauchy stress is given by:

$$\boldsymbol{\sigma} = 2\begin{bmatrix} \lambda^{\frac{1+10\upsilon}{3}} - \lambda^{\frac{-5+4\upsilon}{3}} & 0 & 0 \\ 0 & 0 & 0 \\ 0 & 0 & 0 \end{bmatrix}\frac{\partial W}{\partial \bar{I}_1} + 2\begin{bmatrix} \lambda^{\frac{-1+8\upsilon}{3}} - \lambda^{\frac{-7+2\upsilon}{3}} & 0 & 0 \\ 0 & 0 & 0 \\ 0 & 0 & 0 \end{bmatrix}\frac{\partial W}{\partial \bar{I}_2} \qquad (4.2.3)$$

and the nominal stress is given by

$$N_{11} = \frac{F_{11}}{A_{1,0}} = \left(\lambda^{\frac{1+4\upsilon}{3}} - \lambda^{\frac{-5-2\upsilon}{3}}\right)\frac{\partial W}{\partial \bar{I}_1} + \left(\lambda^{\frac{-1+2\upsilon}{3}} - \lambda^{\frac{-7-4\upsilon}{3}}\right)\frac{\partial W}{\partial \bar{I}_2} \qquad (4.2.4)$$

$\upsilon(\lambda)$ can be found from volume changes in simple extension but because there is only one component of stress, $\frac{\partial W}{\partial \bar{I}_1}(\lambda)$ and $\frac{\partial W}{\partial \bar{I}_2}(\lambda)$ cannot be deduced from a SE/C (simple extension/compression) test alone.

Putting $\lambda = 1 + \varepsilon$, equation 4.2.3 or 4.2.4 gives, for small strain (ε):

$$\sigma_{11} \approx N_{11} \approx 2(1+\upsilon)\cdot 2\cdot\left(\frac{\partial W}{\partial \bar{I}_1} + \frac{\partial W}{\partial \bar{I}_2}\right)\varepsilon \qquad (4.2.5)$$

Putting

$$\mu = 2\cdot\left(\frac{\partial W}{\partial \bar{I}_1} + \frac{\partial W}{\partial \bar{I}_2}\right) \text{ and } \nu = \upsilon$$

equation 4.2.5 can be seen to be in agreement with the usual infinitesimal strain expression:

$$\sigma_{11} = 2(1+\nu)\mu\varepsilon = E\varepsilon \qquad (4.2.6)$$

The Poisson index (υ) and the nominal stress can be measured in simple extension/compression and then equation 4.2.5 can be used to establish to what extent υ changes and to what extent $\left(\partial W/\partial \bar{I}_1 + \partial W/\partial \bar{I}_2\right)$ changes at small strains.

4.2.3 Equibiaxial extension/compression (EBE/C)

Consider a cuboid of material, with sides aligned with the principal axes of deformation, with normal stresses applied to the 1 and the 2 faces. The 3 faces are stress free. λ is the extension ratio in the 1 direction and in the 2 direction. For a GBK material description, the Cauchy stress is given by:

$$\boldsymbol{\sigma} = 2\begin{bmatrix} \lambda^{-\frac{2}{3}\cdot\frac{2-7\upsilon}{1-\upsilon}} - \lambda^{-\frac{2}{3}\cdot\frac{5-4\upsilon}{1-\upsilon}} & 0 & 0 \\ 0 & \lambda^{-\frac{2}{3}\cdot\frac{2-7\upsilon}{1-\upsilon}} - \lambda^{-\frac{2}{3}\cdot\frac{5-4\upsilon}{1-\upsilon}} & 0 \\ 0 & 0 & 0 \end{bmatrix}\frac{\partial W}{\partial \bar{I}_1}$$

$$+2\begin{bmatrix} \lambda^{-\frac{2}{3}\cdot\frac{1-8\upsilon}{1-\upsilon}} - \lambda^{-\frac{2}{3}\cdot\frac{4-5\upsilon}{1-\upsilon}} & 0 & 0 \\ 0 & \lambda^{-\frac{2}{3}\cdot\frac{1-8\upsilon}{1-\upsilon}} - \lambda^{-\frac{2}{3}\cdot\frac{4-5\upsilon}{1-\upsilon}} & 0 \\ 0 & 0 & 0 \end{bmatrix}\frac{\partial W}{\partial \bar{I}_2} \qquad (4.2.7)$$

and the nominal stress is given by

$$\frac{F_{11}}{A_{1,0}} = \frac{F_{22}}{A_{2,0}} = 2\left(\lambda^{-\frac{1}{3}\cdot\frac{1-5\upsilon}{1-\upsilon}} - \lambda^{-\frac{1}{3}\cdot\frac{7+\upsilon}{1-\upsilon}}\right)\frac{\partial W}{\partial \bar{I}_1} + 2\left(\lambda^{\frac{1}{3}\cdot\frac{1+7\upsilon}{1-\upsilon}} - \lambda^{-\frac{1}{3}\cdot\frac{5-\upsilon}{1-\upsilon}}\right)\frac{\partial W}{\partial \bar{I}_2} \qquad (4.2.8)$$

Similarly to the case of SE/C, $\upsilon(\lambda)$ can be found from volume changes in EBE/C but because the two non-zero components of stress are the same, $\frac{\partial W}{\partial \bar{I}_1}(\lambda)$ and $\frac{\partial W}{\partial \bar{I}_2}(\lambda)$ cannot be deduced from an EBE/C test alone.

In fact, SE/C and EBE/C are the only particular cases of plane stress general biaxial deformation which, because of symmetry, do not enable any possible role of $\bar{I}_2$ in W to be distinguished from the role of $\bar{I}_1$. Even considered together, SE/C and EBE/C cannot be used to distinguish the roles of $\bar{I}_1$ and $\bar{I}_2$ because, for the same $\bar{I}_1$, J for SE/C is different from EBE/C.

4.2.4 Fixed width extension/compression (FWE/C)

Consider again a cuboid of material with sides aligned with the principal axes of deformation, with normal stresses applied to the 1 and the 2 faces. The 3 faces are stress free. λ is the extension ratio in the 1 direction and in 2 direction the length is fixed. For a GBK material description, the Cauchy stress is given by:

$\boldsymbol{\sigma}$ =

$$2\begin{bmatrix} \lambda^{\frac{1}{3}\cdot\frac{1+4\upsilon}{1-\upsilon}} - \lambda^{-\frac{1}{3}\cdot\frac{5-4\upsilon}{1-\upsilon}} & 0 & 0 \\ 0 & \lambda^{-\frac{1}{3}\cdot\frac{5-10\upsilon}{1-\upsilon}} - \lambda^{-\frac{1}{3}\cdot\frac{5-4\upsilon}{1-\upsilon}} & 0 \\ 0 & 0 & 0 \end{bmatrix}\frac{\partial W}{\partial \bar{I}_1} + 2\begin{bmatrix} \lambda^{-\frac{1}{3}\cdot\frac{1-8\upsilon}{1-\upsilon}} - \lambda^{-\frac{1}{3}\cdot\frac{7-8\upsilon}{1-\upsilon}} & 0 & 0 \\ 0 & \lambda^{-\frac{1}{3}\cdot\frac{1-8\upsilon}{1-\upsilon}} - \lambda^{-\frac{1}{3}\cdot\frac{1-2\upsilon}{1-\upsilon}} & 0 \\ 0 & 0 & 0 \end{bmatrix}\frac{\partial W}{\partial \bar{I}_2} \tag{4.2.9}$$

and the non-zero nominal stresses are given by

$$\frac{F_{11}}{A_{1,0}} = 2\left(\lambda^{\frac{1}{3}\cdot\frac{1+\upsilon}{1-\upsilon}} - \lambda^{-\frac{1}{3}\cdot\frac{5-\upsilon}{1-\upsilon}}\right)\frac{\partial W}{\partial \bar{I}_1} + 2\left(\lambda^{-\frac{1}{3}\cdot\frac{1-5\upsilon}{1-\upsilon}} - \lambda^{-\frac{1}{3}\cdot\frac{7-5\upsilon}{1-\upsilon}}\right)\frac{\partial W}{\partial \bar{I}_2} \tag{4.2.10a}$$

and

$$\frac{F_{22}}{A_{2,0}} = 2\left(\lambda^{-\frac{2}{3}\cdot\frac{1-2\upsilon}{1-\upsilon}} - \lambda^{-\frac{2}{3}\cdot\frac{1+\upsilon}{1-\upsilon}}\right)\frac{\partial W}{\partial \bar{I}_1} + 2\left(\lambda^{\frac{2}{3}\cdot\frac{1+\upsilon}{1-\upsilon}} - \lambda^{\frac{2}{3}\cdot\frac{1-2\upsilon}{1-\upsilon}}\right)\frac{\partial W}{\partial \bar{I}_2} \tag{4.2.10b}$$

It can be seen that in the case of the stresses for FWE/C there are two different expressions for non-zero stress components; for each value of λ the value of $\frac{\partial W}{\partial \bar{I}_1}$ should be the same for the two stress components – and similarly for $\frac{\partial W}{\partial \bar{I}_2}$. Thus there are two simultaneous equations with two unknowns at each value of λ and we can solve for $\frac{\partial W}{\partial \bar{I}_1}$ and $\frac{\partial W}{\partial \bar{I}_2}$ at each value of λ. So FWE/C seems to be a potentially useful mode of deformation for determining the relative importance of $\frac{\partial W}{\partial \bar{I}_1}$ and $\frac{\partial W}{\partial \bar{I}_2}$, however force would have to be measured in directions parallel to and perpendicular to the applied displacement; this is rarely done – but see Gough et al (1999).

Simple extension/compression (SE/C), equibiaxial extension/compression (EBE/C) and fixed width extension/compression (FWE/C) are particular cases of (pure, plane stress) general biaxial extension/compression. I will now look at some types of deformation other than pure, plane stress) general biaxial extension/compression.

4.2.5 Constant cross-section, or plane, extension/compression

Constant cross-section extension/compression is a particular case of general triaxial deformation. In this mode of test a slab of material whose dimension in the 1 direction is much smaller than in the 2 and 3 directions is tested. Please refer to Figure 2 or Appendix II. The 1 dimension is increased or decreased but, ignoring edge effects, lengths in the 2 and 3 directions remain constant:

$x_1 = \lambda X_1;\ x_2 = X_2;\ x_3 = X_3$

For a GBK material, the Cauchy stress is:

$$\boldsymbol{\sigma} = 2\begin{bmatrix} (\lambda^{1/3} - \lambda^{-r-1}) & 0 & 0 \\ 0 & (\lambda^{-5/3} - \lambda^{-r-1}) & 0 \\ 0 & 0 & (\lambda^{-5/3} - \lambda^{-r-1}) \end{bmatrix} \frac{\partial W}{\partial \bar{I}_1}$$

$$+ 2\begin{bmatrix} (\lambda^{r-1} - \lambda^{-7/3}) & 0 & 0 \\ 0 & (\lambda^{r-1} - \lambda^{-1/3}) & 0 \\ 0 & 0 & (\lambda^{r-1} - \lambda^{-1/3}) \end{bmatrix} \frac{\partial W}{\partial \bar{I}_2} \qquad (4.2.11)$$

The 1,1 component of nominal stress is equal to the 1,1 component of Cauchy stress because there is constant area for this face. For nominal stress the matrix terms for both the 2,2 and for the 3,3 components become $\left(\lambda^{-2/3} - \lambda^{-r}\right)$ and $\left(\lambda^{r} - \lambda^{2/3}\right)$. Here $r = 2(1+\upsilon)/(3(1-2\upsilon))$.

For the shape-volume uncoupled form, for which $W = W_S\left(\bar{I}_1, \bar{I}_2\right) + W_V\left(J\right)$, the Cauchy stress is:

$$\boldsymbol{\sigma} = 2\begin{bmatrix} \frac{2}{3}(\lambda^{1/3} - \lambda^{-5/3}) & 0 & 0 \\ 0 & \frac{1}{3}(\lambda^{-5/3} - \lambda^{1/3}) & 0 \\ 0 & 0 & \frac{1}{3}(\lambda^{-5/3} - \lambda^{1/3}) \end{bmatrix} \frac{\partial W}{\partial \bar{I}_1}$$

$$+ 2\lambda^{-1}\begin{bmatrix} \frac{2}{3}(\lambda^{-1/3} - \lambda^{-7/3}) & 0 & 0 \\ 0 & \frac{1}{3}(\lambda^{-7/3} - \lambda^{-1/3}) & 0 \\ 0 & 0 & \frac{1}{3}(\lambda^{-7/3} - \lambda^{-1/3}) \end{bmatrix} \frac{\partial W}{\partial \bar{I}_2}$$

$$+ \begin{bmatrix} 1 & 0 & 0 \\ 0 & 1 & 0 \\ 0 & 0 & 1 \end{bmatrix} \frac{\partial W}{\partial J} \qquad (4.2.12)$$

In constant cross-section extension/compression, volume is controlled and various components of stress could, in principle, be measured by means along the lines of those used by Gough et al (1999). Differences in the powers present in stress components given by the GBK form could possibly enable $\partial W/\partial \bar{I}_1$, $\partial W/\partial \bar{I}_2$ and υ to be deduced. However, it should be noted that r may vary in $\bar{I}_1, \bar{I}_2$ & J space and would need to be deduced.

For infinitesimal strains, the above expressions (GBK *and* shape-volume uncoupled materials) give:

$$\text{i.e. } \boldsymbol{\sigma} = \mu\begin{bmatrix} (\frac{4}{3}+r)\varepsilon & 0 & 0 \\ 0 & (\frac{-2}{3}+r)\varepsilon & 0 \\ 0 & 0 & (\frac{-2}{3}+r)\varepsilon \end{bmatrix} = \begin{bmatrix} (\frac{4}{3}\mu+K)\varepsilon & 0 & 0 \\ 0 & (K-\frac{2}{3}\mu)\varepsilon & 0 \\ 0 & 0 & (K-\frac{2}{3}\mu)\varepsilon \end{bmatrix} \quad (4.2.13)$$

As expected, equation 4.2.13 gives $K + 4\mu/3$: the plane modulus – see Mott & Roland (2013) for example.

4.2.6 Pure volume change

In the general case, the Cauchy stress can be found from:

$$\boldsymbol{\sigma} = \frac{\partial W}{\partial J}\mathbf{I} \quad (4.2.14)$$

In the particular case of a GBK material, the Cauchy stress is given by:

$$\boldsymbol{\sigma} = 2\left[\left(J^{-1} - J^{-r-1}\right)\frac{\partial W}{\partial \bar{I}_1} + \left(J^{r-1} - J^{-1}\right)\frac{\partial W}{\partial \bar{I}_2}\right]\mathbf{I} \quad (4.2.15)$$

Here $r = 2(1+\upsilon)/(3(1-2\upsilon))$. Once more, it could be difficult to disentangle the effects of variations in $\partial W / \partial \bar{I}_1, \partial W / \partial \bar{I}_1$ and in υ.

For a shape-volume uncoupled material ($W = W_s + W_v$) the Cauchy stress is, very simply:

$$\boldsymbol{\sigma} = \frac{\partial W}{\partial J}\mathbf{I} = \frac{\partial W_v}{\partial J}\mathbf{I} \quad (4.2.16)$$

4.2.7 Simple shear

Please see Figure 6 and refer to Figure 2 or Appendix II for a schematic diagram of the practical arrangement for simple shear. As was the case for fixed cross-section extension/compression, edge effects are ignored.

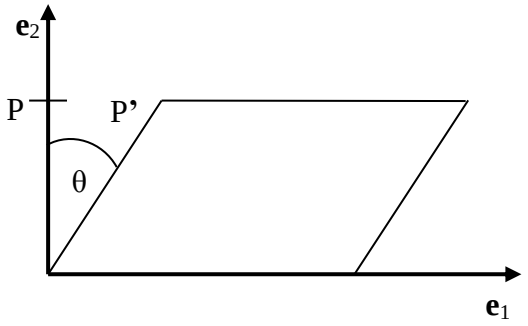

Figure 6. Simple shear: a material point at P in the undeformed condition moves to P'. $\mathbf{e}_1$ and $\mathbf{e}_2$ are unit coordinate vectors.

For simple shear (Figure 6) current coordinates of material points are related to the coordinates in the reference configuration by:

$$x_1 = X_1 + \gamma X_2 ; x_2 + X_2 ; x_3 = X_3 \qquad (4.2.17)$$

Here $\gamma = \tan\theta$.

In the general case of an isotropic hyperelastic material the Cauchy stress is given by:

$$\boldsymbol{\sigma} = 2\begin{bmatrix} \frac{2}{3}\gamma^2 & \gamma & 0 \\ \gamma & -\frac{1}{3}\gamma^2 & 0 \\ 0 & 0 & -\frac{1}{3}\gamma^2 \end{bmatrix}\frac{\partial W}{\partial \bar{I}_1} + 2\begin{bmatrix} \frac{1}{3}\gamma^2 & \gamma & 0 \\ \gamma & -\frac{2}{3}\gamma^2 & 0 \\ 0 & 0 & \frac{1}{3}\gamma^2 \end{bmatrix}\frac{\partial W}{\partial \bar{I}_2} + \begin{bmatrix} 1 & 0 & 0 \\ 0 & 1 & 0 \\ 0 & 0 & 1 \end{bmatrix}\frac{\partial W}{\partial J} \qquad (4.2.18)$$

Because the deformation is simple shear $J = 1$. Now for a shape-volume uncoupled form

$\partial W/\partial J$ must be zero at $J = 1$ - so that the spherical stress is zero at zero volume change. So the

Cauchy stress is given by:

$$\boldsymbol{\sigma} = 2\begin{bmatrix} \frac{2}{3}\gamma^2 & \gamma & 0 \\ \gamma & -\frac{1}{3}\gamma^2 & 0 \\ 0 & 0 & -\frac{1}{3}\gamma^2 \end{bmatrix}\frac{\partial W}{\partial \bar{I}_1} + 2\begin{bmatrix} \frac{1}{3}\gamma^2 & \gamma & 0 \\ \gamma & -\frac{2}{3}\gamma^2 & 0 \\ 0 & 0 & \frac{1}{3}\gamma^2 \end{bmatrix}\frac{\partial W}{\partial \bar{I}_2} \qquad (4.2.19)$$

For a GBK material the Cauchy stress is given by

$$\boldsymbol{\sigma} = 2\begin{bmatrix} \gamma^2 & \gamma & 0 \\ \gamma & 0 & 0 \\ 0 & 0 & 0 \end{bmatrix}\frac{\partial W}{\partial \bar{I}_1} + 2\begin{bmatrix} 0 & \gamma & 0 \\ \gamma & -\gamma^2 & 0 \\ 0 & 0 & 0 \end{bmatrix}\frac{\partial W}{\partial \bar{I}_2} \qquad (4.2.20)$$

As γ tends to zero the nonlinear terms on the diagonals in the above equations disappear leaving only the shear stresses showing that $\left(\frac{\partial W}{\partial \bar{I}_1} + \frac{\partial W}{\partial \bar{I}_2}\right)$ tends to $\frac{\mu}{2}$.

Note that $\sigma_{12} = \sigma_{21} = 2(\partial W/\partial \bar{I}_1 + \partial W/\partial \bar{I}_2)\gamma$ and $\sigma_{11} - \sigma_{22} = 2(\partial W/\partial \bar{I}_1 + \partial W/\partial \bar{I}_2)\gamma^2$

both in equation 4.2.19 and 4.2.20 so both are in accordance with the universal rule described in Beatty (1987) for example – as is 4.2.18.

$$\gamma\sigma_{12} = \sigma_{11} - \sigma_{22} \qquad (4.2.21)$$

Equation 2.2 defining υ in terms of dimensional changes in plane stress indicates that if $\lambda_1\,\lambda_2 = 1$, as is the case in simple shear, then $\lambda_2 = 1$ – i.e. there is plane strain also. Correspondingly equation 4.2.20 shows that for simple shear, which is a plane strain deformation, the GBK material gives plane stress. Examination of equation 4.2.18 shows that this need not be the case. So simple shear seems to be a potentially good way of testing the validity of the GBK approach. It also seems to have the potential to give indications of the relative magnitudes of $\frac{\partial W}{\partial \bar{I}_1}$, $\frac{\partial W}{\partial \bar{I}_2}$ and $\frac{\partial W}{\partial J}$. Unlike in other modes of deformation υ does not appear in the expression for Cauchy stress for simple shear of a GBK material.

Although the main subject of this dissertation is highly compressible elastic materials the theoretical results are also interesting in the context of near-incompressible elasticity. The stress components are quite different in equations 4.2.19 and 4.2.20 - except if $\partial W/\partial \bar{I}_2 = \partial W/\partial \bar{I}_1$. The pressure is always zero in equation 4.2.19 because $J = 1$ and $\partial W/\partial J$ must be zero there for a shape-volume uncoupled form.

However, if an incompressible isotropic elastic material is described as having a Poisson ratio $\upsilon = ½$ it can immediately be seen from equation 2.2, with $\upsilon = ½$ that if $\lambda_1\lambda_2 = 1$ then $\lambda_3 = 1$. That is, for an incompressible isotropic elastic material in shear, plane strain and plane stress can coexist. See also Lai et al (2010).This means that the shape-volume uncoupled material description does not, in general, produce the pressure needed to give the correct stresses as a material tends towards incompressibility. So it seems that the shape-volume uncoupled material description gives the wrong stress components for a near-incompressible material in simple shear and the errors might not be small.

4.3 Further experimental test options considered

The omission of $\partial W/\partial \bar{I}_2$ or $\partial W/\partial \bar{I}_1$ would simplify models for isotropic elastic materials - particularly for foams as this would reduce the $\overline{I_1}$, $\overline{I_2}$, J space to a two-dimensional plane.

In investigating the dependence of W on $\overline{I_1}$, $\overline{I_2}$ and J, the hypothesis would be that $\overline{I_2}$ plays little or no role for foamed elastomers. To support or refute this hypothesis we would need to take a test piece to pairs of states where $\overline{I_1}$ and J are the same but $\overline{I_2}$ is different. The following four test options were considered and loci in $\overline{I_1}$, $\overline{I_2}$, J space were plotted for two of them – please see Appendices III and V. In order to get some idea of what the difference in $\overline{I_2}$ would be for each pair of states, constant Poisson ratio ($\upsilon = 0.25$) was assumed in the calculations performed for options 2 and 3.

Test option 1

This option involved equibiaxial extension plus superposed hydrostatic pressure (or equivalent means to control volume) compared with simple extension.

An equibiaxial extension or simple extension test could be performed within a pressure chamber to allow volume to be controlled. The chamber could be within a second chamber to allow volume change to be monitored (e.g. via liquid column displacement, i.e. a measuring pipette as in section 5.5) and for pressurisation to be uniform. Pressure needed for this will be low - approximately 1 bar because K for the foam is ~0.1MPa; please see chapter 5. Changes in liquid column displacement, and so volume, to be measured optically via a "reinforced" window.

The test piece could be deformed by one of four possible methods; (i) a weight attached to the test piece, tilting the chamber would increase load. This method would only be straightforward for single axis tests. (ii) A fine wire or rotating drive, or drives, through the measuring pipette to actuate a test. (iii) Guided magnets outside the chamber to control soft iron or magnetic test clamps.

Such apparatus could, however, involve a lot of time, effort and cost. Friction could pose problems. Also, an open cell foam could not be used without sealing.

Test option 2

The second option considered was to use (a) equibiaxial extension followed by simple shear of the top surface relative to the bottom surface, compared with (b) simple extension.

Calculations were carried out to examine this option. These showed that with $\overline{I_1}$ and J held at equal values – for (a) and (b) - there was very little difference in $\overline{I_2}$; for this reason this method was discounted. This method could be a lot cheaper and quicker to do than previous option however it is conceptually less "clean" and the mathematics could be more difficult. Attachment of the test piece to the plates could also be a problem.

Test option 3

This option involved using (a) simple extension and comparing this with: (b) plane, i.e. fixed cross-section, extension combined with simple shear.

Calculations were again carried out to examine this option. At $J = 1.5$ and $\overline{I_1} = 4.88$ - and with a simple shear of $\gamma = 1$ for (b) - the value of $\overline{I_2}$ was 4.2 for (a) and 4.45 for (b). This suggested that adequate separation between $\overline{I_2}$ values could be obtained for this option. Option 3 may, though, be experimentally difficult due to problems of attachment of foam to the plates. Various methods including glue and stitching using rubber thread could be tried.

Test option 4.

This final option considered involved a simple shear test. As explained in the literature review and in the theory chapter, different classes of constitutive law for rubbery materials give contrasting patterns of components in the stress tensors produced in simple shear. Experiments in simple shear can be used to give insight about what models should be used – e.g. into whether there should be coupling between *J* and the other principal scalar invariants and into whether it might possible to omit $\bar{I}_1$ or $\bar{I}_2$ from the strain energy density function (*W*).

A shear test will be experimentally less complex to perform than the combined tests considered in previous options – however option 4 is also less generally informative in some respects than other test plans outlined above.

Of the various types of test considered only a selection were to be performed due to limited time and resources. Shear was a first choice as it would be experimentally straightforward and produce useful data. Simple extension would also be useful to test for anisotropy and to obtain data to evaluate the Poisson index.

Practical aspects of further characterisation on the $\overline{I_1}, J$ plane

If *W* did not vary with $\overline{I_2}$ the following approach could be tried. Independently controlled shape change and volume *reduction* should be relatively straightforward to arrive at – for example by simple extension of the rubbery foam - within a sealed envelope of thin rubber membrane if the foam is open - followed by pressurisation. However, independently controlled shape change and volume *increase* is likely to be more difficult to achieve in such a simple and straightforward way; a more complicated method might prove necessary - such as that adopted by Mills (2007): constant cross-section compression or extension of a slab of rubbery foam bonded between two nominally rigid plates, changing $\overline{I_1}$ and J, combined with simple shear of the same slab, changing $\overline{I_1}$ alone. It may be that there are some zones of the I_1, J plane inaccessible to such a test.

5 EXPERIMENTAL WORK

5.1 Materials for experiments

5.1.1 Introduction

For the experimental programme, a material that was close to being isotropic and hyperelastic and which was capable of undergoing quite large strains without failure was required. This was to allow the study of behaviour well above the region of infinitesimal strain. These requirements are difficult to achieve together. For example, polyurethane foam is often produced in a way (a) that results in it "rising" in the mould, rather as true bread does; this almost inevitably leads to elongated cells and the likelihood of anisotropy (Gibson & Ashby, 1997). Other options for manufacturing a rubbery foam include: (b) whipping air into a suitable liquid, then crosslinking this mousse; (c) casting a suitable elastomer around compressible particles or particles that can be washed away subsequently. On further reflection, method (c) was thought unsuitable because the materials produced would either be rather weak - such as when silicone rubber with little or no filler was used as the castable elastomer - or would give too much energy dissipation and history dependence on deformation - such as when silicone with high levels of silica filler was used as the castable elastomer. Similarly a cork-filled polyurethane was expected to give significant amounts of energy dissipation and history dependence on deformation. It should be noted, though, that despite being judged unsuitable for other tests, a cork-filled polyurethane was chosen for the pressure-volume test work to try out the test method in principle. This was because it was believed that the cork-filled polyurethane, unlike the natural rubber latex foam, was essentially a closed cell material so that practical problems in pressure-volume testing would be avoided. Please see section 5.5.

Manufacturing process (b) can be expected to result in an essentially uniform and isotropic foam - provided that the foam is not of very high density; also, natural rubber, without filler, is among the most elastic elastomers but is also highly extensible. Natural rubber does, though, undergo some crystallisation at extreme strains and can become less elastic under these conditions (Treloar, 1975). It should also be noted that natural rubber latex foam fails at lower extensions than does natural rubber without voids (Gent & Thomas, 1959b, 1963).

Several suppliers of natural rubber latex foam were contacted and a number of test pieces were obtained. Unfortunately the natural rubber latex foam obtained in these early attempts was either available only in thicknesses less than 3 mm and judged to be inadequate for the experiments planned or had rather large (~5mm diameter) holes through the thickness and it was felt that the large through-holes would lead to anisotropy.

Eventually, a test piece of 12.5 mm thick open cell natural rubber latex foam with no through-thickness holes was obtained from Pentonville Foam, 104/106 Pentonville Road, London N1 9JB, UK. From figure 7 it can be seen that the structure is rather irregular with pore sizes ranging from approximately 0.1mm to 1mm.

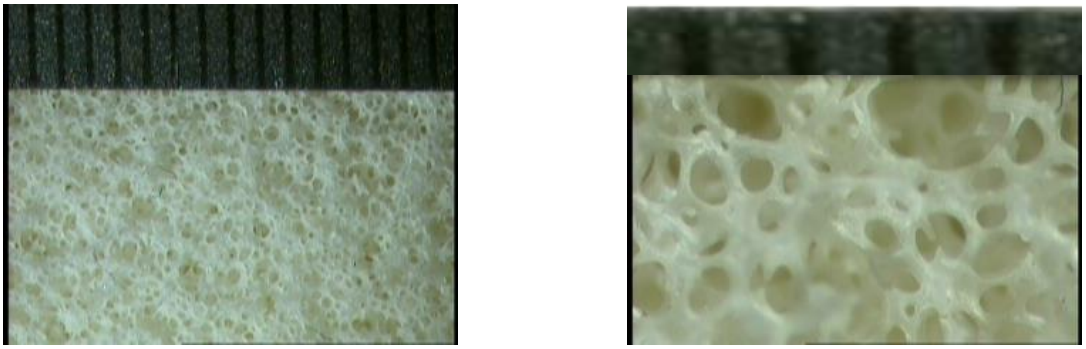

Figure 7. Pentonville Foam natural rubber latex foam with mm rule to show scale of cells. Face shown is the opposite side to the face with "skin" and as received condition.

5.1.2 Measurement of the density of the natural rubber latex foam

The volume (V_f) of a cuboid slab of the Pentonville Foam natural rubber latex foam was found by measuring the length (l), breadth (b) and thickness (h); its mass (m_f) was found by weighing. The error in measured volume was estimated to be ±2%; this was due to slight irregularity in the cut surfaces of the cuboid and was much larger than the percentage error for mass measurement. The density of air was ignored in calculating the density of the foam (ρ_f).

$$\rho_f = \frac{m_f}{V_f} = \frac{m_f}{l \times b \times h} = \frac{125.3\text{g}}{1163\text{cm}^3} = 0.108\text{g/cm}^3 = 108\text{kg/m}^3 \pm 2\% \tag{5.1.1}$$

5.1.3 Finding the volume fraction of rubber in the foam

Taking a figure for the density of unfilled natural rubber $\rho_{NR} = 950\text{kg/m}^3$ ±1% (MRPRA, 1984) the volume fraction of rubber in the foam was calculated to be

$$\Phi = \frac{\rho_f}{\rho_{NR}} = \frac{108}{950} = 0.114 \pm 3\% \quad \text{i.e. } 0.114 +/- 0.003 \tag{5.1.2}$$

5.1.4 Finding the volume fraction of closed cells in the foam

The volume of water (V_w) needed to saturate a known volume of the foam (V_f) was measured so as to find the sum of the volume fraction of rubber (Φ) plus the volume fraction enclosed within closed cells (Φ_{closed}) for the natural rubber latex foam. A cuboid of the foam material ($V_f = 1232 +/- 25\text{cm}^3$) was placed within a perspex container constructed to fit snugly against the cube faces. The top level of the foam was marked on the container before water was added in order to check that the final saturated volume was equal to the initial volume.

The perspex container and the foam test piece were both submerged in a tank of water and the foam thoroughly squeezed by hand to remove all air bubbles before being placed into the container. This method allowed the foam to be fully saturated and also allowed it to regain its original dimensions before being fitted into the container. (An earlier method involved adding water to the dry foam in the perspex container. This made it difficult to remove all of the air and there were also problems in regaining the original height of the test piece due to the friction of the container sides.) Once the foam was at the original height the excess water was removed so that the water surface was level with this height. The water had a small amount of liquid detergent added to reduce the possible repellent effect that may have been caused by greasiness on the surface of the rubber: 10ml of detergent was added to 5 litres of water.

A total of 1074 +/– 3cm^3 of water (V_w) was needed to saturate the foam. The volume of water was measured by subtracting the dry weight from the final weight using laboratory scales.

$$\frac{V_w}{V_f} = \frac{1074}{1232} \pm 2\% = 0.872 \pm 0.017 = 1 - \Phi - \Phi_{closed}$$

$$\therefore \ \Phi_{closed} = 1 - 0.128 \pm 0.017 - 0.114 \pm 0.003 = 0.014 \pm 0.02 \quad (5.1.3)$$

This indicated that in the natural rubber latex foam the, volume, proportion of the voids that were closed [$\Phi_{closed}/(1- \Phi)$] was most likely to be approximately 0.014/0.89 or about 1½% - however the experimental errors could mean that Φ_{closed} could be as low as zero or possibly as high as 0.134. That is between 0% and 15%, by volume, of the cells are closed. It seems likely that the experimental errors given are high estimates and that therefore the percentage by volume of closed cells was close to zero.

5.1.5 Removal of "skin" from the Pentonville Foam natural rubber latex foam

The natural rubber latex foam supplied by Pentonville Foam had a continuous rubber skin on one major face. The skin was approximately 1.5mm thick. It was felt that this could lead to anisotropy so experimental results were carefully examined.

Having examined results it was decided that in initial simple extension experiments the rubber skin was leading to an anisotropic response and so the skin was removed. This was carried out by carefully peeling away the skin. Once a few centimetres was detached this could be gripped and carefully pulled by hand. The removed layer had a fairly consistent thickness of about 1.5mm.

5.1.6 Conditioning of the test piece

As explained in the literature review rubbery test pieces are often subjected to conditioning ("scragging") cycles so as to reduce energy dissipation. However, I followed the guidance of Gough et al (1999) and did not aim to "scrag" the material routinely. This was to try to minimise deformation-induced anisotropy. In order to minimise energy dissipation in my tests deformation was slow for simple shear (SS) and very slow for simple extension/compression (SE/C).

5.2 Simple shear test

5.2.1 Apparatus and experimental procedure

A simple shear test was performed on the natural rubber latex foam test piece supplied by Pentonville Foam in the as received condition. Dimensions of the test piece were 100mm x 100mm x 12.5mm. The large faces of the test piece were bonded by means of a contact adhesive to two parallel steel plates. The thicknesses of the plates were 5mm. The lower plate was attached to a heavy duty (5.55kN) low noise low friction linear bearing and driven by a hydraulic ram. The upper plate was attached to a load cell; capacity of this was: F_1 = 2500N, F_2 = 5000N, F_3=2500N. Please see figures 8 and 9. The height of the plate was adjusted by means of a parallelogram mechanism that kept the plates aligned. The parallelogram mechanism was then locked in place so that no tensile or compressive load would be applied to the undeformed test piece. In the experiment the components of force in the 1 and 2 directions were measured: F_1 and F_2 corresponding to σ_{21} and σ_{22}. Please see figures 9 and 10. Displacement of the sliding, lower, plate was measured using a linear variable differential transformer (LVDT). The test was performed to a maximum shear strain, γ, of 1. A cycle was performed with a triangular variation of displacement with time and with a time period of 32s per cycle; $|\,d\gamma/dt\,| = 0.125s^{-1}$. It was therefore possible for any energy dissipation, "hysteresis", to be observed.

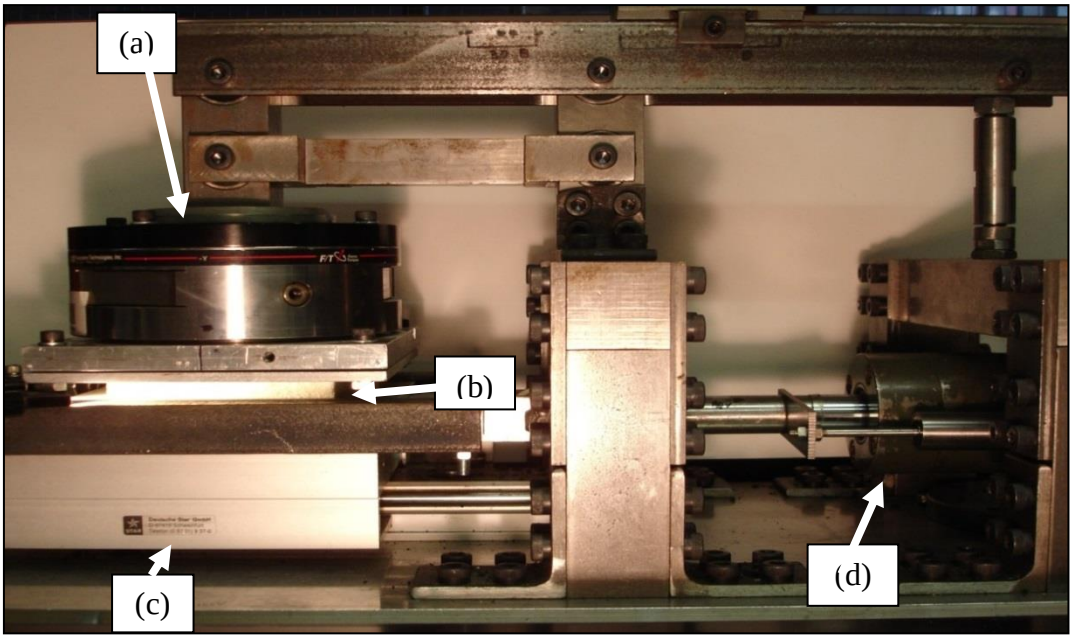

Figure 8. Simple shear test apparatus. (Scale can be judged from the rubber foam test piece which is 100mm long)

(a) 6 degree-of-freedom load cell (able to measure 3 components of force F_1, F_2, F_3 and 3 components of moment M_1, M_2, M_3).
(b) Shear test piece 100mm x 100mm x 12.5mm of natural rubber latex foam supplied by Pentonville Foam.
(c) Low noise, low friction linear bearing. Deutsch star, model D97419.
(d) Hydraulic ram under servohydraulic control. LVDT attached to ram.

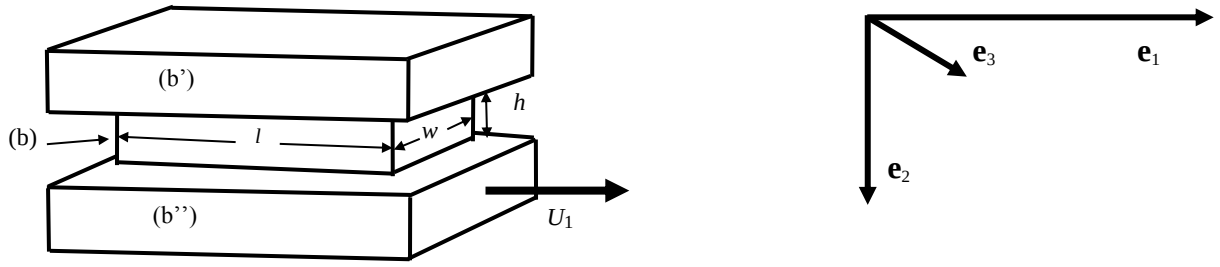

Figure 9. Diagram illustrating shear test piece comprising natural rubber latex foam (b)

(l = w = 100mm, h = 12.5mm) and steel plates (b' and b'') for simple shear test. Unit vectors for coordinate system also shown.

The larger arrow in figure 9 indicates the direction of displacement of the bottom plate, u_1 to produce shear in the test piece. Shear strain (γ) was calculated from the hydraulic ram displacement divided by the foam thickness (h).

Use of the displacement of the hydraulic ram to measure displacement of the lower plate of the test piece and, so, the shear strain in the foam, was justified, apart from edge effects and some edge peeling, because the foam was firmly bonded to rigid plates and because of the very high rigidity of the parallelogram mechanism, the linear bearing, the hydraulic ram and relevant connections. The foam thickness also remained constant due to the rigidity of the locked parallelogram mechanism and accurate alignment of the linear bearing. Please see figure 8.

5.2.2 Results and discussion for simple shear test

Results from these tests were compared with stress components given by a coupled and an uncoupled material model in order to clarify the extent to which either model is appropriate. As mentioned above, there were some problems with the foam peeling away from the plates at the extreme ends as shear took place, and the test piece showed some energy dissipation, "hysteresis", and history dependence.

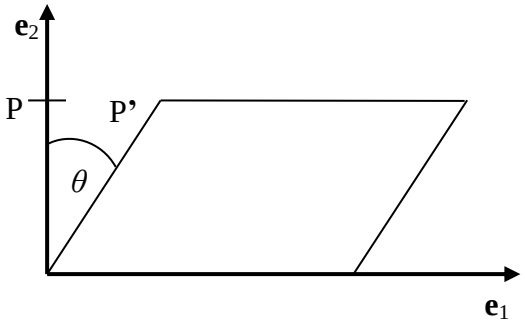

Figure 10. Simple shear. Shear strain $\gamma = \tan\theta$.

Simple shear is shown in figure 10. The deformation is plane strain and constant volume (J = 1). For shear strain γ:

$$x_1 = X_1 + \gamma x_2; x_2 + X_2; x_3 = X_3 \qquad (5.2.1)$$

Referring to section 4.2.7 in this dissertation, and rewriting the equations here for convenience, the Cauchy stress for a general isotropic elastic material in simple shear is given by:

(i)

$$\boldsymbol{\sigma} = 2\begin{bmatrix} \frac{2}{3}\gamma^2 & \gamma & 0 \\ \gamma & -\frac{1}{3}\gamma^2 & 0 \\ 0 & 0 & -\frac{1}{3}\gamma^2 \end{bmatrix}\frac{\partial W}{\partial \bar{I}_1} + 2\begin{bmatrix} \frac{1}{3}\gamma^2 & \gamma & 0 \\ \gamma & -\frac{2}{3}\gamma^2 & 0 \\ 0 & 0 & \frac{1}{3}\gamma^2 \end{bmatrix}\frac{\partial W}{\partial \bar{I}_2} + \begin{bmatrix} 1 & 0 & 0 \\ 0 & 1 & 0 \\ 0 & 0 & 1 \end{bmatrix}\frac{\partial W}{\partial J} \tag{5.2.2}$$

(ii) For a GBK material description:

$$\boldsymbol{\sigma} = 2\begin{bmatrix} \gamma^2 & \gamma & 0 \\ \gamma & 0 & 0 \\ 0 & 0 & 0 \end{bmatrix}\frac{\partial W}{\partial \bar{I}_1} + 2\begin{bmatrix} 0 & \gamma & 0 \\ \gamma & -\gamma^2 & 0 \\ 0 & 0 & 0 \end{bmatrix}\frac{\partial W}{\partial \bar{I}_2} \tag{5.2.3}$$

This indicates that a simple shear test appears to be a potential way of distinguishing between the roles of $\bar{I}_1$ and $\bar{I}_2$. If the role of $\bar{I}_1$ was found to be dominant, the dependence of $\frac{\partial W}{\partial \bar{I}_1}$ on $\bar{I}_1$ could be easily found because $\bar{I}_1 = \gamma^2 + 3$.

(iii) For the shape-volume uncoupled material description:

$$\boldsymbol{\sigma} = 2\begin{bmatrix} \frac{2}{3}\gamma^2 & \gamma & 0 \\ \gamma & -\frac{1}{3}\gamma^2 & 0 \\ 0 & 0 & -\frac{1}{3}\gamma^2 \end{bmatrix}\frac{\partial W}{\partial \bar{I}_1} + 2\begin{bmatrix} \frac{1}{3}\gamma^2 & \gamma & 0 \\ \gamma & -\frac{2}{3}\gamma^2 & 0 \\ 0 & 0 & \frac{1}{3}\gamma^2 \end{bmatrix}\frac{\partial W}{\partial \bar{I}_2} \tag{5.2.4}$$

At $\gamma = 1$ the shape-volume uncoupled material description gives
$\sigma_{33} = 2(\partial W/\partial \bar{I}_2) - \partial W/\partial \bar{I}_1)/3$ but the GBK material description gives $\sigma_{33} = 0$.

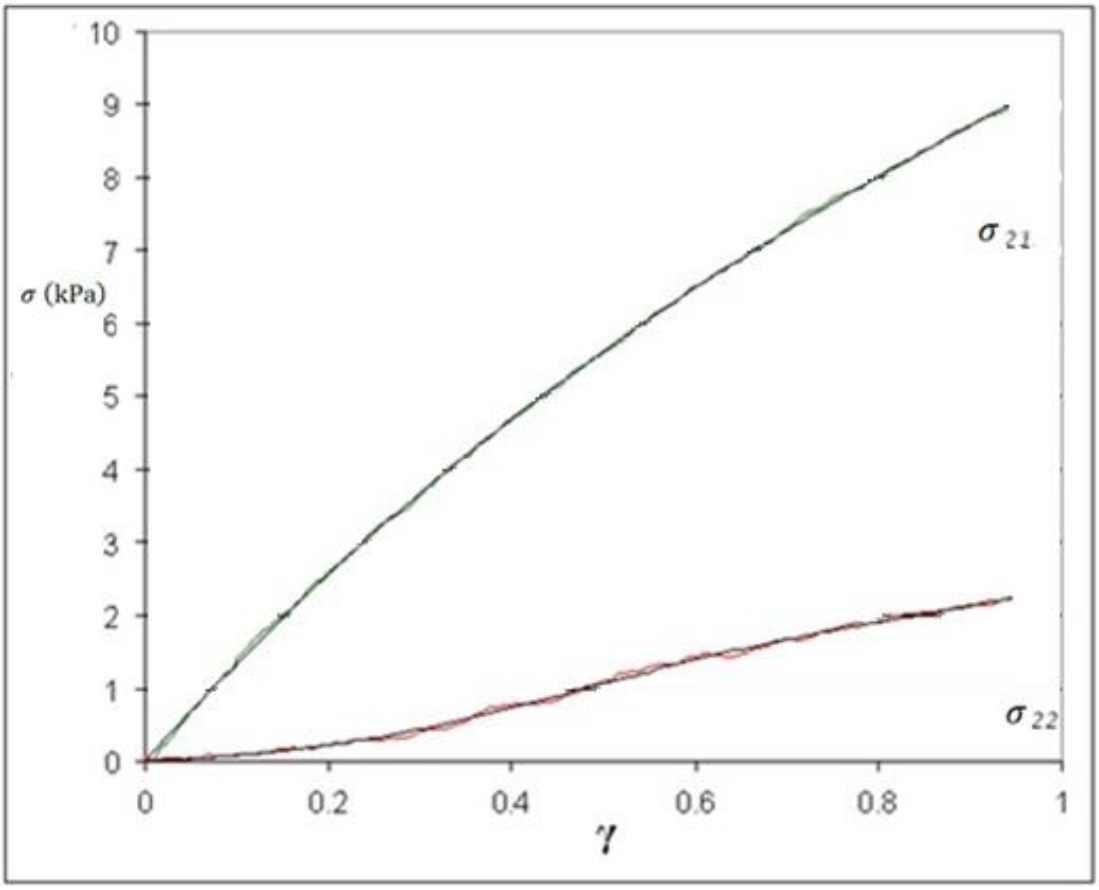

Figure 11. Plots of σ_{21} and σ_{22} against γ for simple shear test.

In figure 11 it can be seen that σ_{21} at $\gamma = 0.1$ is about 1.5 kPa, corresponding to a shear modulus $\mu \approx 15$kPa, and at $\gamma = 1$ it is about 10kPa.This indicates that $(\partial W / \partial \bar{I}_1 + \partial W / \partial \bar{I}_2)$ decreases by only about a third between $\gamma = 0$ and $\gamma = 1$. During shear the number 3 and the number 1 surfaces of the test piece became slightly concave. The fact that σ_{33} is positive suggests that $\frac{\partial W}{\partial \bar{I}_2}$ is greater than $\frac{\partial W}{\partial \bar{I}_1}$ or that $\frac{\partial W}{\partial J}$ is large. The fact that σ_{22} is positive is also consistent with $\frac{\partial W}{\partial J}$ being large. The results appear to indicate that neither the GBK nor the shape volume uncoupled forms are correct.

5.3 Simple extension tests

5.3.1 Apparatus

Simple extension tests were carried out on a natural rubber foam test piece cut from a foam sheet supplied by Pentonville Foam, as described above. An Instron 4204 single axis screw driven electromechanical test machine was used to perform these tests. Please see figure 12. The standard maximum distance between grips for the Instron 4204 test machine was 1000mm. However as the unstrained sample measured 850mm, increasing to 1275mm at $\lambda_1 =$ 1.4 the upper grip needed to be offset. This was achieved by attaching the upper grip to an essentially rigid aluminium strut which gave a new extended range between grips of up to 1900mm. In order to measure tensile force a load cell was attached at the fixed end of the sample. This was a 100lb RDP model 31 load cell which was first calibrated using laboratory weights. Please see figure 12.

To avoid any possible problems caused by end effects the test piece was made 90% longer than the central region to be measured, namely the gauge length . The additional lengths of 200mm at each end allowed the central region to contract laterally with no restriction due to clamping. The width of the undeformed test piece was 60mm and the total length between grips was 850mm; the thickness was 12.5mm. The distance between the pointers used to measure extension ratio, λ_1 was 450mm; please see points marked (b) in figure 12.

The test piece was held using wooden grips with large tapered “lead ins” so as to avoid breakage at high extensions. Grips were produced in-house for this purpose. Both pairs of grips were faced with 400 grit abrasive paper to prevent slippage.

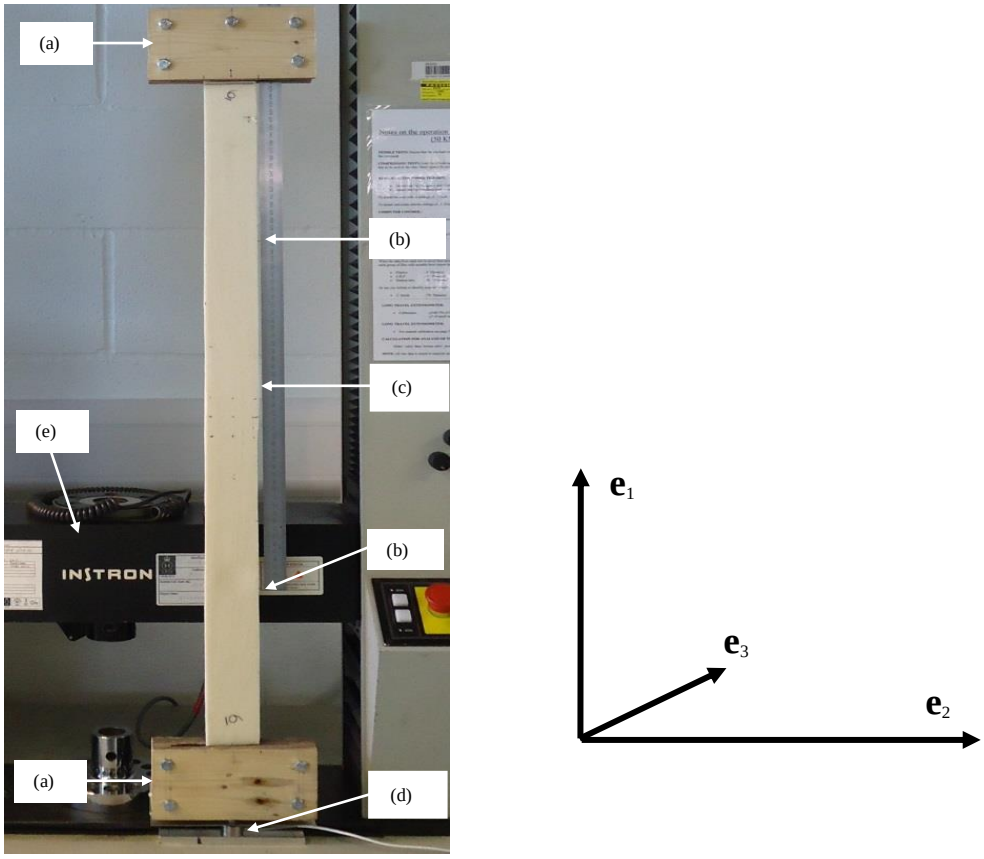

Figure 12. Simple extension test piece, grips and coordinate system.

(a) Tapered wooden grips with abrasive paper on gripping surfaces.

(b) Pointers aligned with mm scale. (Note that the steel rule shown is 700mm long; scale can be judged from this.)

(c) Natural rubber latex foam test piece.

(d) Load cell.

(e) Movable crosshead.

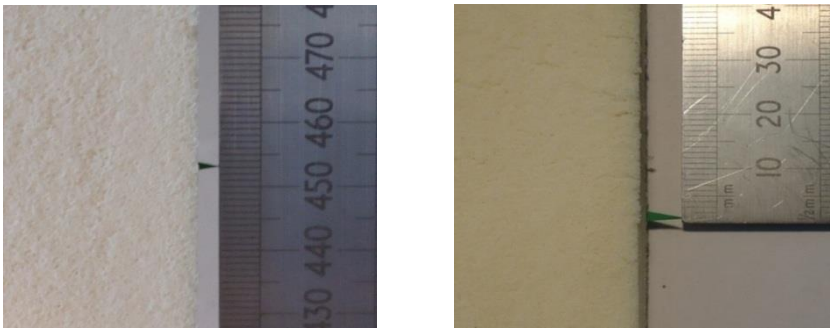

Figure 13. (a) and (b) Details of upper and lower pointers and mm scale.

Figure 14. Side view of tapered wooden grip holding foam test piece. Abrasive paper can be seen on the tapered edges. Each half of wooden grip was 18.5mm thick, from which the scale can be judged.

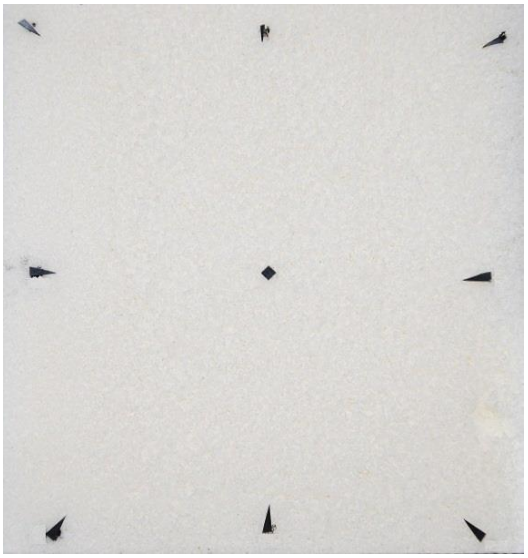

Figure 15. Details of arrangement of central markers.

Figure 16. Detail of rigid aluminium strut used to offset upper grip.

5.3.2 Deformation measurement

One practical issue was deformation measurement as this could not be done using standard methods available in the structures laboratory.

The following standard methods were considered but none found to be suitable:

(i) Conventional contact extensometry as for "normal", i.e. hard, materials. This was not suitable because of problems with attachment to the foam material. In addition the range of travel for these devices would be far too low for this type of test.

(ii) Change in total distance between grips (via crosshead displacement) would not be suitable on its own in these experiments because lateral strains also needed to be measured.

(iii) Video extensometry systems are available from Instron. Such standard video extensometry could possibly work, however with a rubbery foam material the displacements could be much greater than those systems are designed for. It is possible that software could be modified to allow such a system to be used, although further information would be needed to confirm this. Cost was also an issue.

To overcome the measurement problem a high resolution method based on optical principles was successfully developed which enabled the extension ratios in the axial and lateral directions to be measured (λ_1 and λ_2). An arrangement of nine very small (~2.5mm) pointed adhesive markers were attached to the central region and a count of pixels was used to obtain strain measurements for both λ_1 and λ_2. A pair of additional fine adhesive pointers and a mm scale were attached and these were used to quickly estimate and set principal extension ratio λ_1 to the required values during tests. Please see figures 12 – 15.

5.3.3 Experimental procedure

Extension tests were performed very slowly. The extension was increased in graduated steps and paused for 30 seconds at each step to allow a photograph to be taken - a high resolution (10 megapixel) digital camera with tripod was used - and data was obtained from these photographs. For all tests the extension was increased until the principal extension ratio λ_1 had increased to 1.4. A scale level with the surface to be measured was visible in all photographs.

5.4 Simple compression tests

5.4.1 Apparatus and procedures

Simple compression tests were carried out on a 112.5mm cube of natural rubber latex foam which was constructed from a stack of nine squares each of thickness 12.5mm. The foam was the same natural rubber latex foam referred to previously that was supplied by Pentonville Foam. As was the case for the simple extension tests, the "skin" was peeled off prior to assembly of the cube.

The Instron 4204 test machine used for the simple extension tests was used to perform these compression tests. Some practical difficulties were encountered. One problem was with deformation measurement as this could not be done using standard extensometers available in the structures laboratory as their range was too small. To solve this problem the same high resolution optical method as used for the simple extension tests was used and, viewing from the front, this allowed deformation in the vertical and horizontal directions, 1 and 2 directions, to be measured. Please see figures 17 and 18. In figure 18 the pattern of 13 small markers is also shown. As in the simple extension tests, the simple compression tests were performed with a very low strain rate. The crosshead was moved in 2.5mm increments up to a maximum displacement of 67.5mm ($\lambda_1 = 0.4$). After each increment the crosshead was paused for 30 seconds after which a photograph was taken.

Contrary to expectation, initial tests indicated that end effects were small – there was little or no "barrelling" as judged by the markers and the outline of the test piece. There was also little or no "lead in" – initial nonlinearity - of force against displacement. For subsequent tests the positions of the top and bottom lines of three markers were not used in the calculation of extension ratios. Please refer to figure 18. The remaining markers were used to calculate principal extension ratio λ_2. Because the test apparatus was essentially rigid compared with the natural rubber latex foam test piece and because of the lack of end effects and "lead in", the displacement of the cross-head of the test machine was used to calculate principal extension ratio λ_1. Checks confirmed that this method of calculating λ_1 conformed with calculations of λ_1 by the markers method.

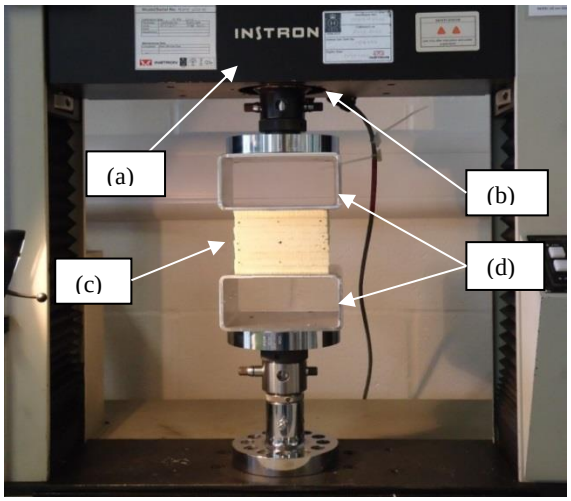

Figure 17. Apparatus for simple compression test.
(a) Moveable crosshead; (b) Load cell within crosshead;
(c) Natural rubber latex foam test piece; (d) Upper and lower platens.

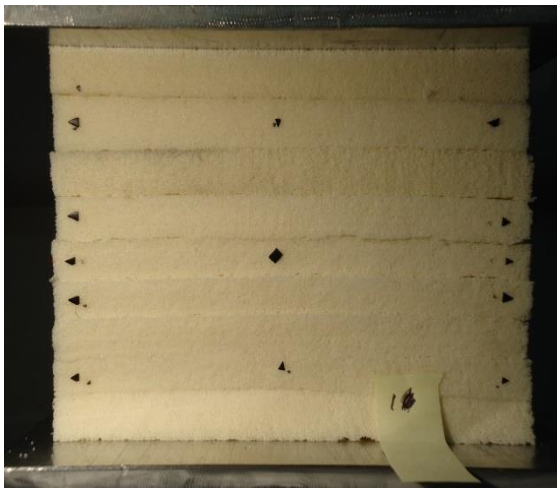

(a)

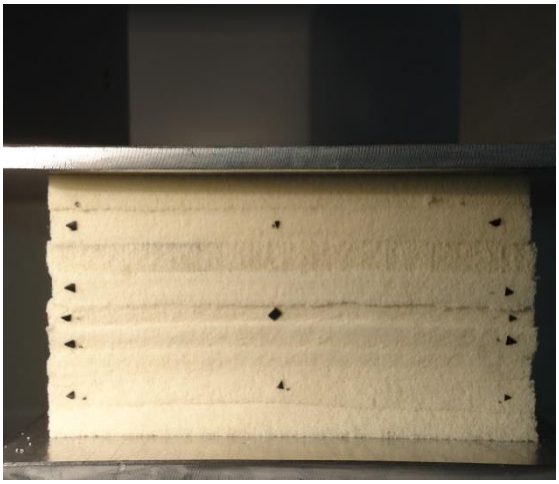

(b)

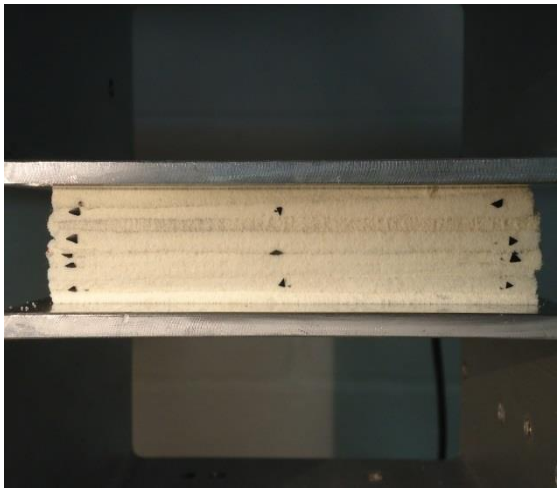

(c)

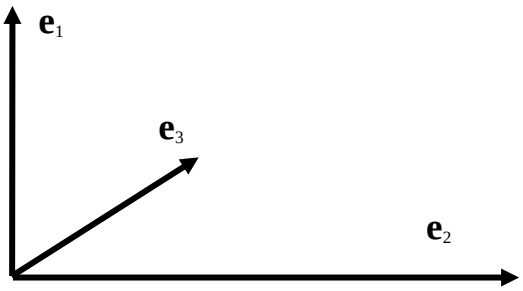

Figure 18. Simple compression test (a) $\lambda_1 = 1$ (b) $\lambda_1 = 0.7$ (c) $\lambda_1 = 0.4$ (d) coordinate system.

5.4.2 Results and discussion for simple extension and compression tests

The results from these tests were qualitatively similar to those of Gent & Thomas (1959, 1963) and figure 19 shows that in simple extension nominal stress against extension ratio (N against λ_1) is largely linear although my results show higher stiffness than theirs. The results from the compression tests were closer to those of Gent & Thomas than in extension. As expected, the foam used in my tests was much softer in compression than in extension. It should be noted that although there appeared to be a discontinuity of slope in N against λ_1 near $\lambda = 1$ closer inspection showed that although the slope did change quite sharply the change was continuous – with the change happening in the range $\lambda_1 \approx$ 0.995 to 0.990. As was the case for Gent & Thomas (1959, 1963), the dependence of nominal stress (N) against extension ratio (λ_1) in extension was remarkably near linear in the tests I performed. My data indicates the near linearity extending to the highest extension ratio reached: $\lambda_1 \approx 1.4$. The Young's modulus implied was about 100kPa.

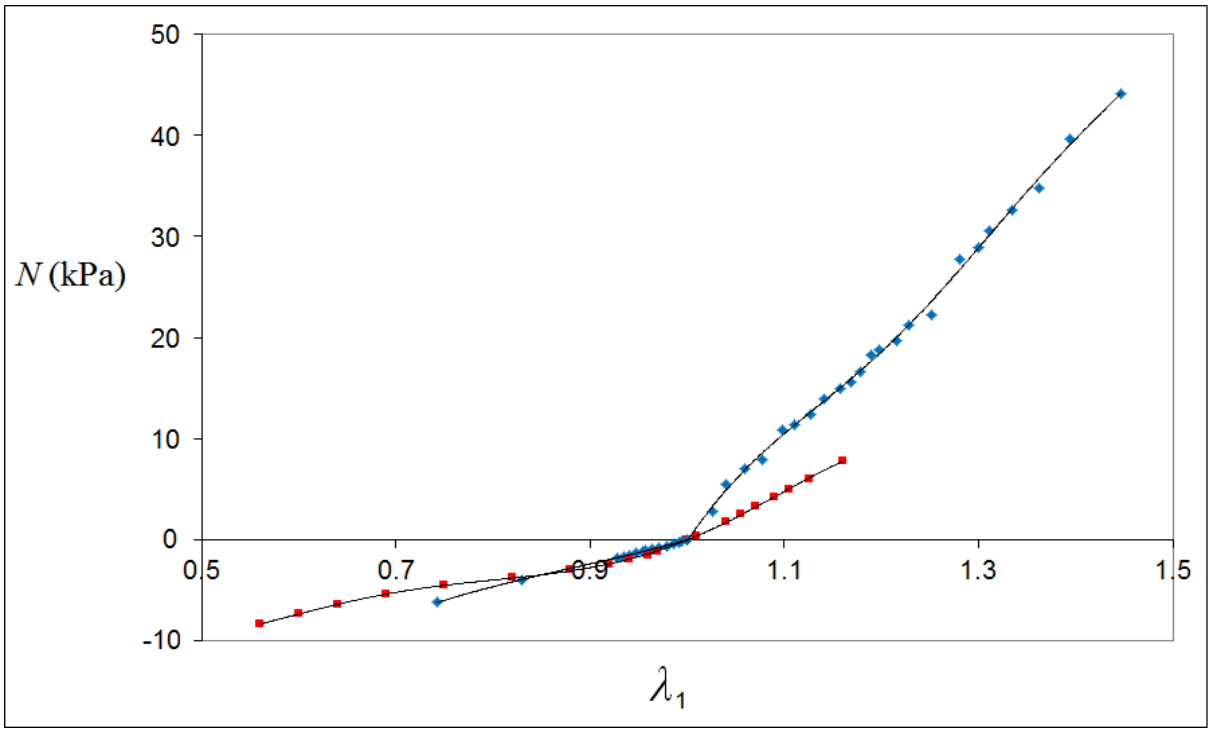

(Data from current tests: blue squares. Data of Gent & Thomas (1959, 1963): red squares.)

Figure 19. Nominal stress (1,1 component N) against extension ratio (λ_1).

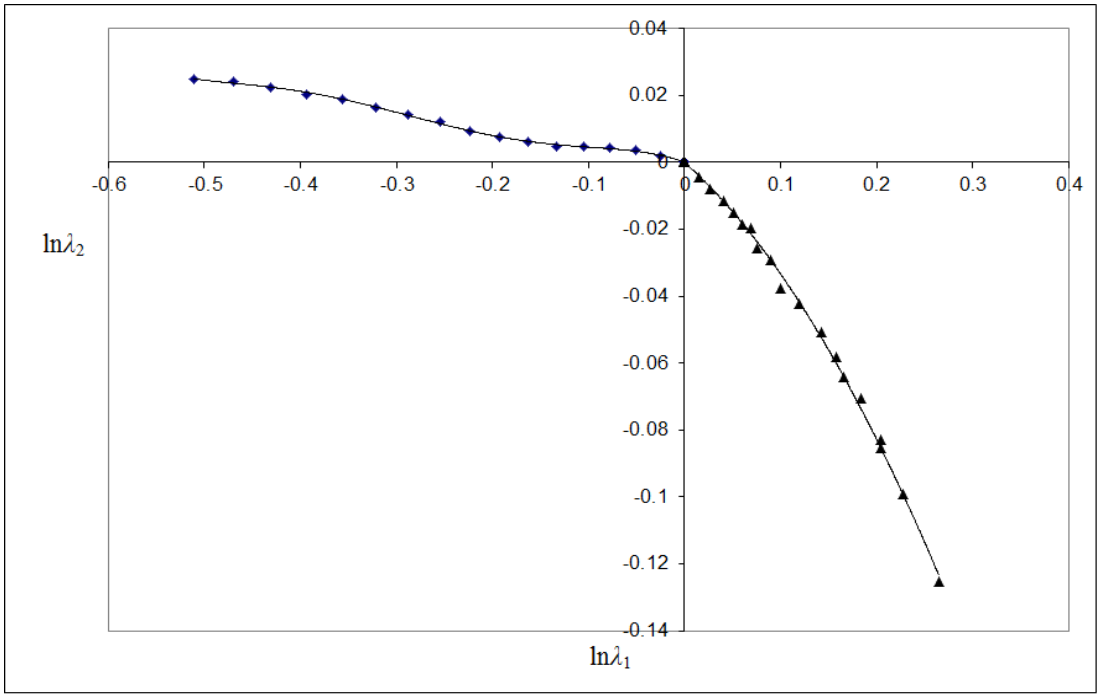

Figure 20. Lateral Hencky ($\ln\lambda_2$) strain against longitudinal Hencky strain ($\ln\lambda_1$).

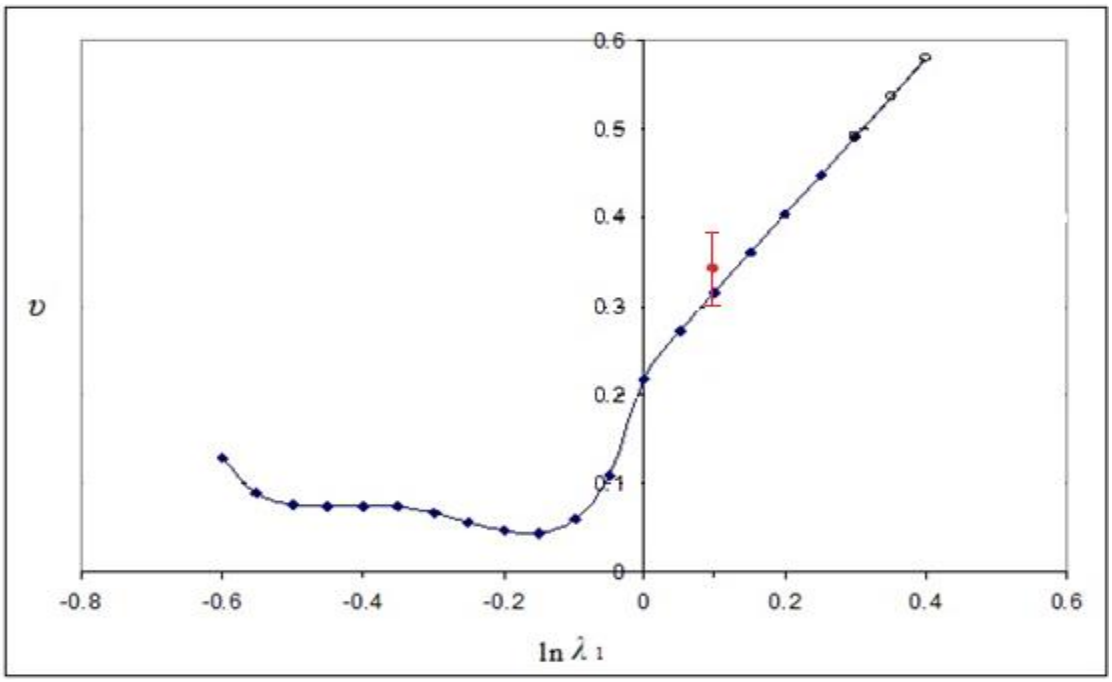

Figure 21. Poisson index (υ) versus $\ln\lambda_1$. (Open circles indicate test results beyond the normally expected value of $\upsilon = 0.5$. The red point is the summary value given by Gent & Thomas (1959); the standard deviation of their values is indicated by the error bar.)

Lateral logarithmic strain ($\ln\lambda_2$) against longitudinal logarithmic strain ($\ln\lambda_1$) is shown in Figure 20. From this the Poisson index (υ) against $\ln\lambda_1$ was found (figure 21). Unlike Blatz & Ko (1962) and Storakers (1986) my data did not show that υ was constant in extension, instead υ increased approximately linearly with $\ln\lambda_1$. υ increased from close to 0.22 to more than ½ - indicating volume reduction in extension, please see open circles on the graph - but not as much as El-Ratal & Mallick (1996) reported. The variation of υ with lambda λ_1 was surprising at first but the experiments were repeated several times and data carefully checked and rechecked and found to be as shown. This gives a high degree of confidence that the variation of υ shown in the figure is a true reflection of the behaviour of this natural rubber latex foam.

These results also indicate that υ falls quite steeply as $\ln\lambda_1$ decreases in simple compression however υ does not seem to reach quite such low values as those of Pierron (2010), although he did not quote his results in quite the same way. Examining stress and υ in figures 19 and 21at $\ln\lambda_1$ = 0.1 and -0.1 – i.e. λ_1 = 1.105 and 0.905 - it can be seen that ($\partial W/\partial \bar{I}_1 + \partial W/\partial \bar{I}_2$) is much lower even at this quite modest compression than in extension. Please refer to equation 4.2.5.

The available experimental data, including that generated in the course of this MPhil, supports the view that, depending on the precise material and test procedure, the Poisson index (υ) can be approximately constant with simple extension or can vary considerably. Also the available experimental data casts doubt on the view that the Poisson ratio of a rubbery foam - and therefore the Poisson index at very small strains - can always be taken as equal to 0.33.

TheYoung modulus ($E \approx 100$kPa) and the Poisson ratio ($\nu \approx 0.22$) of the natural rubber latex foam in simple extension will now be considered alongside its shear modulus measured in simple shear ($\mu \approx$ 15kPa). Using the usual infinitesimal strain relationship [$E = 2(1+\nu)\mu$] it can be seen that the foregoing values are mutually inconsistent: $2(1+\nu)\mu$ gives a value of 37 kPa whereas the value of E measured in simple extension was 100kPa. Calculations and calibrations were checked and rechecked and likely experimental errors were estimated at ≈ 10% at the very most and so could not account for the large discrepancy. Possible explanations for the large discrepancy could be: edge effects, some misalignment or slight pre -deformation in the simple shear test. It is noted that at very small strains the Poisson index - and so the Poisson ratio - is close to 0.2 but that υ changes quite strongly with strain. Could such behaviour indicate that the normal small strain relationships can no longer be used in the usual way for such complex materials? (See also Mott & Roland, 2009, 2013.) Indeed if a "compressive Young's modulus" "E_c" is calculated by dividing stress by engineering strain ($\varepsilon_1 = \lambda_1 - 1$)at λ_1 = 0.9 we get "E_c" ≈ 33kPa. This is in reasonable agreement with $2(1+\nu)\mu$ with $\mu \approx$ 15kPa as before and ν = 0. The question mark over agreement between the simple extension and shear tests does cast some doubt on some of the provisional conclusions reached from the shear tests.

5.5 Pressure-volume tests

5.5.1 Apparatus and procedures

Measurement of the pressure-volume behaviour of a highly compressible rubbery material would add to the data against which any constitutive law can be tested. Data for simple extension gives elastic constants Young's modulus (E) and Poisson's ratio (ν) and these constants can be examined with shear modulus (μ) and bulk modulus (K) for mutual consistency via the usual inter-relationships between small strain elastic constants. Accurate measurement of the pressure-volume behaviour of an open-cell rubbery foam would be very difficult so, as first step, the pressure-volume behaviour of two closed-cell materials were measured.

The materials studied were cork-filled polyurethane elastomers (PU); experiments were performed to measure the quasi-static pressure-volume (p-V) characteristics of these composite materials. Two grades (PR1 and PR5) were obtained from Dr Antunes of University of Minho, Portugal. PR1 and PR5 had densities of approximately 750 kg/m^3 and 585 kg/m^3 respectively and the density of the PU was around 960 kg/m^3 (ρ_1; Antunes, 2008). Please see figure 22 below.

Figure 22(a) PR1.

Figure 22(b) PR5.

The test-piece diameter is 30mm and this indicates scale in both photographs.

The density of cork (ρ_2) is expected to be around 200kg/m^3 and this value seems broadly consistent with formulations and density information given by Antunes (2008); Gibson et al (1981) give a value of 170kg/m^3 for the density of the cork they studied. The bulk modulus of polyurethane elastomer is expected to be approximately 2000MPa (Roland, 2011, page 201). Cork is an anisotropic material but approximately 0.25 seems to be a typical value of the Poisson ratio equivalent and around 3MPa seems to be a typical value of the shear modulus equivalent (Gibson et al, 1981). Using $K = \frac{2(1+\nu)}{3(1-2\nu)}\mu$ (Rees, 1990 and Appendix I) with ν = 0.25 and μ = 3 MPa gives a bulk modulus of around 5 MPa for cork. Consider now volume V of a cork-filled PU - with V_1 the volume of PU and V_2 the volume of cork. The density of the cork-filled PU

$$\rho = (V_1 \rho_1 + V_2 \rho_2)/V \quad (5.5.1)$$

$$\therefore \rho = \frac{V - V_2}{V}\rho_1 + \frac{V_2}{V}\rho_2 = \rho_1 - \frac{V_2}{V}\rho_1 + \frac{V_2}{V}\rho_2 \quad (5.5.2)$$

$$\therefore \rho - \rho_1 = -\frac{V_2}{V}(\rho_1 - \rho_2) \quad (5.5.3)$$

So the volume fraction of cork in PR1 can be estimated:

$$\frac{V_2}{V} = \frac{\rho_1 - \rho}{\rho_1 - \rho_2} \approx \frac{960 - 750}{960 - 200} = 0.28 \quad (5.5.4)$$

Similarly, the volume fraction of cork in PR5 can be estimated:

$$\frac{V_2}{V} \approx \frac{960 - 585}{960 - 200} = 0.49 \quad (5.5.5)$$

The volume strains of (1) the PU and (2) the cork within the composite ($\varepsilon_{Vi} = \Delta V_i/V_i = J\text{-}1$) are related to a purely spherical stress ($-p$):

$$\varepsilon_{V1} = -\frac{p}{K_1}; \varepsilon_{V2} = -\frac{p}{K_2}$$

$$\therefore \Delta V = \Delta V_1 + \Delta V_2 = -p\left(\frac{V_1}{K_1} + \frac{V_2}{K_2}\right) \quad (5.5.6)$$

$$\therefore \varepsilon_V = \frac{\Delta V}{V} = J - 1 = -p\left(\frac{V_1/V}{K_1} + \frac{V_2/V}{K_2}\right) \quad (5.5.7)$$

Here J is the volume ratio.

So PR1 and PR2 are expected to have bulk moduli

$$K \approx \left(\frac{0.72}{2000} + \frac{0.28}{5}\right)^{-1} \approx 18\,\text{MPa} \text{ and } K \approx \left(\frac{0.51}{2000} + \frac{0.49}{5}\right)^{-1} \approx 10\,\text{MPa} \quad (5.5.8)$$

respectively. So, PR1 is expected to have a bulk modulus just under twice that of PR2; this is because the polyurethane has a bulk modulus that is so much higher than cork's.

In order to minimise the influence on volume measurements of changes in container volume caused by pressure increase, a dilatometer was used within a pressure chamber (figure 23). The narrow window for viewing the dilatometer had an external width of 16mm and was fitted with 17mm thick borosilicate glass. The internal cavity within the aluminium pressure chamber closely followed the shape of the dilatometer which it accommodated – minimising the volume of the fluid (air) in the pressure chamber so as to minimise associated stored energy. The dilatometer (figure 24) - made in-house by attaching a graduated glass tube (from a 1ml pipette) to a standard (25ml) specific gravity (SG) bottle - was used within the pressure chamber. The primary pressurising fluid (PPF) within the dilatometer acting on the pieces of compressible rubbery composite was water. The pressure was applied - via air, the secondary pressurising fluid - using a 15 bar compressor and was monitored using a pressure

sensor with a range of 0-25 bar. A computer program allowed images to be captured from a modified webcam as well as recording the pressure. Data was logged at typically one measurement per second.

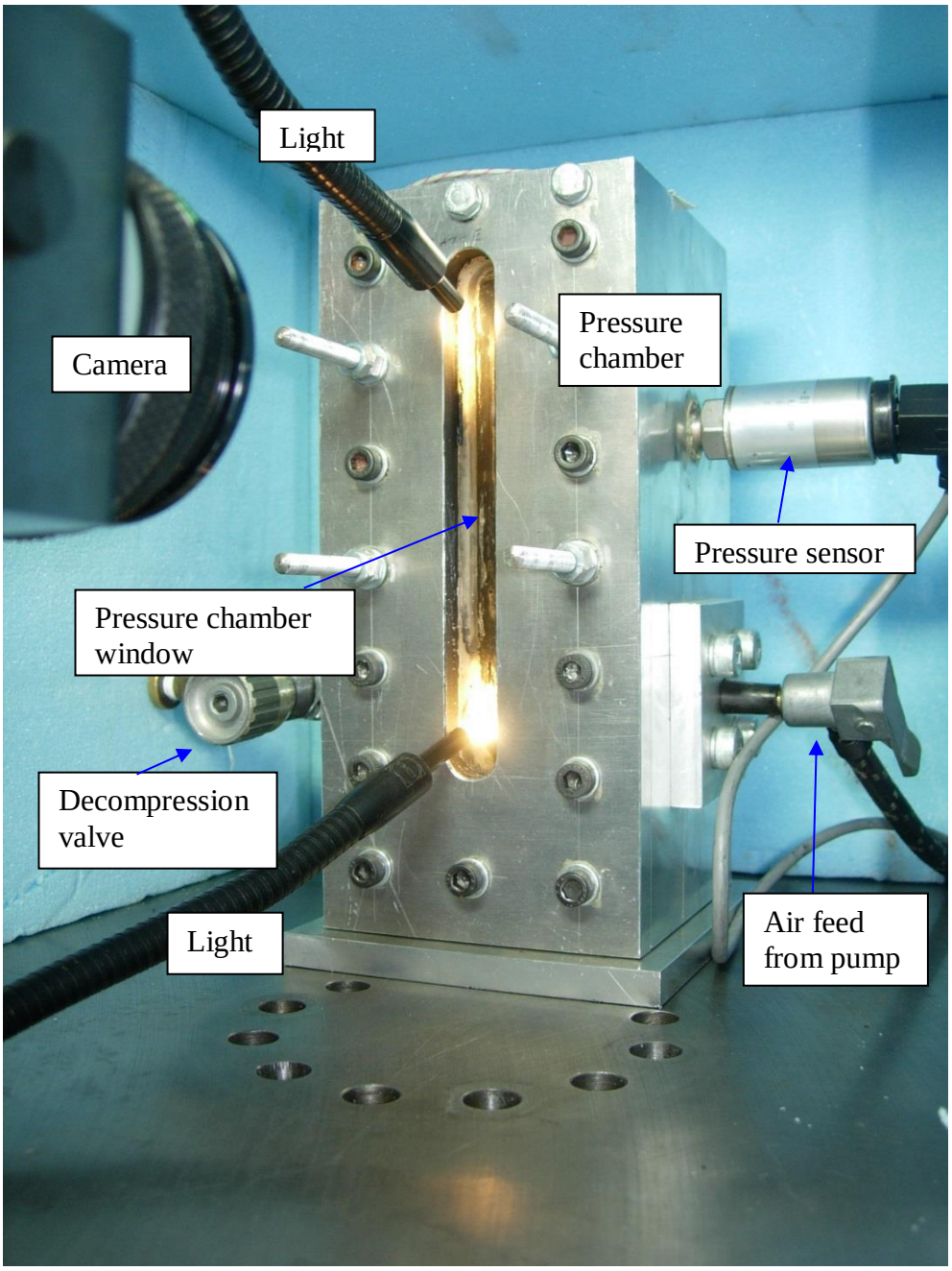

Figure 23. Photograph of the pressure chamber in situ, showing fibre-optic lights etc. The height of the pressure chamber was 235mm inclusive of the base - and its width and depth – both exclusive of the base - were 100mm and 110mm respectively; these dimensions indicate scale.

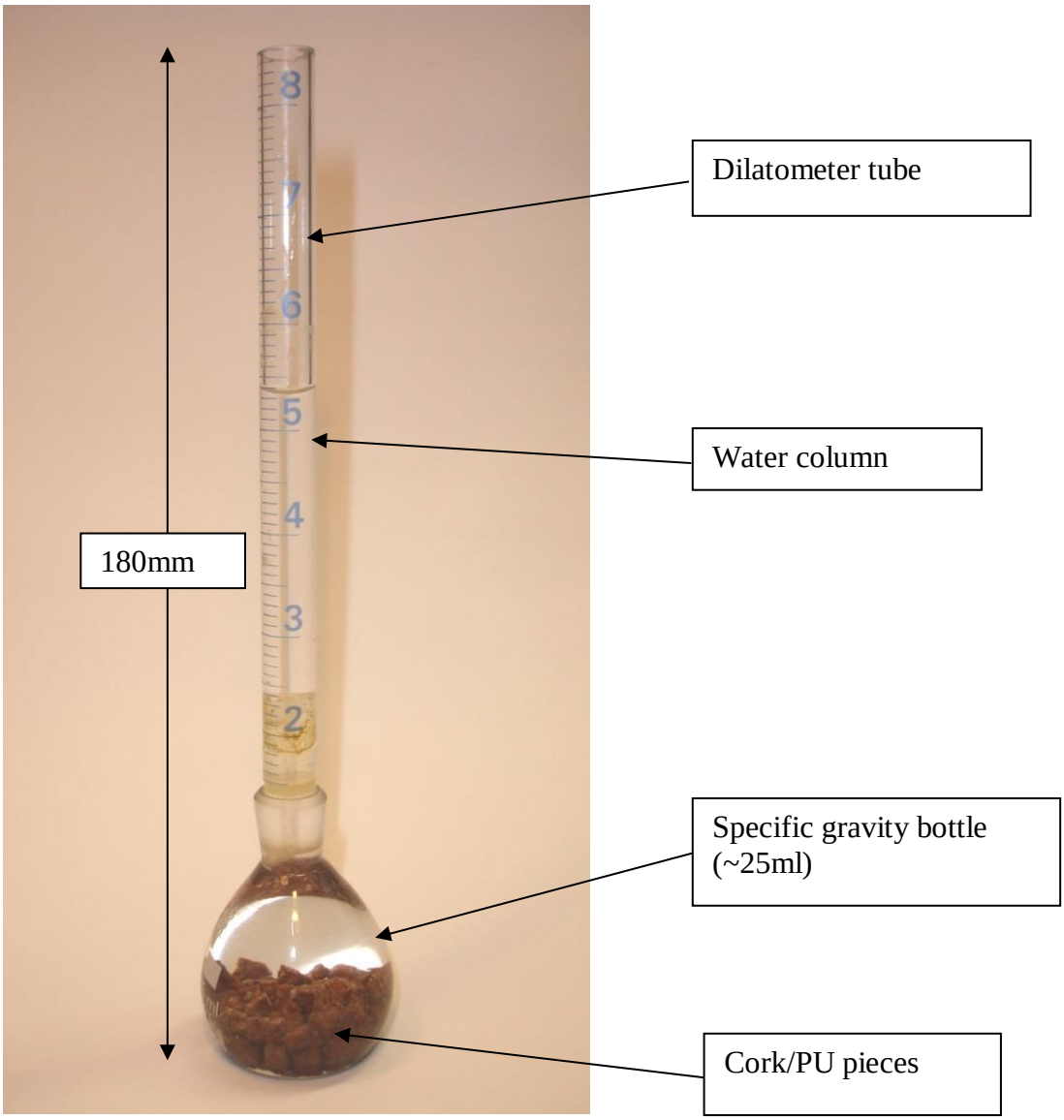

Figure 24**.** Dilatometer and cork-filled polyurethane (cork/PU) pieces.

5.5.2 Experimental method

Pieces of test material were chopped into smaller pieces (~ 2 x 2 x 6mm) to facilitate insertion into the dilatometer which was then topped up with the primary pressurising fluid (PPF). De-ionised water was used as the PPF to facilitate visibility and minimise health hazards. The volumes of the PPF and test material were determined by weight and knowledge of density. In all tests, recently-boiled water at or below 60°C was poured into the dilatometer; on cooling in situ this eliminated bubbles. In addition several cycles of a combination of gentle heating at ~50ºC - by placing the dilatometer into a water bath -

and degassing were performed to ensure all trapped air was removed from the dilatometer.

Next the dilatometer was sealed into the pressure chamber and left in a temperature-controlled room, at 23±3ºC, for 24 hours before pressure-volume (*p*-*V*) testing. The height of the PPF column was recorded via the computer triggered camera. The images and pressure values were logged onto the PC. Volume measurements were obtained via computer-generated cross-hairs acting on the captured images of the dilatometer tube (figure 25).

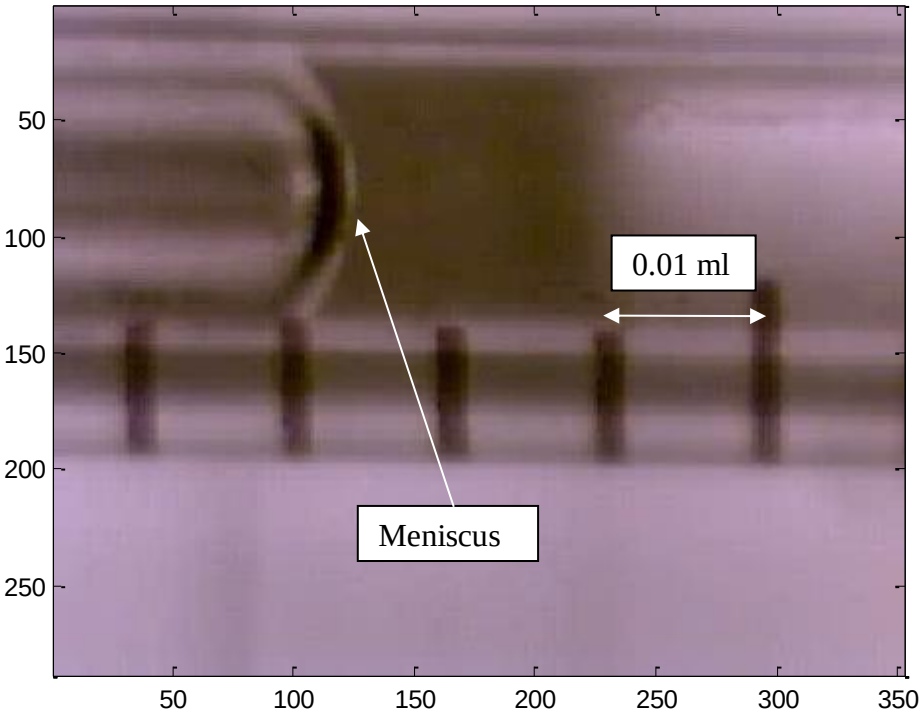

Figure 25. Typical image showing part of dilatometer tube.

(Axes show pixel numbers. Note image is rotated 90° anticlockwise).

Since water was being used as the PPF there was potential for significant differences between advancing and receding contact angles; in order to avoid this problem, extremely slow decompression was used; in addition a drop of paraffin oil was floated on the water in the graduated neck of the dilatometer as it produced a more stable contact angle, and therefore meniscus, than water alone during the *p*-*V* test.

For each *p*-*V* test the following procedure was followed: one cycle to 13 bar (above atmospheric pressure) and back to atmospheric pressure (p_{atm}) then rest for 24 hours; a repeat cycle to 13 bar and back to p_{atm} was then performed.

5.5.3 Results and discussion for pressure-volume tests

The normalised, or fractional, volume reduction was calculated: $\frac{V_0 - V}{V_0} = 1 - J$ (J is the volume ratio) and pressure-volume plots were made (figures 26 and 27).

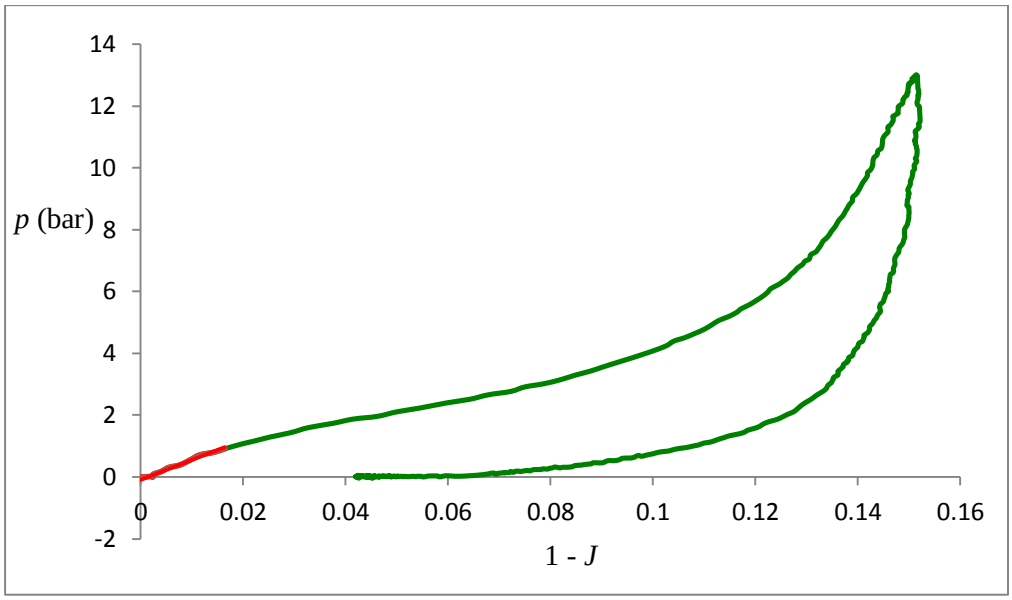

Figure 26. Plot of pressure against fractional decrease in volume (1-*J*) for cork filled polyurethane, PR1.

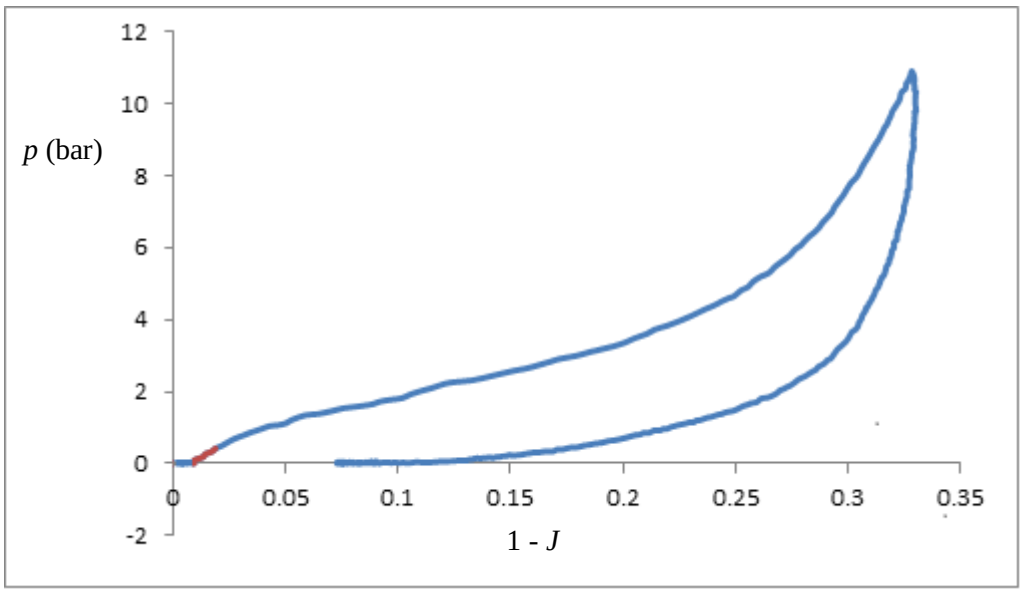

Figure 27. Plot of pressure against fractional decrease in volume (1-*J*) for cork filled polyurethane, PR5.

The bulk modulus (K) for each of the two cork-filled materials was found by fitting a straight line, by least squares, to the low strain portion of each of the plots of pressure (p) against volume strain ($1-J$) - with the "lead in" sections of the curves ignored - shown in red in figures 26 and 27. A value for K of 6.4+/-0.2 MPa was found for PR1 and a value for K of 2+/-0.2 MPa was found for PR2. Thus the estimated value for K was almost three times the measured value for PR1. For PR5 the estimated value for K was five times the measured value. The measured values for K of the cork-filled PU materials correspond to a value of around 1MPa for the effective bulk modulus of cork. The low experimental values for K might also be because there were voids in the finished cork-filled polyurethane materials that were additional to those in the cork cells themselves, or might be because of other effects of local inhomogeneity or anisotropy.

At values of $1-J$ above about 0.03, the curve of p against $1-J$ is significantly non-linear for both composite materials tested. The gradient of the pressure-volume curve first begins to decrease; this probably corresponds to buckling of cell walls within the cork material. At large volume reductions ($1-J \approx 0.12$ for PR1 and $1-J \approx 0.25$ for PR5) the gradient becomes much steeper and this probably corresponds to cells closing within the cork. There is also a high degree of hysteresis shown in the results. This is probably due to hysteresis in the p-V characteristic of the cork material – Gibson et al (1981) also observed high hysteresis for pure cork in simple compression. Other factors contributing to hysteresis could be slippage and friction at the polymer/cork interface and/or mass transport of water and/or air in the cork-filled PU.

6 CONCLUSIONS & RECOMMENDATIONS

Published experimental data and experiments done in these MPhil studies support the view that, depending on the precise rubbery foam and test procedure used, the Poisson index (υ) can either be approximately constant as length more than doubles in simple extension or can increase considerably with stretch and exceed ½ - as here. Published experimental data and experiments done in these MPhil studies also cast doubt on the view that the Poisson index (ν) – and therefore υ at very small strains – can reliably be taken to be equal to be 0.33 for a rubbery foam. For the normal open-cell natural rubber latex foam (*the foam*) studied here, it was found that ν was close to 0.22.

For *the foam* it has been confirmed that υ drops substantially at strains of a few percent in simple; υ remained below 0.1 until *the foam* was at less than half its original height. The results also indicate that $\partial W / \partial \bar{I}_1 + \partial W / \partial \bar{I}_2$ drops sharply at strains ~1% or less as *the foam* goes into simple compression. Here W is the strain energy density and $\bar{I}_1$ and $\bar{I}_2$ are the first and second principal invariants of the volume neutralised Cauchy-Green deformation tensor.

The tests used by Blatz & Ko (1962) and Storåckers (1986) were not adequate for thorough examination of the suitability of the types of constitutive laws they considered for rubbery foams. If J is volume ratio, the coverage of $\bar{I}_1, \bar{I}_2, J$ space was poor: $J < 1$ was not examined and the loci for fixed width extension (FWE) and simple extension were likely to have had rather similar $\bar{I}_1$ and $\bar{I}_2$ values. Also, only one component of stress was measured in FWE.

Theoretical examination of stress tensors for isotropic ideally elastic materials indicated that simple shear was a promising mode of test for probing aspects of the validity of constitutive laws – especially those using the Poisson index (υ).

Simple shear experiments on *the foam* were performed in relation to a class of constitutive law using υ (generalised Blatz & Ko laws, GBK) and one in which the dependence of W on shape changes and its dependence on volume changes are mutually independent (shape-volume uncoupled). The results indicated that $\partial W / \partial \bar{I}_1 + \partial W / \partial \bar{I}_2$ varied only weakly with shear strain (γ). However the results also suggested that neither GBK nor shape-volume uncoupled laws were valid. The results should, though, be treated with some caution because at small strains it was found that $E >> 2(1 + \nu)\mu$. Here μ is the shear modulus, ν the Poisson ratio and E the Young modulus in simple extension. However it was found that $E_C \approx 2(1+\nu_C)\mu$ where ν_C is the apparent Poisson ratio and E_C the apparent Young modulus of *the foam* at approximately 10% simple compression.

More work is needed to determine the behaviour of rubbery foams in more detail so that constitutive laws can be fully checked and to prepare the path for development of new ones.

APPENDIX I. SMALL STRAIN ELASTICITY (THE FRAMEWORK OF ELASTICITY THEORY AT INFINITESIMAL STRAINS FOR ISOTROPIC MATERIALS SOMETIMES CALLED THE GENERALISED HOOKEAN FRAMEWORK OR THE LAMÉ FRAMEWORK)

Linear elastic, isotropic solids, are characterised, at infinitesimal strains, by any two of five very commonly used elastic constants: Λ, μ, K, E and ν : the 1st Lamé constant, the 2nd Lamé constant or shear modulus, the bulk modulus, the Young modulus and the Poisson ratio. Equations relating the constants include:

$$E = 2(1+\nu)\mu \quad \text{(a)}; \quad K = \frac{2(1+\nu)}{3(1-2\nu)}\mu \quad \text{(b)}; \quad K = \frac{E}{3(1-2\nu)} \quad \text{(c)}; \quad \nu = \frac{3K-2\mu}{2(3K+\mu)} \quad \text{(d)};$$

$$\Lambda = K - \frac{2}{3}\mu = \frac{2\nu\mu}{1-2\nu} = \frac{\nu E}{(1+\nu)(1-2\nu)} \quad \text{(e)};$$

$$\frac{9}{E} = \frac{3}{\mu} + \frac{1}{K} \quad \text{(f)}; \qquad (\mathbf{I}.1)$$

(Rees, 1990; Gould, 2013).

E, the Young modulus, is given by direct stress divided by the, longitudinal, direct strain in simple extension or simple compression - see (a) in figure 2 in the main text or Appendix II.

ν, the Poisson ratio, is given by minus the lateral strain divided by the, longitudinal, direct strain in simple extension or simple compression – see (a) in figure 2 in the main text or Appendix II.

μ, the second Lamé constant or shear modulus or rigidity modulus is given by the shear stress divided by the shear strain in simple shear– see (e) in figure 2 in the main text or Appendix II.

K is the bulk modulus: the fractional increase in volume (*J*-1) divided by the increase in applied spherical stress ("hydrostatic" component of stress, e.g. decrease in applied pressure) – see (f) in figure 2 or Appendix II.

Other elastic constants are sometimes used. The plane modulus (*M*) is an example (Mott & Roland, 2009):

$$M = K + \frac{4}{3}\mu \qquad (\mathbf{I}.2)$$

M is given by the direct stress divided by direct strain obtained when a piece of material undergoes (homogeneous) compression or extension at fixed cross section. – see (c) in figure 2 in the main text or Appendix II.

Now,

$$\sigma_{33} = \Lambda\varepsilon_{11} + \Lambda\varepsilon_{22} + (2\mu + \Lambda)\varepsilon_{33}$$
$$= \Lambda\varepsilon_{11} + \Lambda\varepsilon_{22} + \left(\frac{1-2\nu}{\nu}\Lambda + \Lambda\right)\varepsilon_{33}$$

So, if there is plane stress $\sigma_{33} = 0$:

$$\varepsilon_{33} = \frac{-\nu}{1-\nu}(\varepsilon_{11} + \varepsilon_{22}) \qquad (\mathbf{I}.3)$$

APPENDIX II DESCRIPTION OF TESTING METHODS

The following are commonly used modes of test for rubbery materials. In each of (a) to (e) the displacements of the ends of the gauge length and/or of the whole test piece are recorded and the force is recorded.

a. *Simple extension test:* a relatively long, thin specimen is secured at each end in a tensile or universal test machine and loaded in tension.

b. *Fixed width or planar extension test:* a wide thin piece of material is gripped in a universal test machine. The width should be much greater than the length to minimise end effects. The width should in turn be much greater than the thickness.

c. *Constant cross section or plane compression test:* a relatively long and wide but thin piece of material is bonded between rigid plates to form the test piece. The test piece loaded in a compression or universal test machine.

d. *General biaxial extension test:* a square sheet of material is loaded in two axis directions simultaneously. The faces in the positive and negative third axis directions are stress free. For this, specialist apparatus is required to allow each edge to be securely held so that load can be applied whilst allowing the edges to extend during the test. This can be achieved using a series of fixing points along each edge connected by long cables to an actuator or using another suitable mechanism. If the strains are equal for the two axes, there is equibiaxial extension.

e. *Simple shear:* a relatively thin piece of material is bonded between plates and so that one plate is displaced linearly relative to the other but the distance between the plates (*t)* remains constant. This test can be conducted in a universal or compression test machine or using specialist apparatus.

f. *Pure volume decrease:* a piece of material is tested in a pressure chamber. The increase in pressure and the decrease in volume of the piece of material are carefully measured.

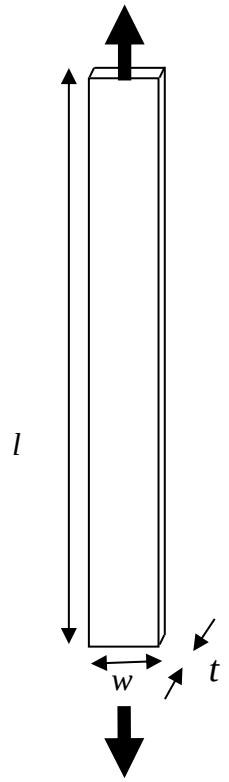

a. Simple extension
($l >> w$; $l >> t$)

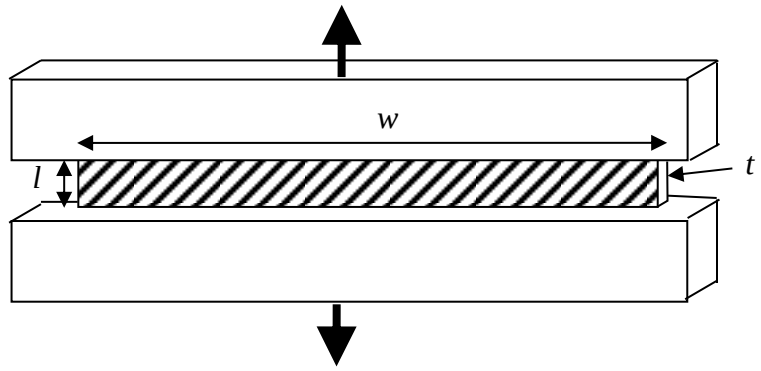

b. Fixed width or planar extension
($w >> l > t$ to minimise end effect)

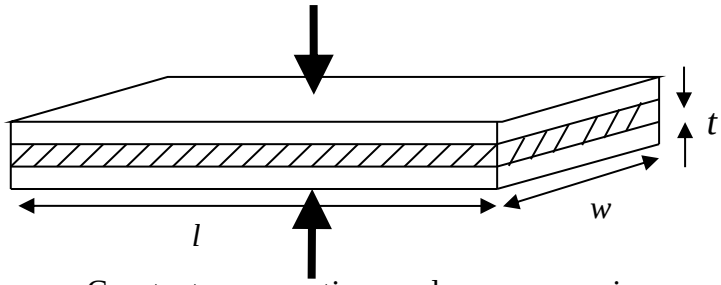

c. Constant cross section or plane compression
(l & $w >> t$ and bonded to rigid plates)

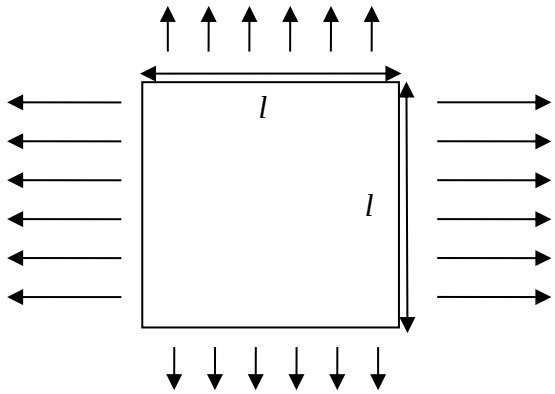

d. General biaxial extension

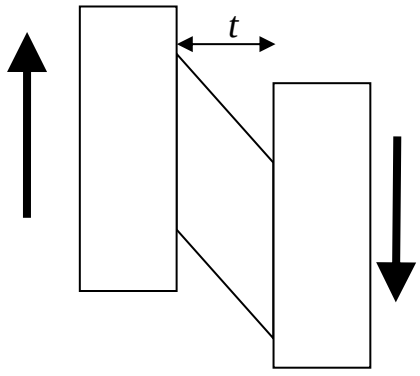

e. Simple shear
(l & $w >> t$ and bonded to plates - see (c))

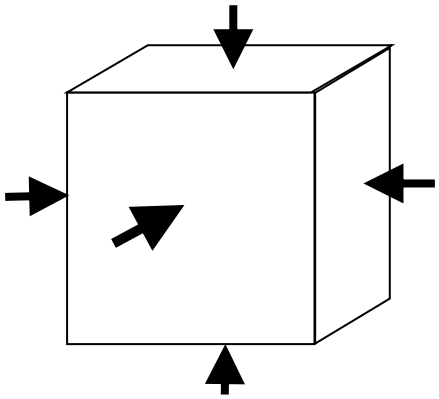

f. Pure volume decrease

Figure II.I. Modes of test for material properties

APPENDIX III MEASURES OF DEFORMATION FOR FINITE DEFORMATION

The starting point for many measures of finite deformation is the deformation gradient **F** also sometimes written **g.**

The deformation gradient tensor is written $\mathbf{F} = \frac{\partial \mathbf{x}}{\partial \mathbf{X}}$ or $F_{ij} = \frac{\partial x_i}{\partial X_j}$ in component form.

For simple pure homogeneous strain, the **F** matrix is a diagonal matrix of the principal extension ratios (or stretches) λ_i. For simple shear **F** is not symmetrical.

B, sometimes written **b**, is the Cauchy tensor or left Cauchy-Green deformation tensor. $\mathbf{B} = \mathbf{F}\mathbf{F}^{\mathrm{T}}$.

The matrices for **B** and also $\mathbf{B}^{-1}$ are symmetrical for simple shear;

C, sometimes written **G**, is the Green tensor or right Cauchy-Green deformation tensor. $\mathbf{C} = \mathbf{F}^{\mathrm{T}}\mathbf{F}$.

The volume neutralised deformation tensors do not change if just the volume changes:

$\overline{\mathbf{F}} = J^{-1/3}\mathbf{F}; \overline{\mathbf{B}} = J^{-2/3}\mathbf{B}; \ \overline{\mathbf{C}} = J^{-2/3}\mathbf{C}$. J is the volume ratio.

I_1, I_2, I_3 are the principal scalar "invariants" of **B** or **C**. And $I_3 = J^2$.

$\lambda_1^2, \lambda_2^2, \lambda_3^2$, the squares of the principal extension ratios, are the eigenvalues of **B** or **C**.

Volume neutralised extension ratios $\overline{\lambda}_i = \lambda_i / J^{1/3}$

$\overline{\lambda}_1^2, \overline{\lambda}_2^2, \overline{\lambda}_3^2$ (squares of the volume neutralised principal extension ratios) are the eigenvalues of $\overline{\mathbf{B}}$ or $\overline{\mathbf{C}}$.

Principal invariants $\bar{I}_1$ and $\bar{I}_2$ are the principal scalar invariants of $\overline{\mathbf{B}}$ or $\overline{\mathbf{C}}$.

$\bar{I}_1 = I_1 / J^{2/3}; \bar{I}_2 = I_2 / J^{4/3}$

$\bar{I}_1 = \overline{\lambda}_1^2 + \overline{\lambda}_2^2 + \overline{\lambda}_3^2$ indicates the amount of shape change in direct form.

$\bar{I}_2 = \overline{\lambda}_1^{-2} + \overline{\lambda}_2^{-2} + \overline{\lambda}_3^{-2}$ indicates the amount of shape change in inverse form.

$J = \lambda_1 \lambda_2 \lambda_3$ indicates the amount of volume change.

In combination, $\bar{I}_1$ and $\bar{I}_2$ can be used to distinguish between different types of shape change.

In simple shear $\bar{I}_1 = \bar{I}_2 = \gamma^2 + 3$.

At small strain there is no distinction between $\bar{I}_1$ and $\bar{I}_2$.

Rivlin (1992) explains why I_1, I_2, I_3 are sufficient to give a strain energy density function W that is completely general for an isotropic, elastic continuum. Use of I_1, I_2, I_3 or especially of $\bar{I}_1$, $\bar{I}_2$ and J, mainstream in large strain FEA, enables relatively easy calculation of complicated cases such as simple shear.

The Hencky principal strains are sometimes used to represent finite deformation:

$e_i = \ln \lambda_i$. At infinitesimal strains, $e_i = \lambda_i - 1 = \varepsilon_i$ the engineering strain.

APPENDIX IV STRESS AT FINITE DEFORMATION

Calculating stress from derivatives of the strain energy density

Bower (2009) gives the following formula for Cauchy stress in component form:

$$\sigma_{ij} = \frac{2}{J^{5/3}}\left(\frac{\partial W}{\partial \bar{I}_1} + \bar{I}_1 \frac{\partial W}{\partial \bar{I}_2}\right)B_{ij} - \frac{2}{3J}\left(\bar{I}_1 \frac{\partial W}{\partial \bar{I}_1} + 2\bar{I}_2 \frac{\partial W}{\partial \bar{I}_2}\right)\delta_{ij} - \frac{2}{J^{7/3}}\frac{\partial W}{\partial \bar{I}_2} B_{ik}B_{kj} + \frac{\partial W}{\partial J}\delta_{ij} \quad \text{(IV.I)}$$

Here B_{ij} is the left Cauchy Green tensor **B** in component form and δ_{ij} is the Kronecker delta. δ_{ij} = 1 if $i = j$ and is zero otherwise, so δ_{ij} is **I** in component form.
Now the Finger tensor is related to the volume neutralised left Cauchy Green deformation tensor by:

$$\mathbf{B} = J^{2/3}\overline{\mathbf{B}}$$

So

$$\sigma_{ij} = \frac{2}{J}\frac{\partial W}{\partial \bar{I}_1}\overline{B}_{ij} + \frac{2}{J}\bar{I}_1\frac{\partial W}{\partial \bar{I}_2}\overline{B}_{ij} - \frac{2}{3J}\bar{I}_1\frac{\partial W}{\partial \bar{I}_1}\delta_{ij} - \frac{4}{3J}\bar{I}_2\frac{\partial W}{\partial \bar{I}_2}\delta_{ij} - \frac{2}{J}\frac{\partial W}{\partial \bar{I}_2}\overline{B}_{ik}\overline{B}_{kj} + \frac{\partial W}{\partial J}\delta_{ij} \quad \text{(IV.2)}$$

Therefore, writing $\overline{\mathbf{B}} \cdot \overline{\mathbf{B}} = \overline{\mathbf{B}}^2$:

$$\boldsymbol{\sigma} = \frac{2}{J}\frac{\partial W}{\partial \bar{I}_1}\overline{\mathbf{B}} + \frac{2}{J}\bar{I}_1\frac{\partial W}{\partial \bar{I}_2}\overline{\mathbf{B}} - \frac{2}{3J}\bar{I}_1\frac{\partial W}{\partial \bar{I}_1}\mathbf{I} - \frac{4}{3J}\bar{I}_2\frac{\partial W}{\partial \bar{I}_2}\mathbf{I} - \frac{2}{J}\frac{\partial W}{\partial \bar{I}_2}\overline{\mathbf{B}}^2 + \frac{\partial W}{\partial J}\mathbf{I} \quad \text{(IV.3)}$$

$$\therefore \boldsymbol{\sigma} = \frac{2}{J}\left[\overline{\mathbf{B}} - \frac{1}{3}\bar{I}_1\mathbf{I}\right]\frac{\partial W}{\partial \bar{I}_1} + \frac{2}{J}\left[\bar{I}_1\overline{\mathbf{B}} - \overline{\mathbf{B}}^2 - \frac{2}{3}\bar{I}_2\mathbf{I}\right]\frac{\partial W}{\partial \bar{I}_2} + \frac{\partial W}{\partial J}\mathbf{I} \quad \text{(IV.4)}$$

The above equation, one of many used to find stress from derivatives of the strain energy density *W*, is widely used in this dissertation. See also Chagnon (2003).

APPENDIX V STRESS PREDICTIONS FOR A GENERALISED BLATZ & KO (GBK) AND OTHER FORMS

V.1 Cases of pure homogeneous strain for a generalised Blatz & Ko (GBK) and other materials

Three particular cases of plane stress general biaxial deformation will now be considered: simple extension/compression (SE/C), equibiaxial extension/compression (EBE/C) and fixed width extension/compression (FWE/C). Please refer to Figure 2 in the main text or to Appendix II for diagrams of test modes.

V.1.1 Simple extension/compression (SE/C)

Consider extension/compression in the 1 direction and put $\lambda_1 = \lambda$

$$\text{Now, } \bar{\lambda}_1\bar{\lambda}_2\bar{\lambda}_3 = \frac{\lambda_1\lambda_2\lambda_3}{J^{1/3}J^{1/3}J^{1/3}} = \frac{J}{J} = 1$$

$$\text{Also, by symmetry, } \lambda_2 = \lambda_3$$

$$\therefore \bar{\lambda}_2 = \bar{\lambda}_3 = \bar{\lambda}^{-1/2}$$

The volume neutralised deformation gradient

$$\bar{\mathbf{F}} = \mathbf{F}/J^{1/3} = \begin{bmatrix} \bar{\lambda} & 0 & 0 \\ 0 & \bar{\lambda}^{-1/2} & 0 \\ 0 & 0 & \bar{\lambda}^{-1/2} \end{bmatrix} = \bar{\mathbf{F}}^T$$

So the volume neutralised left Cauchy-Green deformation tensor

$$\bar{\mathbf{B}} = \bar{\mathbf{F}}\,\bar{\mathbf{F}}^T = \begin{bmatrix} \bar{\lambda}^2 & 0 & 0 \\ 0 & \bar{\lambda}^{-1} & 0 \\ 0 & 0 & \bar{\lambda}^{-1} \end{bmatrix} \qquad \text{(V.1.1.1)}$$

and

$$\bar{\mathbf{B}}^2 = \begin{bmatrix} \bar{\lambda}^4 & 0 & 0 \\ 0 & \bar{\lambda}^{-2} & 0 \\ 0 & 0 & \bar{\lambda}^{-2} \end{bmatrix} \qquad \text{(V.1.1.2)}$$

The first two principal invariants of $\bar{\mathbf{B}}$ are

$$\bar{I}_1 = \bar{\lambda}_1^{\,2} + \bar{\lambda}_2^{\,2} + \bar{\lambda}_3^{\,2} = \bar{\lambda}^{\,2} + 2\bar{\lambda}^{\,-1}$$

$$\bar{I}_2 = \bar{\lambda}_2^{\,2}\bar{\lambda}_3^{\,2} + \bar{\lambda}_1^{\,2}\bar{\lambda}_3^{\,2} + \bar{\lambda}_1^{\,2}\bar{\lambda}_2^{\,2} = \bar{\lambda}_1^{\,-2} + \bar{\lambda}_2^{\,-2} + \bar{\lambda}_3^{\,-2} = \bar{\lambda}^{\,-2} + 2\bar{\lambda}$$

For a GBK material in plane stress general biaxial deformation

$\lambda_3 = (\lambda_1\lambda_2)^{\frac{-\upsilon}{1-\upsilon}}$ and $J = \lambda_1\lambda_2\lambda_3 = \lambda_1\lambda_2(\lambda_1\lambda_2)^{\frac{-\upsilon}{1-\upsilon}} = (\lambda_1\lambda_2)^{\frac{1-2\upsilon}{1-\upsilon}}$

In the particular case of simple extension, $\lambda_3 = \lambda_2$.

So $\lambda_2 = (\lambda_1\lambda_2)^{\frac{-\upsilon}{1-\upsilon}} \therefore \lambda_2^{\frac{1-\upsilon}{1-\upsilon}} = \lambda_1^{\frac{-\upsilon}{1-\upsilon}}\lambda_2^{\frac{-\upsilon}{1-\upsilon}} \therefore \lambda_2^{\frac{1-\upsilon+\upsilon}{1-\upsilon}} = \lambda_2^{\frac{1}{1-\upsilon}} = \lambda_1^{\frac{-\upsilon}{1-\upsilon}} \therefore \lambda_2 = \lambda_3 = \lambda_1^{-\upsilon}$

and the volume ratio $J = \lambda_1\lambda_2\lambda_3 = \lambda\lambda^{-\upsilon}\lambda^{-\upsilon} = \lambda^{1-2\upsilon}$

$$\therefore J^{-1} = \lambda^{-(1-2\upsilon)} = \lambda^{-1+2\upsilon} \qquad \text{(V.1.1.3)}$$

and $J^{-1/3} = \lambda^{-\frac{1-2\upsilon}{3}}$

Also $r = \frac{2}{3}.\frac{1+\upsilon}{1-2\upsilon}$ and equals K/μ at infinitesimal strain so

$$J^{-r} = J^{-\frac{2}{3}.\frac{1+\upsilon}{1-2\upsilon}} = \left(\lambda^{1-2\upsilon}\right)^{-\frac{2}{3}.\frac{1+\upsilon}{1-2\upsilon}} = \lambda^{-\frac{2}{3}.\frac{(1-2\upsilon)(1+\upsilon)}{1-2\upsilon}} = \lambda^{-\frac{2}{3}.(1+\upsilon)} \qquad \text{(V.1.1.4)}$$

$$\text{and } J^{r} = \lambda^{\frac{2}{3}.(1+\upsilon)} \qquad \text{(V.1.1.5)}$$

Also $\bar{\lambda} = \lambda J^{-1/3} = \lambda.\lambda^{\frac{-1+2\upsilon}{3}} = \lambda^{\frac{2+2\upsilon}{3}} = \lambda^{\frac{2}{3}(1+\upsilon)}$,

$\bar{\lambda}^2 = \lambda^{\frac{4}{3}(1+\upsilon)}$,

$\bar{\lambda}^4 = \lambda^{\frac{8}{3}(1+\upsilon)}$,

$\bar{\lambda}^{-1} = \lambda^{-\frac{2}{3}(1+\upsilon)}$,

$\bar{\lambda}^{-2} = \lambda^{-\frac{4}{3}(1+\upsilon)}$.

$$\bar{\mathbf{B}} = \begin{bmatrix} \lambda^{\frac{4}{3}.(1+\upsilon)} & 0 & 0 \\ 0 & \lambda^{-\frac{2}{3}.(1+\upsilon)} & 0 \\ 0 & 0 & \lambda^{-\frac{2}{3}.(1+\upsilon)} \end{bmatrix} \qquad \text{(V.1.1.6)}$$

$$\bar{\mathbf{B}}^2 = \begin{bmatrix} \lambda^{\frac{8}{3}.(1+\upsilon)} & 0 & 0 \\ 0 & \lambda^{-\frac{4}{3}.(1+\upsilon)} & 0 \\ 0 & 0 & \lambda^{-\frac{4}{3}.(1+\upsilon)} \end{bmatrix} \qquad \text{(V.1.1.7)}$$

So $\bar{I}_1 = \lambda^{\frac{4}{3}(1+\upsilon)} + 2\lambda^{-\frac{2}{3}(1+\upsilon)}$ (V.1.1.8)

and $\bar{I}_2 = \lambda^{-\frac{4}{3}(1+\upsilon)} + 2\lambda^{\frac{2}{3}(1+\upsilon)}$ (V.1.1.9)

The Cauchy stress for a GBK material can be written:

$$\boldsymbol{\sigma} = \frac{2}{J}\left[\bar{\mathbf{B}} - J^{-r}\mathbf{I}\right]\frac{\partial W}{\partial \bar{I}_1} + \frac{2}{J}\left[\bar{I}_1\bar{\mathbf{B}} - \bar{\mathbf{B}}^2 + \left(J^{r} - \bar{I}_2\right)\mathbf{I}\right]\frac{\partial W}{\partial \bar{I}_2} = \text{Term1}.\frac{\partial W}{\partial \bar{I}_1} + \text{Term2}.\frac{\partial W}{\partial \bar{I}_2} \qquad \text{(V.1.1.10)}$$

Now we substitute V.1.1.1 to V.1.1.9 into V.1.1.10. Term by term we get the following.

$$\text{Term1} = \frac{2}{J}\left[\bar{\mathbf{B}} - J^{-r}\mathbf{I}\right]$$

$$= 2\lambda^{-1+2\upsilon}\begin{bmatrix} \lambda^{\frac{4}{3}(1+\upsilon)} & 0 & 0 \\ 0 & \lambda^{-\frac{2}{3}(1+\upsilon)} & 0 \\ 0 & 0 & \lambda^{-\frac{2}{3}(1+\upsilon)} \end{bmatrix} - \lambda^{-\frac{2}{3}(1+\upsilon)}\begin{bmatrix} 1 & 0 & 0 \\ 0 & 1 & 0 \\ 0 & 0 & 1 \end{bmatrix}$$

$$= 2\lambda^{-1+2\upsilon}\begin{bmatrix} \lambda^{\frac{4}{3}(1+\upsilon)} - \lambda^{-\frac{2}{3}(1+\upsilon)} & 0 & 0 \\ 0 & \lambda^{-\frac{2}{3}(1+\upsilon)} - \lambda^{-\frac{2}{3}(1+\upsilon)} & 0 \\ 0 & 0 & \lambda^{-\frac{2}{3}(1+\upsilon)} - \lambda^{-\frac{2}{3}(1+\upsilon)} \end{bmatrix}$$

$$= 2\begin{bmatrix} \lambda^{\frac{-3+6\upsilon+4+4\upsilon}{3}} - \lambda^{\frac{-3+6\upsilon-2-2\upsilon}{3}} & 0 & 0 \\ 0 & 0 & 0 \\ 0 & 0 & 0 \end{bmatrix}$$

$$= 2\begin{bmatrix} \lambda^{\frac{1+10\upsilon}{3}} - \lambda^{\frac{-5+4\upsilon}{3}} & 0 & 0 \\ 0 & 0 & 0 \\ 0 & 0 & 0 \end{bmatrix}$$

$$\text{Term2} = \frac{2}{J}\left[\bar{I}_1\overline{\mathbf{B}} - \overline{\mathbf{B}}^2 + \left(J^r - \bar{I}_2\right)\mathbf{I}\right]$$

$$= 2\lambda^{-1+2\upsilon}\left\{[\lambda^{\frac{4}{3}(1+\upsilon)} + 2\lambda^{-\frac{2}{3}(1+\upsilon)}]\begin{bmatrix} \lambda^{\frac{4}{3}(1+\upsilon)} & 0 & 0 \\ 0 & \lambda^{-\frac{2}{3}(1+\upsilon)} & 0 \\ 0 & 0 & \lambda^{-\frac{2}{3}(1+\upsilon)} \end{bmatrix} - \begin{bmatrix} \lambda^{\frac{8}{3}(1+\upsilon)} & 0 & 0 \\ 0 & \lambda^{-\frac{4}{3}(1+\upsilon)} & 0 \\ 0 & 0 & \lambda^{-\frac{4}{3}(1+\upsilon)} \end{bmatrix}\right\}$$

$$+ 2\lambda^{-1+2\upsilon}\begin{bmatrix} \lambda^{\frac{2}{3}(1+\upsilon)} - \lambda^{-\frac{4}{3}(1+\upsilon)} - 2\lambda^{\frac{2}{3}(1+\upsilon)} & 0 & 0 \\ 0 & \lambda^{\frac{2}{3}(1+\upsilon)} - \lambda^{-\frac{4}{3}(1+\upsilon)} - 2\lambda^{\frac{2}{3}(1+\upsilon)} & 0 \\ 0 & 0 & \lambda^{\frac{2}{3}(1+\upsilon)} - \lambda^{-\frac{4}{3}(1+\upsilon)} - 2\lambda^{\frac{2}{3}(1+\upsilon)} \end{bmatrix}$$

$$\text{Putting term2} = 2\lambda^{-1+2\upsilon}\begin{bmatrix} a_{11} & 0 & 0 \\ 0 & a_{22} & 0 \\ 0 & 0 & a_{33} \end{bmatrix}$$

$$a_{11} = \lambda^{\frac{8}{3}(1+\upsilon)} + 2\lambda^{\frac{2}{3}(1+\upsilon)} - \lambda^{\frac{8}{3}(1+\upsilon)} + \lambda^{\frac{2}{3}(1+\upsilon)} - \lambda^{-\frac{4}{3}(1+\upsilon)} - 2\lambda^{\frac{2}{3}(1+\upsilon)}$$

$$a_{22} = a_{33} = \lambda^{\frac{2}{3}(1+\upsilon)} + 2\lambda^{-\frac{4}{3}(1+\upsilon)} - \lambda^{-\frac{4}{3}(1+\upsilon)} + \lambda^{\frac{2}{3}(1+\upsilon)} - \lambda^{-\frac{4}{3}(1+\upsilon)} - 2\lambda^{\frac{2}{3}(1+\upsilon)}$$

$$\therefore \text{Term2} = 2\lambda^{-1+2\upsilon}\begin{bmatrix} \lambda^{\frac{2}{3}(1+\upsilon)} - \lambda^{-\frac{4}{3}(1+\upsilon)} & 0 & 0 \\ 0 & 0 & 0 \\ 0 & 0 & 0 \end{bmatrix}$$

$$= 2\begin{bmatrix} \lambda^{\frac{-3+2+6\upsilon+2\upsilon}{3}} - \lambda^{\frac{-3-4+6\upsilon-4\upsilon}{3}} & 0 & 0 \\ 0 & 0 & 0 \\ 0 & 0 & 0 \end{bmatrix}$$

$$= 2\begin{bmatrix} \lambda^{\frac{-1+8\upsilon}{3}} - \lambda^{\frac{-7+2\upsilon}{3}} & 0 & 0 \\ 0 & 0 & 0 \\ 0 & 0 & 0 \end{bmatrix}$$

Adding the terms gives:

$$\boldsymbol{\sigma} = 2\begin{bmatrix} \lambda^{\frac{1+10\upsilon}{3}} - \lambda^{\frac{-5+4\upsilon}{3}} & 0 & 0 \\ 0 & 0 & 0 \\ 0 & 0 & 0 \end{bmatrix}\frac{\partial W}{\partial \bar{I}_1} + 2\begin{bmatrix} \lambda^{\frac{-1+8\upsilon}{3}} - \lambda^{\frac{-7+2\upsilon}{3}} & 0 & 0 \\ 0 & 0 & 0 \\ 0 & 0 & 0 \end{bmatrix}\frac{\partial W}{\partial \bar{I}_2} \qquad \text{(V.1.1.11)}$$

V.1.2 Equibiaxial extension/compression (EBE/C)

Consider equibiaxial extension/compression (EBE/C) in the 1 and 2 directions. The deformation gradient

$$\mathbf{F} = \begin{bmatrix} \lambda_1 & 0 & 0 \\ 0 & \lambda_2 & 0 \\ 0 & 0 & \lambda_3 \end{bmatrix}$$

For EBE/C, $\lambda_1 = \lambda_2 = \lambda$

$\therefore \bar{\lambda}_1 = \bar{\lambda}_2 = \lambda \ / J^{1/3} = \bar{\lambda}$

$\bar{\lambda}_1\bar{\lambda}_2\bar{\lambda}_3 = \bar{\lambda}^2\bar{\lambda}_3 = 1$

$\therefore \bar{\lambda}_3 = \bar{\lambda}^{-2}$

So $\bar{\mathbf{F}} = \mathbf{F}J^{-\frac{1}{3}} = \begin{bmatrix} \bar{\lambda} & 0 & 0 \\ 0 & \bar{\lambda} & 0 \\ 0 & 0 & \bar{\lambda}^{-2} \end{bmatrix} = \bar{\mathbf{F}}^T$;

$\therefore \bar{\mathbf{B}} = \bar{\mathbf{F}}\bar{\mathbf{F}}^T = \begin{bmatrix} \bar{\lambda}^2 & 0 & 0 \\ 0 & \bar{\lambda}^2 & 0 \\ 0 & 0 & \bar{\lambda}^{-4} \end{bmatrix}$ (V.1.2.1)

and $\bar{\mathbf{B}}^2 = \begin{bmatrix} \bar{\lambda}^4 & 0 & 0 \\ 0 & \bar{\lambda}^4 & 0 \\ 0 & 0 & \bar{\lambda}^{-8} \end{bmatrix}$ (V.1.2.2)

So $\bar{I}_1 = 2\bar{\lambda}^2 + \bar{\lambda}^{-4}$ (V.1.2.3)

and $\bar{I}_2 = 2\bar{\lambda}^{-2} + \bar{\lambda}^4$ (V.1.2.4)

For a GBK material in general (plane stress) biaxial deformation
$\lambda_3 = (\lambda_1\lambda_2)^{\frac{-\upsilon}{1-\upsilon}}$ and $J = \lambda_1\lambda_2\lambda_3 = \lambda_1\lambda_2(\lambda_1\lambda_2)^{\frac{-\upsilon}{1-\upsilon}} = (\lambda_1\lambda_2)^{\frac{1-2\upsilon}{1-\upsilon}}$;

in the particular case of EBE/C, $\lambda_1 = \lambda_2 = \lambda$.

So $\lambda_3 = (\lambda\ \lambda)^{\frac{-\upsilon}{1-\upsilon}} = \lambda^{\frac{-2\upsilon}{1-\upsilon}}$

and $J = \lambda_1\lambda_2\lambda_3 = \lambda^2\lambda^{-\frac{2\upsilon}{1-\upsilon}} = \lambda^{\frac{2-2\upsilon-2\upsilon}{1-\upsilon}} = \lambda^{\frac{2-4\upsilon}{1-\upsilon}} = \lambda^{2\cdot\frac{1-2\upsilon}{1-\upsilon}}$.

Also $J^{-1} = \lambda^{-2\cdot\frac{1-2\upsilon}{1-\upsilon}} = \lambda^{\frac{-2+4\upsilon}{1-\upsilon}}$ (V.1.2.5),

$J^{-1/3} = \lambda^{-\frac{2}{3}\cdot\frac{1-2\upsilon}{1-\upsilon}} = \lambda^{\frac{-2+4\upsilon}{3-3\upsilon}}$,

$J^{-r} = J^{-\frac{2}{3}\cdot\frac{1+\upsilon}{1-2\upsilon}} = \left(\lambda^{2\cdot\frac{1-2\upsilon}{1-\upsilon}}\right)^{-\frac{2}{3}\cdot\frac{1+\upsilon}{1-2\upsilon}} = \lambda^{-\frac{4}{3}\cdot\frac{1+\upsilon}{1-\upsilon}}$ (V.1.2.6),

and $J^r = \lambda^{\frac{4}{3}\cdot\frac{1+\upsilon}{1-\upsilon}}$ (V.1.2.7)

Here $r = \frac{2}{3}\cdot\frac{1+\upsilon}{1-2\upsilon}$.

Also $\bar{\lambda} = \lambda J^{-1/3} = \lambda.\lambda^{\frac{-2+4\upsilon}{3-3\upsilon}} = \lambda^{\frac{3-3\upsilon-2+4\upsilon}{3-3\upsilon}} = \lambda^{\frac{1+\upsilon}{3-3\upsilon}} = \lambda^{\frac{1}{3}\cdot\frac{1+\upsilon}{1-\upsilon}}$

$\bar{\lambda}^2 = \lambda^{\frac{2+2\upsilon}{3-3\upsilon}} = \lambda^{\frac{2}{3}\cdot\frac{1+\upsilon}{1-\upsilon}}$,

$\bar{\lambda}^4 = \lambda^{\frac{4+4\upsilon}{3-3\upsilon}} = \lambda^{\frac{4}{3}\frac{1+\upsilon}{1-\upsilon}}$,

$\bar{\lambda}^{-4} = \lambda^{\frac{-4-4\upsilon}{3-3\upsilon}} = \lambda^{-\frac{4}{3}\frac{1+\upsilon}{1-\upsilon}}$,

$\bar{\lambda}^{-1} = \lambda^{\frac{-1-\upsilon}{3-3\upsilon}} = \lambda^{-\frac{1}{3}\frac{1+\upsilon}{1-\upsilon}}$,

and $\bar{\lambda}^{-2} = \lambda^{\frac{-2-2\upsilon}{3-3\upsilon}} = \lambda^{-\frac{2}{3}\frac{1+\upsilon}{1-\upsilon}}$.

Making use of the foregoing:

$$\bar{\mathbf{B}} = \begin{bmatrix} \bar{\lambda}^2 & 0 & 0 \\ 0 & \bar{\lambda}^2 & 0 \\ 0 & 0 & \bar{\lambda}^{-4} \end{bmatrix} = \begin{bmatrix} \lambda^{\frac{2}{3}\frac{1+\upsilon}{1-\upsilon}} & 0 & 0 \\ 0 & \lambda^{\frac{2}{3}\frac{1+\upsilon}{1-\upsilon}} & 0 \\ 0 & 0 & \lambda^{-\frac{4}{3}\frac{1+\upsilon}{1-\upsilon}} \end{bmatrix} \tag{V.1.2.8}$$

$$\bar{\mathbf{B}}^2 = \begin{bmatrix} \lambda^{\frac{4}{3}\frac{1+\upsilon}{1-\upsilon}} & 0 & 0 \\ 0 & \lambda^{\frac{4}{3}\frac{1+\upsilon}{1-\upsilon}} & 0 \\ 0 & 0 & \lambda^{-\frac{8}{3}\frac{1+\upsilon}{1-\upsilon}} \end{bmatrix} \tag{V.1.2.9}$$

,

$$\bar{I}_1 = 2\bar{\lambda}^2 + \bar{\lambda}^{-4} = 2\lambda^{\frac{2}{3}\frac{1+\upsilon}{1-\upsilon}} + \lambda^{-\frac{4}{3}\frac{1+\upsilon}{1-\upsilon}} \tag{V.1.2.10}$$

,

and

$$\bar{I}_2 = 2\bar{\lambda}^{-2} + \bar{\lambda}^4 = 2\lambda^{-\frac{2}{3}\frac{1+\upsilon}{1-\upsilon}} + \lambda^{\frac{4}{3}\frac{1+\upsilon}{1-\upsilon}} \tag{V.1.2.11}$$

The Cauchy stress for a GBK material can be written:

$$\boldsymbol{\sigma} = \frac{2}{J}\left[\bar{\mathbf{B}} - J^{-r}\mathbf{I}\right]\frac{\partial W}{\partial \bar{I}_1} + \frac{2}{J}\left[\bar{I}_1\bar{\mathbf{B}} - \bar{\mathbf{B}}^2 + \left(J^r - \bar{I}_2\right)\mathbf{I}\right]\frac{\partial W}{\partial \bar{I}_2} = \text{Term1}.\frac{\partial W}{\partial \bar{I}_1} + \text{Term2}.\frac{\partial W}{\partial \bar{I}_2} \tag{V.1.2.12}$$

Now we substitute V.1.2.5 to V.1.2.11into V.1.1.12. Term by term we get the following.

$$\text{Term1} = \frac{2}{J}\left[\bar{\mathbf{B}} - J^{-r}\mathbf{I}\right] = 2\lambda^{\frac{-2+4\upsilon}{1-\upsilon}}\begin{bmatrix} \lambda^{\frac{2}{3}\frac{1+\upsilon}{1-\upsilon}} - \lambda^{-\frac{4}{3}\frac{1+\upsilon}{1-\upsilon}} & 0 & 0 \\ 0 & \lambda^{\frac{2}{3}\frac{1+\upsilon}{1-\upsilon}} - \lambda^{-\frac{4}{3}\frac{1+\upsilon}{1-\upsilon}} & 0 \\ 0 & 0 & \lambda^{-\frac{4}{3}\frac{1+\upsilon}{1-\upsilon}} - \lambda^{-\frac{4}{3}\frac{1+\upsilon}{1-\upsilon}} \end{bmatrix}$$

$$= 2\begin{bmatrix} \lambda^{\frac{-6+12\upsilon+2+2\upsilon}{3(1-\upsilon)}} - \lambda^{\frac{-6+12\upsilon-4-4\upsilon}{3(1-\upsilon)}} & 0 & 0 \\ 0 & \lambda^{\frac{-6+12\upsilon+2+2\upsilon}{3(1-\upsilon)}} - \lambda^{\frac{-6+12\upsilon-4-4\upsilon}{3(1-\upsilon)}} & 0 \\ 0 & 0 & 0 \end{bmatrix}$$

$$= 2\begin{bmatrix} \lambda^{\frac{-4+14\upsilon}{3(1-\upsilon)}} - \lambda^{\frac{-10+8\upsilon}{3(1-\upsilon)}} & 0 & 0 \\ 0 & \lambda^{\frac{-4+14\upsilon}{3(1-\upsilon)}} - \lambda^{\frac{-10+8\upsilon}{3(1-\upsilon)}} & 0 \\ 0 & 0 & 0 \end{bmatrix}$$

$$= 2\begin{bmatrix} \lambda^{-\frac{2}{3}\cdot\frac{2-7\upsilon}{1-\upsilon}} - \lambda^{-\frac{2}{3}\cdot\frac{5-4\upsilon}{1-\upsilon}} & 0 & 0 \\ 0 & \lambda^{-\frac{2}{3}\cdot\frac{2-7\upsilon}{1-\upsilon}} - \lambda^{-\frac{2}{3}\cdot\frac{5-4\upsilon}{1-\upsilon}} & 0 \\ 0 & 0 & 0 \end{bmatrix}$$

$$\text{Term2} = \frac{2}{J}\left[\bar{I}_1\overline{\mathbf{B}} - \overline{\mathbf{B}}^2 + \left(J^r - \bar{I}_2\right)\mathbf{I}\right]$$

$$= 2\lambda^{\frac{-2+4\upsilon}{1-\upsilon}}\left\{\left(2\lambda^{\frac{2}{3}\cdot\frac{1+\upsilon}{1-\upsilon}} + \lambda^{-\frac{4}{3}\cdot\frac{1+\upsilon}{1-\upsilon}}\right)\begin{bmatrix} \lambda^{\frac{2}{3}\cdot\frac{1+\upsilon}{1-\upsilon}} & 0 & 0 \\ 0 & \lambda^{\frac{2}{3}\cdot\frac{1+\upsilon}{1-\upsilon}} & 0 \\ 0 & 0 & \lambda^{-\frac{4}{3}\cdot\frac{1+\upsilon}{1-\upsilon}} \end{bmatrix} - \begin{bmatrix} \lambda^{\frac{4}{3}\cdot\frac{1+\upsilon}{1-\upsilon}} & 0 & 0 \\ 0 & \lambda^{\frac{4}{3}\cdot\frac{1+\upsilon}{1-\upsilon}} & 0 \\ 0 & 0 & \lambda^{-\frac{8}{3}\cdot\frac{1+\upsilon}{1-\upsilon}} \end{bmatrix}\right\}$$

$$+ 2\lambda^{\frac{-2+4\upsilon}{1-\upsilon}}\begin{bmatrix} \lambda^{\frac{4}{3}\cdot\frac{1+\upsilon}{1-\upsilon}} - 2\lambda^{-\frac{2}{3}\cdot\frac{1+\upsilon}{1-\upsilon}} - \lambda^{\frac{4}{3}\cdot\frac{1+\upsilon}{1-\upsilon}} & 0 & 0 \\ 0 & \lambda^{\frac{4}{3}\cdot\frac{1+\upsilon}{1-\upsilon}} - 2\lambda^{-\frac{2}{3}\cdot\frac{1+\upsilon}{1-\upsilon}} - \lambda^{\frac{4}{3}\cdot\frac{1+\upsilon}{1-\upsilon}} & 0 \\ 0 & 0 & \lambda^{\frac{4}{3}\cdot\frac{1+\upsilon}{1-\upsilon}} - 2\lambda^{-\frac{2}{3}\cdot\frac{1+\upsilon}{1-\upsilon}} - \lambda^{\frac{4}{3}\cdot\frac{1+\upsilon}{1-\upsilon}} \end{bmatrix}$$

$$\text{Term2} = 2\lambda^{\frac{-2+4\upsilon}{1-\upsilon}}\begin{bmatrix} a_{11} & 0 & 0 \\ 0 & a_{22} & 0 \\ 0 & 0 & a_{33} \end{bmatrix}$$

Here $a_{11} = a_{22} = 2\lambda^{\frac{4}{3}\cdot\frac{1+\upsilon}{1-\upsilon}} + \lambda^{-\frac{2}{3}\cdot\frac{1+\upsilon}{1-\upsilon}} - \lambda^{\frac{4}{3}\cdot\frac{1+\upsilon}{1-\upsilon}} + \lambda^{\frac{4}{3}\cdot\frac{1+\upsilon}{1-\upsilon}} - 2\lambda^{-\frac{2}{3}\cdot\frac{1+\upsilon}{1-\upsilon}} - \lambda^{\frac{4}{3}\cdot\frac{1+\upsilon}{1-\upsilon}}$

and $a_{33} = 2\lambda^{-\frac{2}{3}\cdot\frac{1+\upsilon}{1-\upsilon}} + \lambda^{-\frac{8}{3}\cdot\frac{1+\upsilon}{1-\upsilon}} - \lambda^{-\frac{8}{3}\cdot\frac{1+\upsilon}{1-\upsilon}} + \lambda^{\frac{4}{3}\cdot\frac{1+\upsilon}{1-\upsilon}} - 2\lambda^{-\frac{2}{3}\cdot\frac{1+\upsilon}{1-\upsilon}} - \lambda^{\frac{4}{3}\cdot\frac{1+\upsilon}{1-\upsilon}}$

So, term2 $= 2\lambda^{\frac{-2+4\upsilon}{1-\upsilon}}\begin{bmatrix} \lambda^{\frac{4}{3}\cdot\frac{1+\upsilon}{1-\upsilon}} - \lambda^{-\frac{2}{3}\cdot\frac{1+\upsilon}{1-\upsilon}} & 0 & 0 \\ 0 & \lambda^{\frac{4}{3}\cdot\frac{1+\upsilon}{1-\upsilon}} - \lambda^{-\frac{2}{3}\cdot\frac{1+\upsilon}{1-\upsilon}} & 0 \\ 0 & 0 & 0 \end{bmatrix}$

$= 2\lambda^{\frac{-2+4\upsilon}{1-\upsilon}}\begin{bmatrix} \lambda^{\frac{1}{3}\cdot\frac{4+4\upsilon}{1-\upsilon}} - \lambda^{\frac{1}{3}\cdot\frac{-2-2\upsilon}{1-\upsilon}} & 0 & 0 \\ 0 & \lambda^{\frac{1}{3}\cdot\frac{4+4\upsilon}{1-\upsilon}} - \lambda^{\frac{1}{3}\cdot\frac{-2-2\upsilon}{1-\upsilon}} & 0 \\ 0 & 0 & 0 \end{bmatrix}$

$= 2\begin{bmatrix} \lambda^{\frac{1}{3}\cdot\frac{-6+12\upsilon+4+4\upsilon}{1-\upsilon}} - \lambda^{\frac{1}{3}\cdot\frac{-6+12\upsilon-2-2\upsilon}{1-\upsilon}} & 0 & 0 \\ 0 & \lambda^{\frac{1}{3}\cdot\frac{-6+12\upsilon+4+4\upsilon}{1-\upsilon}} - \lambda^{\frac{1}{3}\cdot\frac{-6+12\upsilon-2-2\upsilon}{1-\upsilon}} & 0 \\ 0 & 0 & 0 \end{bmatrix}$

$= 2\begin{bmatrix} \lambda^{\frac{1}{3}\cdot\frac{-2+16\upsilon}{1-\upsilon}} - \lambda^{\frac{1}{3}\cdot\frac{-8+10\upsilon}{1-\upsilon}} & 0 & 0 \\ 0 & \lambda^{\frac{1}{3}\cdot\frac{-2+16\upsilon}{1-\upsilon}} - \lambda^{\frac{1}{3}\cdot\frac{-8+10\upsilon}{1-\upsilon}} & 0 \\ 0 & 0 & 0 \end{bmatrix}$

$= 2\begin{bmatrix} \lambda^{-\frac{2}{3}\cdot\frac{1-8\upsilon}{1-\upsilon}} - \lambda^{-\frac{2}{3}\cdot\frac{4-5\upsilon}{1-\upsilon}} & 0 & 0 \\ 0 & \lambda^{-\frac{2}{3}\cdot\frac{1-8\upsilon}{1-\upsilon}} - \lambda^{-\frac{2}{3}\cdot\frac{4-5\upsilon}{1-\upsilon}} & 0 \\ 0 & 0 & 0 \end{bmatrix}$

Therefore

$$\boldsymbol{\sigma} = 2\begin{bmatrix} \lambda^{-\frac{2}{3}\cdot\frac{2-7\upsilon}{1-\upsilon}} - \lambda^{-\frac{2}{3}\cdot\frac{5-4\upsilon}{1-\upsilon}} & 0 & 0 \\ 0 & \lambda^{-\frac{2}{3}\cdot\frac{2-7\upsilon}{1-\upsilon}} - \lambda^{-\frac{2}{3}\cdot\frac{5-4\upsilon}{1-\upsilon}} & 0 \\ 0 & 0 & 0 \end{bmatrix}\frac{\partial W}{\partial \bar{I}_1} + 2\begin{bmatrix} \lambda^{-\frac{2}{3}\cdot\frac{1-8\upsilon}{1-\upsilon}} - \lambda^{-\frac{2}{3}\cdot\frac{4-5\upsilon}{1-\upsilon}} & 0 & 0 \\ 0 & \lambda^{-\frac{2}{3}\cdot\frac{1-8\upsilon}{1-\upsilon}} - \lambda^{-\frac{2}{3}\cdot\frac{4-5\upsilon}{1-\upsilon}} & 0 \\ 0 & 0 & 0 \end{bmatrix}\frac{\partial W}{\partial \bar{I}_2}$$

(V.1.2.13)

V.1.3 Fixed width extension/compression (FWE/C)

Consider extension in the 1 direction with dimensions in the 2 direction fixed

Put $\lambda_1 = \lambda; \lambda_2 = 1 \therefore \lambda_3 = (\lambda_1\lambda_2)^{\frac{-\upsilon}{1-\upsilon}} = \lambda^{\frac{-\upsilon}{1-\upsilon}}$

The volume ratio $J = \lambda_1\lambda_2\lambda_3 = \lambda\lambda^{\frac{-\upsilon}{1-\upsilon}} = \lambda^{\frac{1-\upsilon-\upsilon}{1-\upsilon}} = \lambda^{\frac{1-2\upsilon}{1-\upsilon}}$

$$\therefore J^{-1} = \lambda^{\frac{-1+2\upsilon}{1-\upsilon}} \qquad \text{(V.1.3.1)}$$

$$J^{-1/3} = \lambda^{\frac{-1+2\upsilon}{3-3\upsilon}} \qquad \text{(V.1.3.2)}$$

Now

$$r = \frac{2}{3}.\frac{1+\upsilon}{1-2\upsilon}$$

$$\therefore J^{-r} = \lambda^{\frac{-1+2\upsilon}{1-\upsilon}.\frac{2}{3}.\frac{1+\upsilon}{1-2\upsilon}} = \lambda^{-\frac{2}{3}.\frac{1+\upsilon}{1-\upsilon}} = \lambda^{\frac{-2-2\upsilon}{3-3\upsilon}} \qquad \text{(V.1.3.3)}$$

$$\text{and } J^{r} = \lambda^{\frac{2+2\upsilon}{3-3\upsilon}} \qquad \text{(V.1.3.4)}$$

Unlike SE/C and EBE/C for FWE/C there is not symmetry in $\bar{\lambda}_i$ so we cannot go straight to $\bar{\mathbf{F}}$ in the same way. (For FWE/C $\bar{\lambda}_2 \neq \bar{\lambda}_3$ and $\bar{\lambda}_1 \neq \bar{\lambda}_2$, also $\bar{\lambda}_2 \neq 1$ despite λ_2 being equal to1.) Here, the deformation gradient

$$\mathbf{F} = \begin{bmatrix} \lambda_1 & 0 & 0 \\ 0 & \lambda_2 & 0 \\ 0 & 0 & \lambda_3 \end{bmatrix} = \begin{bmatrix} \lambda & 0 & 0 \\ 0 & 1 & 0 \\ 0 & 0 & \lambda^{\frac{-\upsilon}{1-\upsilon}} \end{bmatrix} = \mathbf{F}^{\mathrm{T}}$$

$$\therefore \bar{\mathbf{F}} = J^{-1/3}\mathbf{F} = \lambda^{\frac{-1+2\upsilon}{3-3\upsilon}} \begin{bmatrix} \lambda & 0 & 0 \\ 0 & 1 & 0 \\ 0 & 0 & \lambda^{\frac{-\upsilon}{1-\upsilon}} \end{bmatrix} = \begin{bmatrix} \lambda^{\frac{3-3\upsilon-1+2\upsilon}{3-3\upsilon}} & 0 & 0 \\ 0 & \lambda^{\frac{-1+2\upsilon}{3-3\upsilon}} & 0 \\ 0 & 0 & \lambda^{\frac{-3\upsilon-1+2\upsilon}{3-3\upsilon}} \end{bmatrix} = \begin{bmatrix} \lambda^{\frac{2-\upsilon}{3-3\upsilon}} & 0 & 0 \\ 0 & \lambda^{\frac{-1+2\upsilon}{3-3\upsilon}} & 0 \\ 0 & 0 & \lambda^{\frac{-1-\upsilon}{3-3\upsilon}} \end{bmatrix}$$

$$= \begin{bmatrix} \bar{\lambda}_1 & 0 & 0 \\ 0 & \bar{\lambda}_2 & 0 \\ 0 & 0 & \bar{\lambda}_3 \end{bmatrix}$$

$$\therefore \bar{\mathbf{B}} = \bar{\mathbf{F}}\bar{\mathbf{F}}^{T} = \begin{bmatrix} \lambda^{\frac{4-2\upsilon}{3-3\upsilon}} & 0 & 0 \\ 0 & \lambda^{\frac{-2+4\upsilon}{3-3\upsilon}} & 0 \\ 0 & 0 & \lambda^{\frac{-2-2\upsilon}{3-3\upsilon}} \end{bmatrix} \qquad \text{(V.1.3.5)}$$

and $\overline{\mathbf{B}}^2 = \begin{bmatrix} \lambda^{\frac{8-4\upsilon}{3-3\upsilon}} & 0 & 0 \\ 0 & \lambda^{\frac{-4+8\upsilon}{3-3\upsilon}} & 0 \\ 0 & 0 & \lambda^{\frac{-4-4\upsilon}{3-3\upsilon}} \end{bmatrix}$ (V.1.3.6)

$$\therefore \bar{I}_1 = \bar{\lambda}_1^2 + \bar{\lambda}_2^2 + \bar{\lambda}_3^2 = \lambda^{\frac{4-2\upsilon}{3-3\upsilon}} + \lambda^{\frac{-2+4\upsilon}{3-3\upsilon}} + \lambda^{\frac{-2-2\upsilon}{3-3\upsilon}} \quad \text{(V.1.3.7)}$$

and

$$\bar{I}_2 = \bar{\lambda}_1^{-2} + \bar{\lambda}_2^{-2} + \bar{\lambda}_3^{-2} = \lambda^{\frac{-4+2\upsilon}{3-3\upsilon}} + \lambda^{\frac{2-4\upsilon}{3-3\upsilon}} + \lambda^{\frac{2+2\upsilon}{3-3\upsilon}} \quad \text{(V.1.3.8)}$$

From equations V.1.3.4 and V.1.3.8 we have

$$J^r - \bar{I}_2 = -\lambda^{\frac{-4+2\upsilon}{3-3\upsilon}} - \lambda^{\frac{2-4\upsilon}{3-3\upsilon}}$$

Now,

$$\boldsymbol{\sigma} = \frac{2}{J}\left[\overline{\mathbf{B}} - J^{-r}\mathbf{I}\right]\frac{\partial W}{\partial \bar{I}_1} + \frac{2}{J}\left[\bar{I}_1\overline{\mathbf{B}} - \overline{\mathbf{B}}^2 + \left(J^r - \bar{I}_2\right)\mathbf{I}\right]\frac{\partial W}{\partial \bar{I}_2}.$$

Substituting we get:

$$\frac{2}{J}\left[\overline{\mathbf{B}} - J^{-r}\mathbf{I}\right] = 2\lambda^{\frac{-1+2\upsilon}{1-\upsilon}}\left\{\begin{bmatrix} \lambda^{\frac{4-2\upsilon}{3-3\upsilon}} & 0 & 0 \\ 0 & \lambda^{\frac{-2+4\upsilon}{3-3\upsilon}} & 0 \\ 0 & 0 & \lambda^{\frac{-2-2\upsilon}{3-3\upsilon}} \end{bmatrix} - \begin{bmatrix} \lambda^{\frac{-2-2\upsilon}{3-3\upsilon}} & 0 & 0 \\ 0 & \lambda^{\frac{-2-2\upsilon}{3-3\upsilon}} & 0 \\ 0 & 0 & \lambda^{\frac{-2-2\upsilon}{3-3\upsilon}} \end{bmatrix}\right\}$$

$$= 2\lambda^{\frac{-3+6\upsilon}{3-3\upsilon}}\begin{bmatrix} \lambda^{\frac{4-2\upsilon}{3-3\upsilon}} - \lambda^{\frac{-2-2\upsilon}{3-3\upsilon}} & 0 & 0 \\ 0 & \lambda^{\frac{-2+4\upsilon}{3-3\upsilon}} - \lambda^{\frac{-2-2\upsilon}{3-3\upsilon}} & 0 \\ 0 & 0 & 0 \end{bmatrix}$$

$$= 2\begin{bmatrix} \lambda^{\frac{-3+6\upsilon+4-2\upsilon}{3-3\upsilon}} - \lambda^{\frac{-3+6\upsilon-2-2\upsilon}{3-3\upsilon}} & 0 & 0 \\ 0 & \lambda^{\frac{-3+6\upsilon-2+4\upsilon}{3-3\upsilon}} - \lambda^{\frac{-3+6\upsilon-2-2\upsilon}{3-3\upsilon}} & 0 \\ 0 & 0 & 0 \end{bmatrix}$$

$$= 2\begin{bmatrix} \lambda^{\frac{1+4\upsilon}{3-3\upsilon}} - \lambda^{\frac{-5+4\upsilon}{3-3\upsilon}} & 0 & 0 \\ 0 & \lambda^{\frac{-5+10\upsilon}{3-3\upsilon}} - \lambda^{\frac{-5+4\upsilon}{3-3\upsilon}} & 0 \\ 0 & 0 & 0 \end{bmatrix}$$

$$= 2\begin{bmatrix} \lambda^{\frac{1}{3}\cdot\frac{1+4\upsilon}{1-\upsilon}} - \lambda^{-\frac{1}{3}\cdot\frac{5-4\upsilon}{1-\upsilon}} & 0 & 0 \\ 0 & \lambda^{-\frac{1}{3}\cdot\frac{5-10\upsilon}{1-\upsilon}} - \lambda^{-\frac{1}{3}\cdot\frac{5-4\upsilon}{1-\upsilon}} & 0 \\ 0 & 0 & 0 \end{bmatrix}$$

Also

$$\frac{2}{J}\left[\bar{I}_1\overline{\mathbf{B}} - \overline{\mathbf{B}}^2 + \left(J^r - \bar{I}_2\right)\mathbf{I}\right] = \frac{2}{J}\left\{\bar{I}_1\overline{\mathbf{B}} - \overline{\mathbf{B}}^2\right\} + \frac{2}{J}\left[\left(J^r - \bar{I}_2\right)\mathbf{I}\right] =$$

$$2\lambda^{\frac{-1+2\upsilon}{1-\upsilon}}\left\{\left(\lambda^{\frac{4-2\upsilon}{3-3\upsilon}} + \lambda^{\frac{-2+4\upsilon}{3-3\upsilon}} + \lambda^{\frac{-2-2\upsilon}{3-3\upsilon}}\right)\begin{bmatrix} \lambda^{\frac{4-2\upsilon}{3-3\upsilon}} & 0 & 0 \\ 0 & \lambda^{\frac{-2+4\upsilon}{3-3\upsilon}} & 0 \\ 0 & 0 & \lambda^{\frac{-2-2\upsilon}{3-3\upsilon}} \end{bmatrix} - \begin{bmatrix} \lambda^{\frac{8-4\upsilon}{3-3\upsilon}} & 0 & 0 \\ 0 & \lambda^{\frac{-4+8\upsilon}{3-3\upsilon}} & 0 \\ 0 & 0 & \lambda^{\frac{-4-4\upsilon}{3-3\upsilon}} \end{bmatrix}\right\}$$

$$+ 2\lambda^{\frac{-1+2\upsilon}{1-\upsilon}}\begin{bmatrix} \lambda^{\frac{2+2\upsilon}{3-3\upsilon}} - \lambda^{\frac{-4+2\upsilon}{3-3\upsilon}} - \lambda^{\frac{2-4\upsilon}{3-3\upsilon}} - \lambda^{\frac{2+2\upsilon}{3-3\upsilon}} & 0 & 0 \\ 0 & \lambda^{\frac{2+2\upsilon}{3-3\upsilon}} - \lambda^{\frac{-4+2\upsilon}{3-3\upsilon}} - \lambda^{\frac{2-4\upsilon}{3-3\upsilon}} - \lambda^{\frac{2+2\upsilon}{3-3\upsilon}} & 0 \\ 0 & 0 & \lambda^{\frac{2+2\upsilon}{3-3\upsilon}} - \lambda^{\frac{-4+2\upsilon}{3-3\upsilon}} - \lambda^{\frac{2-4\upsilon}{3-3\upsilon}} - \lambda^{\frac{2+2\upsilon}{3-3\upsilon}} \end{bmatrix}$$

$$=$$

$$2\lambda^{\frac{-3+6\upsilon}{3-3\upsilon}}\left\{\begin{bmatrix}\lambda^{\frac{8-4\upsilon}{3-3\upsilon}}+\lambda^{\frac{2+2\upsilon}{3-3\upsilon}}+\lambda^{\frac{2-4\upsilon}{3-3\upsilon}} & 0 & 0\\ 0 & \lambda^{\frac{2+2\upsilon}{3-3\upsilon}}+\lambda^{\frac{-4+8\upsilon}{3-3\upsilon}}+\lambda^{\frac{-4+2\upsilon}{3-3\upsilon}} & 0\\ 0 & 0 & \lambda^{\frac{2-4\upsilon}{3-3\upsilon}}+\lambda^{\frac{-4+2\upsilon}{3-3\upsilon}}+\lambda^{\frac{-4-4\upsilon}{3-3\upsilon}}\end{bmatrix}-\begin{bmatrix}\lambda^{\frac{8-4\upsilon}{3-3\upsilon}} & 0 & 0\\ 0 & \lambda^{\frac{-4+8\upsilon}{3-3\upsilon}} & 0\\ 0 & 0 & \lambda^{\frac{-4-4\upsilon}{3-3\upsilon}}\end{bmatrix}\right\}$$

$$+2\lambda^{\frac{-3+6\upsilon}{3-3\upsilon}}\begin{bmatrix}-\lambda^{\frac{-4+2\upsilon}{3-3\upsilon}}-\lambda^{\frac{2-4\upsilon}{3-3\upsilon}} & 0 & 0\\ 0 & -\lambda^{\frac{-4+2\upsilon}{3-3\upsilon}}-\lambda^{\frac{2-4\upsilon}{3-3\upsilon}} & 0\\ 0 & 0 & -\lambda^{\frac{-4+2\upsilon}{3-3\upsilon}}-\lambda^{\frac{2-4\upsilon}{3-3\upsilon}}\end{bmatrix}$$

$$=2\lambda^{\frac{-3+6\upsilon}{3-3\upsilon}}\begin{bmatrix}\lambda^{\frac{2+2\upsilon}{3-3\upsilon}}-\lambda^{\frac{-4+2\upsilon}{3-3\upsilon}} & 0 & 0\\ 0 & \lambda^{\frac{2+2\upsilon}{3-3\upsilon}}-\lambda^{\frac{2-4\upsilon}{3-3\upsilon}} & 0\\ 0 & 0 & 0\end{bmatrix}$$

$$=\begin{bmatrix}\lambda^{\frac{-1+8\upsilon}{3-3\upsilon}}-\lambda^{\frac{-7+8\upsilon}{3-3\upsilon}} & 0 & 0\\ 0 & \lambda^{\frac{-1+8\upsilon}{3-3\upsilon}}-\lambda^{\frac{-1+2\upsilon}{3-3\upsilon}} & 0\\ 0 & 0 & 0\end{bmatrix}$$

So

$$\boldsymbol{\sigma}=\frac{2}{J}\left[\overline{\mathbf{B}}-J^{-r}\mathbf{I}\right]\frac{\partial W}{\partial \bar{I}_1}+\frac{2}{J}\left[\bar{I}_1\overline{\mathbf{B}}-\overline{\mathbf{B}}^2+\left(J^r-\bar{I}_2\right)\mathbf{I}\right]\frac{\partial W}{\partial \bar{I}_2}$$

$$=2\begin{bmatrix}\lambda^{\frac{1}{3}\cdot\frac{1+4\upsilon}{1-\upsilon}}-\lambda^{-\frac{1}{3}\cdot\frac{5-4\upsilon}{1-\upsilon}} & 0 & 0\\ 0 & \lambda^{-\frac{1}{3}\cdot\frac{5-10\upsilon}{1-\upsilon}}-\lambda^{-\frac{1}{3}\cdot\frac{5-4\upsilon}{1-\upsilon}} & 0\\ 0 & 0 & 0\end{bmatrix}\frac{\partial W}{\partial \bar{I}_1}+2\begin{bmatrix}\lambda^{\frac{-1+8\upsilon}{3-3\upsilon}}-\lambda^{\frac{-7+8\upsilon}{3-3\upsilon}} & 0 & 0\\ 0 & \lambda^{\frac{-1+8\upsilon}{3-3\upsilon}}-\lambda^{\frac{-1+2\upsilon}{3-3\upsilon}} & 0\\ 0 & 0 & 0\end{bmatrix}\frac{\partial W}{\partial \bar{I}_2}$$

$$=2\begin{bmatrix}\lambda^{\frac{1}{3}\cdot\frac{1+4\upsilon}{1-\upsilon}}-\lambda^{-\frac{1}{3}\cdot\frac{5-4\upsilon}{1-\upsilon}} & 0 & 0\\ 0 & \lambda^{-\frac{1}{3}\cdot\frac{5-10\upsilon}{1-\upsilon}}-\lambda^{-\frac{1}{3}\cdot\frac{5-4\upsilon}{1-\upsilon}} & 0\\ 0 & 0 & 0\end{bmatrix}\frac{\partial W}{\partial \bar{I}_1}+2\begin{bmatrix}\lambda^{-\frac{1}{3}\cdot\frac{1-8\upsilon}{1-\upsilon}}-\lambda^{-\frac{1}{3}\cdot\frac{7-8\upsilon}{1-\upsilon}} & 0 & 0\\ 0 & \lambda^{-\frac{1}{3}\cdot\frac{1-8\upsilon}{1-\upsilon}}-\lambda^{-\frac{1}{3}\cdot\frac{1-2\upsilon}{1-\upsilon}} & 0\\ 0 & 0 & 0\end{bmatrix}\frac{\partial W}{\partial \bar{I}_2}$$

(V.1.3.8)

Next, two simple cases of triaxial deformation will be considered: extension/compression with constant cross-section as illustrated in Figure 2 of the main text and in Appendix II.

V.1.4 Constant cross-section extension/compression

Consider extension or compression in the 1 direction with the dimensions in the 2 and 3 directions fixed. Material point coordinates in the current and reference configurations are related by:

$x_1 = \lambda X_1;\ x_2 = X_2;\ x_3 = X_3$

The deformation gradient is therefore given by

$$\mathbf{F} = \begin{bmatrix} \frac{\partial x_1}{\partial X_1} & \frac{\partial x_1}{\partial X_2} & \frac{\partial x_1}{\partial X_3} \\ \frac{\partial x_2}{\partial X_1} & \frac{\partial x_2}{\partial X_2} & \frac{\partial x_2}{\partial X_3} \\ \frac{\partial x_3}{\partial X_1} & \frac{\partial x_3}{\partial X_2} & \frac{\partial x_3}{\partial X_3} \end{bmatrix} = \begin{bmatrix} \lambda & 0 & 0 \\ 0 & 1 & 0 \\ 0 & 0 & 1 \end{bmatrix} = \mathbf{F}^{\mathrm{T}}$$

Also

$$J = \lambda \qquad \text{(V.1.4.1)}$$

So the volume neutralised deformation gradient is

$$\overline{\mathbf{F}} = \overline{\mathbf{F}}^{\mathrm{T}} = \begin{bmatrix} \lambda^{2/3} & 0 & 0 \\ 0 & \lambda^{-1/3} & 0 \\ 0 & 0 & \lambda^{-1/3} \end{bmatrix}$$

$$\text{So } \overline{\mathbf{B}} = \overline{\mathbf{F}}\overline{\mathbf{F}}^{\mathrm{T}} = \begin{bmatrix} \lambda^{4/3} & 0 & 0 \\ 0 & \lambda^{-2/3} & 0 \\ 0 & 0 & \lambda^{-2/3} \end{bmatrix} = \begin{bmatrix} \bar{\mathrm{b}}_{11} & \bar{\mathrm{b}}_{12} & \bar{\mathrm{b}}_{13} \\ \bar{\mathrm{b}}_{21} & \bar{\mathrm{b}}_{22} & \bar{\mathrm{b}}_{23} \\ \bar{\mathrm{b}}_{31} & \bar{\mathrm{b}}_{32} & \bar{\mathrm{b}}_{33} \end{bmatrix} \qquad \text{(V.1.4.2)}$$

$$\overline{\mathbf{B}}^2 = \begin{bmatrix} \lambda^{8/3} & 0 & 0 \\ 0 & \lambda^{-4/3} & 0 \\ 0 & 0 & \lambda^{-4/3} \end{bmatrix} \qquad \text{(V.1.4.3)}$$

$$\bar{I}_1 = \bar{\mathrm{b}}_{11} + \bar{\mathrm{b}}_{22} + \bar{\mathrm{b}}_{33} = \lambda^{4/3} + 2\lambda^{-2/3} \qquad \text{(V.1.4.4)}$$

$$\text{and } \bar{I}_2 = \begin{vmatrix} \bar{\mathrm{b}}_{22} & \bar{\mathrm{b}}_{32} \\ \bar{\mathrm{b}}_{23} & \bar{\mathrm{b}}_{33} \end{vmatrix} + \begin{vmatrix} \bar{\mathrm{b}}_{11} & \bar{\mathrm{b}}_{21} \\ \bar{\mathrm{b}}_{12} & \bar{\mathrm{b}}_{33} \end{vmatrix} + \begin{vmatrix} \bar{\mathrm{b}}_{11} & \bar{\mathrm{b}}_{31} \\ \bar{\mathrm{b}}_{13} & \bar{\mathrm{b}}_{33} \end{vmatrix} = \begin{vmatrix} \lambda^{-2/3} & 0 \\ 0 & \lambda^{-2/3} \end{vmatrix} + \begin{vmatrix} \lambda^{4/3} & 0 \\ 0 & \lambda^{-2/3} \end{vmatrix} + \begin{vmatrix} \lambda^{4/3} & 0 \\ 0 & \lambda^{-2/3} \end{vmatrix}$$

$$= \lambda^{-4/3} + 2\lambda^{2/3} \qquad \text{(V.1.4.5)}$$

Now for a GBK material we have once more

$$\boldsymbol{\sigma} = \frac{2}{J}\left[\overline{\mathbf{B}} - J^{-r}\mathbf{I}\right]\frac{\partial W}{\partial \bar{I}_1} + \frac{2}{J}\left[\bar{I}_1\overline{\mathbf{B}} - \overline{\mathbf{B}}^2 + \left(J^r - \bar{I}_2\right)\mathbf{I}\right]\frac{\partial W}{\partial \bar{I}_2} \qquad \text{(V.1.4.6)}$$

Substitution into equation 4.1.4.6 gives

$$\boldsymbol{\sigma} = 2\frac{\partial W}{\partial \bar{I}_1}\lambda^{-1}\left\{\begin{bmatrix}\lambda^{4/3} & 0 & 0\\ 0 & \lambda^{-2/3} & 0\\ 0 & 0 & \lambda^{-2/3}\end{bmatrix} + \begin{bmatrix}-\lambda^{-r} & 0 & 0\\ 0 & -\lambda^{-r} & 0\\ 0 & 0 & -\lambda^{-r}\end{bmatrix}\right\}$$
$$+ 2\frac{\partial W}{\partial \bar{I}_2}\lambda^{-1}\left\{(\lambda^{4/3} + \lambda^{-2/3})\begin{bmatrix}\lambda^{4/3} & 0 & 0\\ 0 & \lambda^{-2/3} & 0\\ 0 & 0 & \lambda^{-2/3}\end{bmatrix} + \begin{bmatrix}\lambda^{8/3} & 0 & 0\\ 0 & \lambda^{-4/3} & 0\\ 0 & 0 & \lambda^{-4/3}\end{bmatrix}\right.$$
$$\left. + \begin{bmatrix}(-2\lambda^{2/3} - \lambda^{-4/3}) & 0 & 0\\ 0 & (-2\lambda^{2/3} - \lambda^{-4/3}) & 0\\ 0 & 0 & (-2\lambda^{2/3} - \lambda^{-4/3})\end{bmatrix} + \begin{bmatrix}\lambda^r & 0 & 0\\ 0 & \lambda^r & 0\\ 0 & 0 & \lambda^r\end{bmatrix}\right\}$$

$$= 2\frac{\partial W}{\partial \bar{I}_1}\begin{bmatrix}(\lambda^{1/3} - \lambda^{-r-1}) & 0 & 0\\ 0 & (\lambda^{-5/3} - \lambda^{-r-1}) & 0\\ 0 & 0 & (\lambda^{-5/3} - \lambda^{-r-1})\end{bmatrix}$$
$$+ 2\frac{\partial W}{\partial \bar{I}_2}\left\{\begin{bmatrix}(\lambda^{5/3} + 2\lambda^{-1/3}) & 0 & 0\\ 0 & (\lambda^{-1/3} + 2\lambda^{-7/3}) & 0\\ 0 & 0 & (\lambda^{-1/3} + 2\lambda^{-7/3})\end{bmatrix} + \begin{bmatrix}-\lambda^{5/3} & 0 & 0\\ 0 & -\lambda^{-7/3} & 0\\ 0 & 0 & -\lambda^{-7/3}\end{bmatrix}\right.$$
$$\left. + \begin{bmatrix}(-2\lambda^{-1/3} - \lambda^{-7/3}) & 0 & 0\\ 0 & (-2\lambda^{-1/3} - \lambda^{-7/3}) & 0\\ 0 & 0 & (-2\lambda^{-1/3} - \lambda^{-7/3})\end{bmatrix} + \begin{bmatrix}\lambda^{r-1} & 0 & 0\\ 0 & \lambda^{r-1} & 0\\ 0 & 0 & \lambda^{r-1}\end{bmatrix}\right\}$$

$$\boldsymbol{\sigma} = 2\frac{\partial W}{\partial \bar{I}_1}\begin{bmatrix}(\lambda^{1/3} - \lambda^{-r-1}) & 0 & 0\\ 0 & (\lambda^{-5/3} - \lambda^{-r-1}) & 0\\ 0 & 0 & (\lambda^{-5/3} - \lambda^{-r-1})\end{bmatrix}$$

$$+ 2\frac{\partial W}{\partial \bar{I}_2}\begin{bmatrix}(\lambda^{r-1} - \lambda^{-7/3}) & 0 & 0\\ 0 & (\lambda^{r-1} - \lambda^{-1/3}) & 0\\ 0 & 0 & (\lambda^{r-1} - \lambda^{-1/3})\end{bmatrix} \qquad \text{(V.1.4.7)}$$

Now recall the infinitesimal stress-strain relationships for deformations aligned with the principal axes (see, for example, Hall, 1968, p100):

$$\sigma_1 = (K + \frac{4}{3}\mu)\varepsilon_1 + \Lambda\varepsilon_2 + \Lambda\varepsilon_3 \qquad \text{(V.1.4.8a)}$$

$$\sigma_2 = \Lambda\varepsilon_1 + (K + \frac{4}{3}\mu)\varepsilon_2 + \Lambda\varepsilon_3 \qquad \text{(V.1.4.8b)}$$

$$\sigma_3 = +\Lambda\varepsilon_1 + \Lambda\varepsilon_2 + (K + \frac{4}{3}\mu)\varepsilon_3 \qquad \text{(V.1.4.8c)}$$

Where μ is the shear modulus and the second Lamé constant

$\Lambda = K - \frac{2}{3}\mu$ and $K + \frac{4}{3}\mu = \Lambda + 2\mu$

So $\Lambda = (r - \frac{2}{3})\mu$ and $K + \frac{4}{3}\mu = (r + \frac{4}{3})\mu$

For fixed cross-section extension/compression we have $\varepsilon_2 = \varepsilon_3 = 0$

So $\sigma_1 = (r + \frac{4}{3})\mu\varepsilon_1;\ \sigma_2 = \sigma_3 = (r - \frac{2}{3})\mu\varepsilon_1 \qquad \text{(V.1.4.9)}$

In matrix form

$$\boldsymbol{\sigma} = \mu\begin{bmatrix} (r + \frac{4}{3})\varepsilon_1 & 0 & 0 \\ 0 & (r - \frac{2}{3})\varepsilon_1 & 0 \\ 0 & 0 & (r - \frac{2}{3})\varepsilon_1 \end{bmatrix} \qquad \text{(V.1.4.10)}$$

Now compare with the large strain result, by putting $\lambda = 1 + \varepsilon$:

$$\boldsymbol{\sigma} = 2\frac{\partial W}{\partial \bar{I}_1}\begin{bmatrix} (\lambda^{1/3} - \lambda^{-r-1}) & 0 & 0 \\ 0 & (\lambda^{-5/3} - \lambda^{-r-1}) & 0 \\ 0 & 0 & (\lambda^{-5/3} - \lambda^{-r-1}) \end{bmatrix}$$

$$+ 2\frac{\partial W}{\partial \bar{I}_2}\begin{bmatrix} (\lambda^{r-1} - \lambda^{-7/3}) & 0 & 0 \\ 0 & (\lambda^{r-1} - \lambda^{-1/3}) & 0 \\ 0 & 0 & (\lambda^{r-1} - \lambda^{-1/3}) \end{bmatrix}$$

$$= 2\frac{\partial W}{\partial \bar{I}_1}\begin{bmatrix} ((1+\varepsilon)^{1/3} - (1+\varepsilon)^{-r-1}) & 0 & 0 \\ 0 & ((1+\varepsilon)^{-5/3} - (1+\varepsilon)^{-r-1}) & 0 \\ 0 & 0 & ((1+\varepsilon)^{-5/3} - (1+\varepsilon)^{-r-1}) \end{bmatrix}$$

$$+2\frac{\partial W}{\partial \bar{I}_2}\begin{bmatrix}((1+\varepsilon)^{r-1}-(1+\varepsilon)^{-7/3}) & 0 & 0\\ 0 & ((1+\varepsilon)^{r-1}-(1+\varepsilon)^{-1/3}) & 0\\ 0 & 0 & ((1+\varepsilon)^{r-1}-(1+\varepsilon)^{-1/3})\end{bmatrix}$$

Expanding for small ε gives:

$$\approx 2\frac{\partial W}{\partial \bar{I}_1}\begin{bmatrix}(\frac{1}{3}+r+1)\varepsilon & 0 & 0\\ 0 & (\frac{-5}{3}+r+1)\varepsilon & 0\\ 0 & 0 & (\frac{-5}{3}+r+1)\varepsilon\end{bmatrix}$$

$$+2\frac{\partial W}{\partial \bar{I}_2}\begin{bmatrix}(\frac{7}{3}+r-1)\varepsilon & 0 & 0\\ 0 & (\frac{1}{3}+r-1)\varepsilon & 0\\ 0 & 0 & (\frac{1}{3}+r-1)\varepsilon\end{bmatrix}$$

$$\boldsymbol{\sigma} \approx 2\frac{\partial W}{\partial \bar{I}_1}\begin{bmatrix}(\frac{4}{3}+r)\varepsilon & 0 & 0\\ 0 & (\frac{-2}{3}+r)\varepsilon & 0\\ 0 & 0 & (\frac{-2}{3}+r)\varepsilon\end{bmatrix}$$

$$+2\frac{\partial W}{\partial \bar{I}_2}\begin{bmatrix}(\frac{4}{3}+r)\varepsilon & 0 & 0\\ 0 & (\frac{-2}{3}+r)\varepsilon & 0\\ 0 & 0 & (\frac{-2}{3}+r)\varepsilon\end{bmatrix}$$

i.e. $$\boldsymbol{\sigma} \approx \mu\begin{bmatrix}(\frac{4}{3}+r)\varepsilon & 0 & 0\\ 0 & (\frac{-2}{3}+r)\varepsilon & 0\\ 0 & 0 & (\frac{-2}{3}+r)\varepsilon\end{bmatrix} \qquad \text{(V.1.4.11)}$$

The two expressions are the same, as required. This is a useful check on the large strain result.

Now we consider the stresses in fixed cross-section compression for a shape-volume uncoupled form of strain energy density i.e.

$$W = W_S(\bar{I}_1, \bar{I}_2) + W(J) \qquad \text{(V.1.4.12)}$$

The general formula for Cauchy stress is

$$\boldsymbol{\sigma} = \frac{2}{J}\left[\overline{\mathbf{B}} - \frac{1}{3}\bar{I}_1\mathbf{I}\right]\frac{\partial W}{\partial \bar{I}_1} + \frac{2}{J}\left[\bar{I}_1\overline{\mathbf{B}} - \overline{\mathbf{B}}^2 - \frac{2}{3}\bar{I}_2\mathbf{I}\right]\frac{\partial W}{\partial \bar{I}_2} + \frac{\partial W}{\partial J}\mathbf{I} \qquad \text{(V.1.4.13)}$$

As above we have the following.

The deformation gradient is given by

$$\mathbf{F} = \begin{bmatrix} \lambda & 0 & 0 \\ 0 & 1 & 0 \\ 0 & 0 & 1 \end{bmatrix} = \mathbf{F}^{\mathrm{T}} \qquad \text{(V.1.4.14)}$$

Also

$$J = \lambda \qquad \text{(V.1.4.15)}$$

So the volume neutralised deformation gradient is

$$\overline{\mathbf{F}} = \overline{\mathbf{F}}^{\mathrm{T}} = \begin{bmatrix} \lambda^{2/3} & 0 & 0 \\ 0 & \lambda^{-1/3} & 0 \\ 0 & 0 & \lambda^{-1/3} \end{bmatrix}$$

$$\text{So } \overline{\mathbf{B}} = \overline{\mathbf{F}}\overline{\mathbf{F}}^{\mathrm{T}} = \begin{bmatrix} \lambda^{4/3} & 0 & 0 \\ 0 & \lambda^{-2/3} & 0 \\ 0 & 0 & \lambda^{-2/3} \end{bmatrix} = \begin{bmatrix} \bar{\mathrm{b}}_{11} & \bar{\mathrm{b}}_{12} & \bar{\mathrm{b}}_{13} \\ \bar{\mathrm{b}}_{21} & \bar{\mathrm{b}}_{22} & \bar{\mathrm{b}}_{23} \\ \bar{\mathrm{b}}_{31} & \bar{\mathrm{b}}_{32} & \bar{\mathrm{b}}_{33} \end{bmatrix} \qquad \text{(V.1.4.16)}$$

$$\overline{\mathbf{B}}^2 = \begin{bmatrix} \lambda^{8/3} & 0 & 0 \\ 0 & \lambda^{-4/3} & 0 \\ 0 & 0 & \lambda^{-4/3} \end{bmatrix} \qquad \text{(V.1.4.17)}$$

$$\bar{I}_1 = \bar{\mathrm{b}}_{11} + \bar{\mathrm{b}}_{22} + \bar{\mathrm{b}}_{33} = \lambda^{4/3} + 2\lambda^{-2/3} \qquad \text{(V.1.4.18)}$$

$$\text{and } \bar{I}_2 = \begin{vmatrix} \bar{\mathrm{b}}_{22} & \bar{\mathrm{b}}_{32} \\ \bar{\mathrm{b}}_{23} & \bar{\mathrm{b}}_{33} \end{vmatrix} + \begin{vmatrix} \bar{\mathrm{b}}_{11} & \bar{\mathrm{b}}_{21} \\ \bar{\mathrm{b}}_{12} & \bar{\mathrm{b}}_{33} \end{vmatrix} + \begin{vmatrix} \bar{\mathrm{b}}_{11} & \bar{\mathrm{b}}_{31} \\ \bar{\mathrm{b}}_{13} & \bar{\mathrm{b}}_{33} \end{vmatrix} = \begin{vmatrix} \lambda^{-2/3} & 0 \\ 0 & \lambda^{-2/3} \end{vmatrix} + \begin{vmatrix} \lambda^{4/3} & 0 \\ 0 & \lambda^{-2/3} \end{vmatrix} + \begin{vmatrix} \lambda^{4/3} & 0 \\ 0 & \lambda^{-2/3} \end{vmatrix}$$

$$= \lambda^{-4/3} + 2\lambda^{2/3} \qquad \text{(V.1.4.19)}$$

Substituting into V.1.4.13 we get

$$\boldsymbol{\sigma} = 2\frac{\partial W_S}{\partial \bar{I}_1}\lambda^{-1}\left\{\begin{bmatrix}\lambda^{4/3} & 0 & 0\\ 0 & \lambda^{-2/3} & 0\\ 0 & 0 & \lambda^{-2/3}\end{bmatrix} + \begin{bmatrix}(-\frac{\lambda^{4/3}}{3}-\frac{2}{3}\lambda^{-2/3}) & 0 & 0\\ 0 & (-\frac{\lambda^{4/3}}{3}-\frac{2}{3}\lambda^{-2/3}) & 0\\ 0 & 0 & (-\frac{\lambda^{4/3}}{3}-\frac{2}{3}\lambda^{-2/3})\end{bmatrix}\right\}$$

$$+2\frac{\partial W_S}{\partial \bar{I}_2}\lambda^{-1}\left\{\left(\begin{bmatrix}(\lambda^{8/3}+2\lambda^{2/3}) & 0 & 0\\ 0 & (\lambda^{2/3}+2\lambda^{-4/3}) & 0\\ 0 & 0 & (\lambda^{2/3}+2\lambda^{-4/3})\end{bmatrix} + \begin{bmatrix}-\lambda^{8/3} & 0 & 0\\ 0 & -\lambda^{-4/3} & 0\\ 0 & 0 & -\lambda^{-4/3}\end{bmatrix}\right.\right.$$

$$\left.\left. + \begin{bmatrix}(-\frac{2}{3}\lambda^{-4/3}-\frac{4}{3}\lambda^{2/3}) & 0 & 0\\ 0 & (-\frac{2}{3}\lambda^{-4/3}-\frac{4}{3}\lambda^{2/3}) & 0\\ 0 & 0 & (-\frac{2}{3}\lambda^{-4/3}-\frac{4}{3}\lambda^{2/3})\end{bmatrix}\right)\right\} + \frac{\partial W_2}{\partial J}\begin{bmatrix}1 & 0 & 0\\ 0 & 1 & 0\\ 0 & 0 & 1\end{bmatrix}$$

$$= 2\frac{\partial W_S}{\partial \bar{I}_1}\lambda^{-1}\begin{bmatrix}\frac{2}{3}(\lambda^{4/3}-\lambda^{-2/3}) & 0 & 0\\ 0 & \frac{1}{3}(\lambda^{-2/3}-\lambda^{4/3}) & 0\\ 0 & 0 & \frac{1}{3}(\lambda^{-2/3}-\lambda^{4/3})\end{bmatrix}$$

$$+2\frac{\partial W_S}{\partial \bar{I}_2}\lambda^{-1}\begin{bmatrix}\frac{2}{3}(\lambda^{2/3}-\lambda^{-4/3}) & 0 & 0\\ 0 & \frac{1}{3}(\lambda^{-4/3}-\lambda^{2/3}) & 0\\ 0 & 0 & \frac{1}{3}(\lambda^{-2/3}-\lambda^{4/3})\end{bmatrix}$$

$$+\frac{\partial W_V}{\partial J}\begin{bmatrix}1 & 0 & 0\\ 0 & 1 & 0\\ 0 & 0 & 1\end{bmatrix}$$

$$= 2\frac{\partial W_S}{\partial \bar{I}_1}\begin{bmatrix}\frac{2}{3}(\lambda^{1/3}-\lambda^{-5/3}) & 0 & 0\\ 0 & \frac{1}{3}(\lambda^{-5/3}-\lambda^{1/3}) & 0\\ 0 & 0 & \frac{1}{3}(\lambda^{-5/3}-\lambda^{1/3})\end{bmatrix}$$

$$+2\frac{\partial W_S}{\partial \bar{I}_2}\lambda^{-1}\begin{bmatrix}\frac{2}{3}(\lambda^{-1/3}-\lambda^{-7/3}) & 0 & 0\\ 0 & \frac{1}{3}(\lambda^{-7/3}-\lambda^{-1/3}) & 0\\ 0 & 0 & \frac{1}{3}(\lambda^{-7/3}-\lambda^{-1/3})\end{bmatrix}$$

$$+\frac{\partial W_V}{\partial J}\begin{bmatrix}1 & 0 & 0\\ 0 & 1 & 0\\ 0 & 0 & 1\end{bmatrix}$$

$$=2\frac{\partial W_S}{\partial \bar{I}_1}\begin{bmatrix}\frac{2}{3}(\lambda^{1/3}-\lambda^{-5/3}) & 0 & 0\\ 0 & -\frac{1}{3}(\lambda^{1/3}-\lambda^{-5/3}) & 0\\ 0 & 0 & -\frac{1}{3}(\lambda^{1/3}-\lambda^{-5/3})\end{bmatrix}$$

$$+2\frac{\partial W_S}{\partial \bar{I}_2}\lambda^{-1}\begin{bmatrix}\frac{2}{3}(\lambda^{-1/3}-\lambda^{-7/3}) & 0 & 0\\ 0 & -\frac{1}{3}(\lambda^{-1/3}-\lambda^{-7/3}) & 0\\ 0 & 0 & -\frac{1}{3}(\lambda^{-1/3}-\lambda^{-7/3})\end{bmatrix}$$

$$+\frac{\partial W_V}{\partial J}\begin{bmatrix}1 & 0 & 0\\ 0 & 1 & 0\\ 0 & 0 & 1\end{bmatrix} \qquad \text{(V.1.4.20)}$$

Taking $\lim \lambda \to 1; (1+\varepsilon)^{1/3} \to 1+\frac{1}{3}\varepsilon; -(1+\varepsilon)^{-5/3} \to -1+\frac{5}{3}\varepsilon;$ adding gives 2ε

Also

Lim $\lambda \to 1; (1+\varepsilon)^{-1/3} \to 1-\frac{1}{3}\varepsilon; -(1+\varepsilon)^{-7/3} \to -1+\frac{7}{3}\varepsilon;$ adding gives 2ε

Furthermore,

if, in the infinitesimal strain limit, $W_V = \frac{1}{2}K(J-1)^2$

then $\frac{\partial W_2}{\partial J} = K(J-1) = K(\varepsilon_1+\varepsilon_2+\varepsilon_3) = K(\varepsilon_1+0+0) = K\varepsilon$ here.

So, for infinitesimal strains, the relationships for the uncoupled form gives

$$\boldsymbol{\sigma} = 2\frac{\partial W_S}{\partial \bar{I}_1}\begin{bmatrix} \frac{4}{3}\varepsilon & 0 & 0 \\ 0 & -\frac{2}{3}\varepsilon & 0 \\ 0 & 0 & -\frac{2}{3}\varepsilon \end{bmatrix} + 2\frac{\partial W_S}{\partial \bar{I}_2}\begin{bmatrix} \frac{4}{3}\varepsilon & 0 & 0 \\ 0 & -\frac{2}{3}\varepsilon & 0 \\ 0 & 0 & -\frac{2}{3}\varepsilon \end{bmatrix} + \frac{\partial W_V}{\partial J}\begin{bmatrix} 1 & 0 & 0 \\ 0 & 1 & 0 \\ 0 & 0 & 1 \end{bmatrix}$$

$$= 2\left(\frac{\partial W_1}{\partial \bar{I}_1} + \frac{\partial W_1}{\partial \bar{I}_2}\right)\begin{bmatrix} \frac{4}{3}\varepsilon & 0 & 0 \\ 0 & -\frac{2}{3}\varepsilon & 0 \\ 0 & 0 & -\frac{2}{3}\varepsilon \end{bmatrix} + K\begin{bmatrix} \varepsilon & 0 & 0 \\ 0 & \varepsilon & 0 \\ 0 & 0 & \varepsilon \end{bmatrix}$$

$$= \begin{bmatrix} (\frac{4}{3}\mu + K)\varepsilon & 0 & 0 \\ 0 & (K - \frac{2}{3}\mu)\varepsilon & 0 \\ 0 & 0 & (K - \frac{2}{3}\mu)\varepsilon \end{bmatrix} \qquad \text{(V.1.4.21)}$$

- as required, this is once more in agreement with the result from small strain theory.

V.1.5. Pure volume change

For pure volume change, material point coordinates in the current and reference configurations are related:

$$x_1 = J^{1/3}X_1;\ x_2 = J^{1/3}X_2;\ x_3 = J^{1/3}X_3 \qquad \text{(V.1.5.1)}$$

It follows that

$$\overline{\mathbf{F}} = \overline{\mathbf{F}}^{\mathrm{T}} = \overline{\mathbf{B}} = \overline{\mathbf{B}}^2 = \mathbf{I}$$

and $\bar{I}_1 = \bar{I}_2 = 3$

So, for a GBK material:

$$\boldsymbol{\sigma} = \frac{2}{J}\left[\overline{\mathbf{B}} - J^{-r}\mathbf{I}\right]\frac{\partial W}{\partial \bar{I}_1} + \frac{2}{J}\left[\bar{I}_1\overline{\mathbf{B}} - \overline{\mathbf{B}}^2 - \bar{I}_2\mathbf{I} + J^r\mathbf{I}\right]\frac{\partial W}{\partial \bar{I}_2}$$

$$= \left\{2\frac{\partial W}{\partial \bar{I}_1}\cdot\left(J^{-1} - J^{-r-1}\right) + 2\frac{\partial W}{\partial \bar{I}_2}\cdot\left(J^{r-1} - J^{-1}\right)\right\}\mathbf{I} \qquad \text{(V.1.5.2)}$$

For a shape-volume uncoupled material we have, trivially:

$$\boldsymbol{\sigma} = \frac{\partial W}{\partial J}\mathbf{I} = \frac{\partial W_V}{\partial J}\mathbf{I} \qquad \text{(V.1.5.3)}$$

V.2 Simple shear

Finally simple shear will be considered.

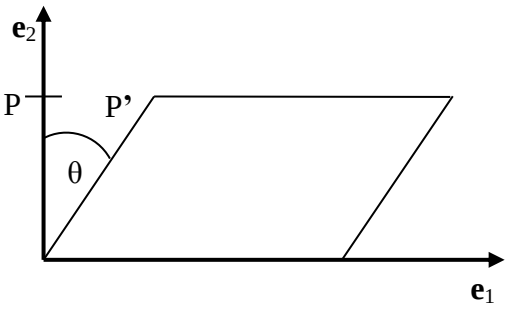

Figure V.1 A piece of material in simple shear.

Material coordinates in the current and reference configurations are related by:

$x_1 = X_1 + \gamma x_2 ; x_2 + X_2 ; x_3 = X_3$ (V.2.1)

Also $J = 1$ (V.2.2)

So barred and unbarred quantities are equivalent here and the deformation gradient is

$$\bar{\mathbf{F}} = \mathbf{F} = \begin{bmatrix} \frac{\partial x_1}{\partial X_1} & \frac{\partial x_1}{\partial X_2} & \frac{\partial x_1}{\partial X_3} \\ \frac{\partial x_2}{\partial X_1} & \frac{\partial x_2}{\partial X_2} & \frac{\partial x_2}{\partial X_3} \\ \frac{\partial x_3}{\partial X_1} & \frac{\partial x_3}{\partial X_2} & \frac{\partial x_3}{\partial X_3} \end{bmatrix} = \begin{bmatrix} 1 & \gamma & 0 \\ 0 & 1 & 0 \\ 0 & 0 & 1 \end{bmatrix}; \quad \bar{\mathbf{F}}^{\mathrm{T}} = \mathbf{F}^{\mathrm{T}} = \begin{bmatrix} 1 & 0 & 0 \\ \gamma & 1 & 0 \\ 0 & 0 & 1 \end{bmatrix}$$

- as Lai et al (2010 page 325). So

$$\bar{\mathbf{B}} = \mathbf{B} = \bar{\mathbf{F}}\bar{\mathbf{F}}^{\mathrm{T}} = \begin{bmatrix} (1+\gamma^2) & \gamma & 0 \\ \gamma & 1 & 0 \\ 0 & 0 & 1 \end{bmatrix} \qquad \text{(V.2.3)}$$

and $\bar{I}_1 = I_1 = \gamma^2 + 3$ (V.2.4)

and $$\bar{I}_2 = I_2 = \begin{vmatrix} 1 & 0 \\ 0 & 1 \end{vmatrix} + \begin{vmatrix} (1+\gamma^2) & \gamma \\ \gamma & 1 \end{vmatrix} + \begin{vmatrix} (1+\gamma^2) & 0 \\ 0 & 1 \end{vmatrix} = \gamma^2 + 3 \qquad \text{(V.2.5)}$$

Also $$\mathbf{B}^2 = \begin{bmatrix} (1+\gamma^2) & \gamma & 0 \\ \gamma & 1 & 0 \\ 0 & 0 & 1 \end{bmatrix} \begin{bmatrix} (1+\gamma^2) & \gamma & 0 \\ \gamma & 1 & 0 \\ 0 & 0 & 1 \end{bmatrix} = \begin{bmatrix} (1+2\gamma^2+\gamma^4+\gamma^2) & (\gamma+\gamma^3+\gamma) & 0 \\ (\gamma+\gamma^3+\gamma) & (\gamma^2+1) & 0 \\ 0 & 0 & 1 \end{bmatrix}$$

$$= \begin{bmatrix} (1+3\gamma^2+\gamma^4) & (2\gamma+\gamma^3) & 0 \\ (2\gamma+\gamma^3) & (1+\gamma^2) & 0 \\ 0 & 0 & 1 \end{bmatrix} \qquad \text{(V.2.6)}$$

Now, for a GBK material

$$\boldsymbol{\sigma} = \frac{2}{J}\left[\overline{\mathbf{B}} - J^{-r}\mathbf{I}\right]\frac{\partial W}{\partial \bar{I}_1} + \frac{2}{J}\left[\bar{I}_1\overline{\mathbf{B}} - \overline{\mathbf{B}}^2 + \left(J^r - \bar{I}_2\right)\mathbf{I}\right]\frac{\partial W}{\partial \bar{I}_2} \quad \text{(V.2.7)}$$

Noting again that in simple shear $J = 1$, so that barred quantities can be unbarred, and substituting in $\bar{I}_1 = \bar{I}_2 = \gamma^2 + 3$ we get:

$$\boldsymbol{\sigma} = 2\left[\mathbf{B} - \mathbf{I}\right]\frac{\partial W}{\partial \bar{I}_1} + 2\left[\left(\gamma^3 + 3\right)\left(\mathbf{B} - \mathbf{I}\right) - \mathbf{B}^2 + \mathbf{I}\right]\frac{\partial W}{\partial \bar{I}_2}$$

$$= 2\frac{\partial W}{\partial \bar{I}_1}\begin{bmatrix} \gamma^2 & \gamma & 0 \\ \gamma & 0 & 0 \\ 0 & 0 & 0 \end{bmatrix}$$

$$+ 2\frac{\partial W}{\partial \bar{I}_2}\left\{\left(\gamma^2 + 3\right)\begin{bmatrix} \gamma^2 & \gamma & 0 \\ \gamma & 0 & 0 \\ 0 & 0 & 0 \end{bmatrix} + \begin{bmatrix} -(1+3\gamma^2+\gamma^4) & -(2\gamma+\gamma^3) & 0 \\ -(2\gamma+\gamma^3) & -(1+\gamma^2) & 0 \\ 0 & 0 & -1 \end{bmatrix} + \begin{bmatrix} 1 & 0 & 0 \\ 0 & 1 & 0 \\ 0 & 0 & 1 \end{bmatrix}\right\}$$

$$= 2\frac{\partial W}{\partial \bar{I}_1}\begin{bmatrix} \gamma^2 & \gamma & 0 \\ \gamma & 0 & 0 \\ 0 & 0 & 0 \end{bmatrix}$$

$$+ 2\frac{\partial W}{\partial \bar{I}_2}\left\{\begin{bmatrix} (\gamma^4+3\gamma^2) & (\gamma^3+3\gamma) & 0 \\ (\gamma^3+3\gamma) & 0 & 0 \\ 0 & 0 & 0 \end{bmatrix} + \begin{bmatrix} -(3\gamma^2+\gamma^4) & -(2\gamma+\gamma^3) & 0 \\ -(2\gamma+\gamma^3) & -\gamma^2 & 0 \\ 0 & 0 & 0 \end{bmatrix}\right\}$$

$$= 2\frac{\partial W}{\partial \bar{I}_1}\begin{bmatrix} \gamma^2 & \gamma & 0 \\ \gamma & 0 & 0 \\ 0 & 0 & 0 \end{bmatrix} + 2\frac{\partial W}{\partial \bar{I}_2}\begin{bmatrix} 0 & \gamma & 0 \\ \gamma & -\gamma^2 & 0 \\ 0 & 0 & 0 \end{bmatrix} \quad \text{(V.2.8)}$$

Now we consider the stresses in simple shear for a shape-volume uncoupled form of strain energy density i.e.

$$W = W_S\left(\bar{I}_1, \bar{I}_2\right) + W(J) \quad \text{(V.2.9)}$$

The general formula for Cauchy stress is

$$\boldsymbol{\sigma} = \frac{2}{J}\left[\overline{\mathbf{B}} - \frac{1}{3}\bar{I}_1\mathbf{I}\right]\frac{\partial W}{\partial \bar{I}_1} + \frac{2}{J}\left[\bar{I}_1\overline{\mathbf{B}} - \overline{\mathbf{B}}^2 - \frac{2}{3}\bar{I}_2\mathbf{I}\right]\frac{\partial W}{\partial \bar{I}_2} + \frac{\partial W}{\partial J}\mathbf{I} \quad \text{(V.2.10)}$$

As above we have the following.

$$\overline{\mathbf{B}} = \mathbf{B} = \overline{\mathbf{F}}\overline{\mathbf{F}}^{\mathrm{T}} = \begin{bmatrix} (1+\gamma^2) & \gamma & 0 \\ \gamma & 1 & 0 \\ 0 & 0 & 1 \end{bmatrix} \qquad \text{(V.2.11)}$$

and $\bar{I}_1 = I_1 = \bar{I}_2 = I_2 = \gamma^2 + 3$ (V.2.12)

Also $\mathbf{B}^2 = \begin{bmatrix} (1+3\gamma^2+\gamma^4) & (2\gamma+\gamma^3) & 0 \\ (2\gamma+\gamma^3) & (1+\gamma^2) & 0 \\ 0 & 0 & 1 \end{bmatrix}$ (V.2.13)

Putting $J = 1$, noting that $\partial W/\partial J = 0$ at $J = 1$ for a shape-volume uncoupled form and substituting equations V.2.11 to V.2.13 into V.2.10 we get:

$$\boldsymbol{\sigma} = 2\left[\overline{\mathbf{B}} - \frac{1}{3}\left(\gamma^2+3\right)\mathbf{I}\right]\frac{\partial W}{\partial \bar{I}_1} + 2\left[\left(\gamma^2+3\right)\overline{\mathbf{B}} - \overline{\mathbf{B}}^2 - \frac{2}{3}\left(\gamma^2+3\right)\mathbf{I}\right]\frac{\partial W}{\partial \bar{I}_2} \qquad \text{(V.2.14)}$$

$$\boldsymbol{\sigma} = 2\left(\begin{bmatrix} \left(1+\gamma^2\right) & \gamma & 0 \\ \gamma & 1 & 0 \\ 0 & 0 & 1 \end{bmatrix} - \begin{bmatrix} (1+\frac{\gamma^2}{3}) & 0 & 0 \\ 0 & (1+\frac{\gamma^2}{3}) & 0 \\ 0 & 0 & (1+\frac{\gamma^2}{3}) \end{bmatrix}\right)\frac{\partial W}{\partial \bar{I}_1}$$

$$+2\left(\begin{bmatrix} \left(3+4\gamma^2+\gamma^4\right) & (3\gamma+\gamma^3) & 0 \\ (3\gamma+\gamma^3) & (3+\gamma^2) & 0 \\ 0 & 0 & (3+\gamma^2) \end{bmatrix} - \begin{bmatrix} \left(1+3\gamma^2+\gamma^4\right) & (2\gamma+\gamma^3) & 0 \\ (2\gamma+\gamma^3) & (1+\gamma^2) & 0 \\ 0 & 0 & 1 \end{bmatrix} - \begin{bmatrix} (2+\frac{2\gamma^2}{3}) & 0 & 0 \\ 0 & (2+\frac{2\gamma^2}{3}) & 0 \\ 0 & 0 & (2+\frac{2\gamma^2}{3}) \end{bmatrix}\right)\frac{\partial W}{\partial \bar{I}_2}$$

$$\therefore \boldsymbol{\sigma} = 2\begin{bmatrix} \frac{2}{3}\gamma^2 & \gamma & 0 \\ \gamma & -\frac{1}{3}\gamma^2 & 0 \\ 0 & 0 & -\frac{1}{3}\gamma^2 \end{bmatrix}\frac{\partial W}{\partial \bar{I}_1} + 2\begin{bmatrix} \frac{1}{3}\gamma^2 & \gamma & 0 \\ \gamma & -\frac{2}{3}\gamma^2 & 0 \\ 0 & 0 & \frac{1}{3}\gamma^2 \end{bmatrix}\frac{\partial W}{\partial \bar{I}_2} \qquad \text{(V.2.15)}$$

Finally, in the completely general case of an isotropic hyperelastic material for which

$W = W\left(\bar{I}_1, \bar{I}_2, J\right)$ (V.2.16)

$\partial W/\partial J$ can no longer be assumed to be zero at $J = 1$. So we have

$$\boldsymbol{\sigma} = 2\left[\overline{\mathbf{B}} - \frac{1}{3}\left(\gamma^2+3\right)\mathbf{I}\right]\frac{\partial W}{\partial \bar{I}_1} + 2\left[\left(\gamma^2+3\right)\overline{\mathbf{B}} - \overline{\mathbf{B}}^2 - \frac{2}{3}\left(\gamma^2+3\right)\mathbf{I}\right]\frac{\partial W}{\partial \bar{I}_2} + \frac{\partial W}{\partial J}\mathbf{I} \qquad \text{(V.2.17)}$$

$$\therefore \boldsymbol{\sigma} = 2\begin{bmatrix} \frac{2}{3}\gamma^2 & \gamma & 0 \\ \gamma & -\frac{1}{3}\gamma^2 & 0 \\ 0 & 0 & -\frac{1}{3}\gamma^2 \end{bmatrix}\frac{\partial W}{\partial \bar{I}_1} + 2\begin{bmatrix} \frac{1}{3}\gamma^2 & \gamma & 0 \\ \gamma & -\frac{2}{3}\gamma^2 & 0 \\ 0 & 0 & \frac{1}{3}\gamma^2 \end{bmatrix}\frac{\partial W}{\partial \bar{I}_2} + \frac{\partial W}{\partial J}\mathbf{I} \qquad \text{(V.2.18)}$$

References

Alderson K L, Alderson A & Evans K E (1997) The interpretation of the strain-dependent Poisson's ratio in auxetic polyethylene. J Strain Analysis vol 32, pp201-212.

Antunes P (2008) Constitutive modelling of cork-polyurethane gel composites. PhD thesis. University of Minho, School of Engineering.

Arruda EM & Boyce MC (1993) A three-dimensional model for the large stretch behavior of rubber elastic materials. J Mech Phys Solids. vol 41, pp389-412.

Attard M M (2004) Finite strain isotropic elasticity. Int J Solids Structs. vol 40, pp4353-4378.

Beatty MF (1987) Topics in finite elasticity: hyperelasticity of rubber, elastomers, and biological tissues—with examples. Applied Mechanics Reviews, vol 40, issue 12, pp1699-1719.

Beatty MF & Stalnaker DO (1987) The Poisson function of finite elasticity. J Appl Mech vol 53, pp807-813.

Bilgili E (2004) Restricting the hyperelastic models for elastomers based on some thermodynamic, mechanical and empirical criteria. J Elastomers and Plastics. vol 36, pp159-175.

Bischoff JE, Arruda EM & Grosh K (2001) A new constitutive model for the compressibility of elastomers at finite deformations. Rubber Chem Technol, vol 74, No. 4, pp541-559.

Blatz PJ & Ko WL (1962) Application of finite elastic theory to the deformation of rubbery materials. Trans Soc Rheology. vol VI, pp223-251.

Bonet J & Wood R D (1997) nonlinear continuum mechanics for finite element analysis. Cambridge University Press.

Bower A F (2009) Applied mechanics of solids. CRC Press.

Boyer R F & Miller R L (1986) Correlations involving the Mooney-Rivlin C2 constant and the number of chain atoms between physical entanglements. Polymer, vol 28, Issue 3, pp399-407.

Boyce & Arruda (2000) Constitutive models of rubber elasticity: A review. Rubber Chem Technol. Vol 73, no 3, pp504-523.

Bruhns OT, Xiao H & Meyers A (2001) Constitutive inequalities for an isotropic elastic strain-energy function based on Hencky's logarithmic strain tensor. Proc. Roy. Soc. A, vol 457, pp2207-2226.

Burgess I W & Levinson M (1972) The instability of slightly compressible rectangular rubberlike solids under biaxial loadings. Int J Solids Structs, vol 8, pp133-148.

Carmichael AJ & Holdaway HW (1961) Phenomenological elastomechanical behavior of rubbers over wide ranges of strain. J Appl Phys, vol 32, pp159-166.

Chagnon G (2003) Modelling of Mullins effect in rubber like materials. PhD thesis, Ecole Centrale de Nantes.

Chagnon G & Coveney VA (2008) Unpublished work.

Chagnon G & Coveney VA (2011) Unpublished work.

Davies CKL, Dilip K &Thomas AG. (1994) Characterisation of the behaviour of rubber for engineering design purposes. Rubber Chem Technol. vol 67, issue 4, pp716-728.

Dienes J K & Solem J C (1999) Nonlinear behavior of some hydrostatically stressed isotropic elastomeric foams. Acta Mechanica. vol 138, pp155-162.

Eihlers W & Eipper G (1998)The simple tension problem at large volumetric strains computed from finite hyperelastic laws. Acta Mechanica, vol 130, pp17-27.

El-Ratal W H & Mallick P K (1996) Elastic response of flexible polyurethane foams in uniaxial tension. J Eng Materials & Tech, vol 118, pp157-161.

Flory P J (1960) Thermodynamic relations for high elastic materials. Trans. Faraday Soc, vol 57, pp829–838.

Fu YB & Ogden RW (2002) Non linear elasticity, theory and applications. Cambridge University Press.

Gan YX, Chen C & Shen YP (2005) Three-dimensional modelling of the mechanical property of linearly elastic open cell foams. Int J Solids & Structures vol 42, pp6628-6642.

Gendy AS & Saleeb AF (2000) Non-linear parameter estimation for characterising hyperelastic large strain models. Computational Mechanics. vol 25, pp66-77.

Gent AN (1999) Elastic instabilities of inflated rubber shells. Rubber Chem Technol. vol 72, pp263-268.

Gent AN (2005) Elastic instabilities in rubber, Int J Nonlinear Mechanics, vol 40, pp165-175.

Gent AN & Cho IS (1999) Surface instabilities in compressed or bent rubber blocks, Rubber Chem Technol, vol 72, pp253-262.

Gent & Rivlin (1952) Experiments on the mechanics of rubber II: The torsion, extension and inflation of a tube. Proc Phys Soc B, vol 65, pp487-501.

Gent AN & Thomas AG (1959) The deformation of foamed elastic materials, Journal of Applied Polymer Science, vol 1, pp107-113.

Gent AN & Thomas AG (1959) Failure of foamed elastic materials, Journal of Applied Polymer Science, vol 2, issue 6, pp354-357.

Gent AN & Thomas AG (1963) Mechanics of foamed elastic materials. Rubber Chem. and Tech. vol 36, pp597-610.

Gibson LJ, Easterling KE & Ashby MF (1981) The structure and mechanics of cork. Proc R Soc Lond A. vol 377, pp99-117.

Gibson LJ & Ashby MF (1982) The mechanics of three-dimensional cellular materials. Proc R Soc Lond A, vol 382, pp43-59.

Gibson LJ & Ashby MF (1997) Cellular solids structure and properties. Cambridge University press.

Gong L, Kyriakides S & Jang K (2004) Compressive response of open-cell foams. Part I: Morphology and elastic properties. Int Journal Solids & Structures. vol 42, pp1355-1379.

Gough J Gregory IH & Muhr AH (1999) Determination of constitutive equations for vulcanized rubber in finite element analysis of elastomers. Boast D & Coveney VA (eds), Professional Engineering Publishing (IMechE), pp5-26.

Gould PL (2013) Introduction to linear elasticity. 3rd edn, Springer.

Greaves GN, Greer AL, Lakes RS & Rouxel T (2011) Poisson's ratio and modern materials. Nature Materials, vol 10, pp823-837.

Green AE & Adkins JE (1960) Large elastic deformations and non-linear continuum mechanics. Clarenden Press, Oxford.

Gregory MJ (1979) The stress-strain behaviour of filled rubbers at moderate strains. Plastics and Rubber: Materials and Applications. vol 4, pp184-188.

Hall IH (1968) Deformation of solids. Nelson.

Hencky H (1928) Über die Form des Elastizitätsgesetzes bei ideal elastischen Stoffen. Zeitschrift für technische Physik, vol 9, pp215-220.

Hencky H (1931) The Law of elasticity for isotropic and quasi-isotropic substances by finite deformations**.** Journal of Rheology, vol 2, issue 2, pp169-187.

Hencky H (1933) The elastic behaviour of vulcanized rubber, Journal Applied Mechanics. vol 6, pp217-224.

Hill JM (1973) On a duality of stress and deformation fields in finite elasticity. Journal of Elasticity, vol 3, no 1. pp51-56.

Hill R (1970) Constitutive inequalities for isotropic elastic solids under finite strain. Proc R Soc Lond A, vol 314, pp457-472.

Hill R (1978) Aspects of invariance in solid mechanics. Adv Appl Mech, vol 18, pp1-75.

Holzapfel GA (2000) reprinted with corrections in 2006. Nonlinear Solid Mechanics: a continuum approach for engineering. Wiley.

Jones DF & Treloar LRG (1975) The properties of rubber in pure homogeneous strain. J Physics D: Appl Physics vol 8, pp1285-1304.

Kawabata S (1973) Fracture and mechanical behavior of rubber-like polymers under finite deformation in biaxial stress field. J Macromol Sci B, vol 8, pp605-630.

Knowles J K & Sternberg E (1975) On the ellipticity of the equations of nonlinear elastostatics for a special material. J Elasticity, vol 5, pp341-361.

Lai WM, Rubin D & Krempl E (2010) Introduction to continuum mechanics. 4th edn, Butterworth-Heinemann.

Lakes R (1987) Foam structures with a negative Poisson's ratio. Science vol 235, pp1038-1040.

Liu CH & Mang HA (1996) A critical assessment of volumetric strain energy functions of hyperelasticity at large strains. Institute for Strength of Materials, University of Technology of Vienna, Karlsplatz 13/202, 1040 Vienna. 1996, vol. 76, SUP5 (593 p.) (6 ref.), pp305-306.

Marlow RS (2003) A general first-invariant hyperelastic constitutive model. In constitutive models for rubber III. JJC Busfield & AH Muhr (eds) , Balkema, ISBN 90 5809 5665, pp157-167.

Mars WV (2006) Heuristic approach for approximating energy release rates of small cracks under finite strain, multiaxial loading. Chapter 7 in Elastomers and components service life prediction – progress and challenges, Coveney VA (ed) Woodhead pp91-111.

Mills NJ (2007) The high strain mechanical response of the wet Kelvin model for open-cell foams. Int J Solids and Structures vol 44, pp51-65.

Mills N J & Gilchrist A (2000a) Modelling the indentation of low density polymer foams. Cellular Polymers, vol 19, pp389-412.

Mills N J & Gilchrist A (2000b) High strain extension of open cell foams. J Eng Matls and Techn ASME vol 122, pp67-73.

Mooney M (1940) A theory of large elastic deformation. J Appl Physics, vol 11, pp582-592.

Mott PH & Roland CM (2009) Limits to Poisson's ratio in isotropic materials. Physical review B, vol 80, pp132104-1-132104-4.

Mott PH & Roland CM (2013) Limits to Poisson's ratio in isotropic materials – general result for arbitrary deformation. Physica Scripta, vol 87 pp055404-1 – 055404-6.

MRPRA (1984) The natural rubber formulary and property index. Published by the Malaysian Rubber Producers' Research Association (MRPRA, now renamed TARRC, at

Brickendonbury, Hertford, UK) a unit of the Malaysian Rubber Research and Development Board.

Muhr AH (2005) Modelling the stress-strain behaviour of rubber. Rubber Chem Tech vol 78, issue 3, pp391-425.

Needleman A **(**1977) Inflation of spherical rubber balloons. Int. J Solids Struct. vol 13, pp409-421.

Oden JT (1972, 2000) Finite elements of nonlinear continua. McGraw-Hill, Dover.

Ogden RW (1972a) Large deformation isotropic elasticity – on the correlation of theory and experiment for incompressible rubber-like solids. Proc R Soc Lond A vol 326 pp565-584.

Ogden RW (1972b) Large deformation isotropic elasticity: on the correlation of theory and experiment for compressible rubber-like solids. Proc R Soc Lond A vol 328 pp567-583.

Ogden RW (1976) Volume changes associated with the deformation of rubber-like solids. J Mech. Phys. Solids, vol 24: pp323-338.

Ogden RW (1986) Recent advances in the phenomenological theory of rubber elasticity. Rubber Chem & Tech. vol 59 pp361-383.

Ogden RW, Saccomandi G & Sgura I (2004) Fitting hyperelastic models to experimental data. Computational Mechanics. vol 34 pp484-582.

Pierron F (2010) Identification of Poisson's ratio of standard and auxetic low density polymeric foams from full field measurements. J Strain Analysis. vol 45 pp223-253.

Price C (1976) Thermodynamics of rubber elasticity. Proc R Soc London A. vol 351 no 1666. pp331-350.

Pucci E & Saccomandi G (2002) A note on the Gent model for rubber-like materials. Rubber Chem and Tech. vol 75 pp839-851.

Rees DWA (1990) Mechanics of solids and structures. McGraw-Hill, London.
Rivlin RS (1948a) Large elastic deformations of isotopic materials. I Fundamental concepts. Phil Trans R Soc A. vol 240 pp459-490.

Rivlin RS (1948b) Large elastic deformations of isotopic materials. IV Further developments of the general theory. Phil Trans R Soc A. vol 241 pp379-397.

Rivlin RS (1992) The elasticity of rubber. Rubber Chem Tech. vol 65 pp51-66.

Rivlin RS & Saunders DW (1951) Large elastic deformations of isotropic materials VII. Experiments on the deformation of rubber. Phil Trans R Soc Lond, A. vol 243 pp251-288.

Rivlin RS & Sawyers KN (1976) The strain energy function for elastomers, Trans Soc Rheology, vol 20, pp545-557.

Roberts AD ed. (1988) Natural rubber science and technology. Oxford University Press.

Roland CM (2011) Viscoelastic behavior of rubbery materials. Oxford University Press.

Schwaber DM (1973) Impact behavior of polymeric foams: A Review. Polymer Plastics Technol. Eng. vol 2. pp231-249.

Seibert DJ & Schöche N (2000) Direct comparison of some recent rubber elasticity models. Rubber Chem Tech, vol 73, pp366–384.

Storakers B (1986) On material representation and constitutive branching in finite compressible elasticity. J Mech Phys Solids vol 34 No. 2 pp125-145.

Treloar LRG (1975) The physics of rubber elasticity. 3rd Edn, Clarendon Press, Oxford.

Treloar LRG (1976) The mechanics of rubber elasticity. Proc Roy Soc. A vol 351. pp301-330.

Truesdell & Noll (2004) The non linear field theories of mechanics. Springer, London.

Valanis KC & Landel RF (1967) The strain-energy density function of a hyperelastic material in terms of the extension ratios. J Appl Physics, vol 38, pp 2997-3002.

Williams J.G (1973) Stress analysis of polymers. Longman group, London.

Yong Xia, W Li, Yuanming (2004) Study on the compressible hyperelastic constitutive model of tire rubber compounds under moderate finite deformation. Rubber Chem Technol, vol 77, pp. 230-241.

Yeoh OH (1990) Characterisation of elastic properties of carbon black filled rubber vulcanizates. Rubber Chem Technol, vol 63, pp792-805.

Yeoh OH (1997) On the Ogden strain energy function. Rubber Chem Technol, vol 70, pp175-182.

Zhang J & Ashby, MF, (1989) Energy absorption of foams and honeycombs. Cambridge University Department of Engineering, internal report.

Zhu HX, Mills NJ & Knott JF. (1996) Analysis of the high strain compression of open cell foams. J Mech. Phys. Solids vol 45. pp1875-1904.